December 2018

Evaluation and Influence of Recycled Concrete Aggregate Base Layers on Hma Pavement Performance

Jessie Daniel Ramirez
University of Wisconsin-Milwaukee

EVALUATION AND INFLUENCE OF RECYCLED CONCRETE AGGREGATE BASE LAYERS ON HMA PAVEMENT PERFORMANCE

by

Jessie Ramirez

A Thesis Submitted in
Partial Fulfillment of the
Requirements for the Degree of

Master of Science
in Engineering

at
The University of Wisconsin-Milwaukee
December 2018

ABSTRACT

EVALUATION AND INFLUENCE OF RECYCLED CONCRETE AGGREGATE BASE LAYERS ON HMA PAVEMENT PERFORMANCE

by

Jessie Ramirez

The University of Wisconsin-Milwaukee, 2018
Under the Supervision of Professor Hani Titi

This research investigated the influence of the RCA base layers on the HMA pavement performance as compared with CA base layers using laboratory tests on collected base layer materials and field tests on corresponding pavement sections. Field and laboratory testing programs were conducted to investigate RCA and CA base layer materials in which identified test sections at the selected pavement sites were subjected to testing using FWD, walking profiler, and DCP. Visual distress surveys were also conducted at the selected pavement sections. RCA and CA base layer samples were collected from these pavement sites and were subjected to a laboratory testing program including: particle size analysis, Micro-Deval abrasion test, absorption, and specific gravity.

Laboratory tests indicated that the investigated RCA base layer materials are in general "finer" than the CA base materials based on the FM and GN values. The RCA base layer materials also possessed higher absorption values compared with CA base materials. In terms of resistance to abrasion, Micro-Deval abrasion test results showed that RCA and CA base layer materials exhibited high mass loss, in general, compared with a mean mass loss of 15.05% for Wisconsin virgin coarse aggregates.

Field tests evaluated the strength and modulus of the investigated RCA and CA base materials and pavement test sections based on DCP and FWD tests. The DCP test results indicated that the CBR and layer moduli values of both RCA and CA base layer types are comparable. The CBR and base layer modulus values obtained from the results of the DCP tests indicated in general good strength and modulus properties of the investigated RCA and CA bases. The FWD test results showed variability in pavement surface deflections within individual test sections and among the various pavement test sections. In general, less deflection D_0 values exhibited by pavement test sections with RCA base layers compared with those with CA base layers. The back-calculated moduli for the RCA and CA base layers (E_{Base}) exhibited significant variability within individual pavement test sections and among pavements. Comparison of the back-calculated layer moduli values E_{base} for RCA and CA base layer pavement show that there are very high values exhibited by RCA base layers for example at STH 78, which could be attributed to the tufa formation.

The results of the visual distress surveys and pavement profile measurements (in terms of calculated PCI and IRI) for investigated pavement test sections showed variability with classified pavement conditions ranging from poor to good. The HMA pavements with RCA base layers exhibited higher PCI values indicating better pavement quality. The HMA pavements with CA base layers exhibited lower IRI values compared with the HMA pavements with CA base layers indicating a smoother ride quality for HMA pavement with CA base layer.

TABLE OF CONTENTS

LIST OF FIGURES

LIST OF TABLES

ACKNOWLEDGEMENTS

I would like to thank a few people for the aid and effort in bringing this thesis to completion. I would first like to thank Dr. Hani Titi for the tremendous support and guidance throughout my undergraduate and graduate years, providing encouragement and knowledge, and for pushing me to always produce the best possible work. Dr. Habib Tabatabai and Dr. Benjamin Church for being a part of the committee and taking the time to evaluate. Mohamad Sooman for the great effort and help collecting data throughout my research. Victor Ramirez for providing valuable input and collecting data for this thesis.

I would like to thank my parents, Demetrio and Eliza Ramirez for all the love, support, and guidance. Finally, I would like to thank my wife, Brittany Ramirez, for supporting me though this journey and always being there for me during those important days.

Chapter 1

Introduction

1.1 Problem Statement

There has been great interest in recent years in using Recycled Concrete Aggregate (RCA) as base course in Wisconsin and elsewhere for the economic and environmental benefits offered by such practice. Recent examples include the I-94 corridor reconstruction in Kenosha, Racine and Milwaukee Counties, and the Beltline reconstruction in Dane County.

Laboratory studies showed that RCA have resilient modulus values equal to or higher than typical natural aggregates and also generally higher durability, in particular to freeze-thaw cycles. However, it is also recognized that RCA exhibits tufa formation and potentially lower drainability than natural aggregates. Wisconsin Department of Transportation (WisDOT) has been using RCA as base course for long time. The qualitative assessment of WisDOT roads constructed with RCA is that they are performing adequately. A quantitative review of WisDOT experience through collection and comparison of pavement distress surveys of roadways using RCA as base course compared with those using natural mineral aggregates is needed.

1.2 Research Objective and Scope

The objective of this study is to evaluate the performance of HMA pavements constructed with RCA base layers as compared with the performance of other HMA pavements

constructed with CA base layers. The scope of this study is limited to performing field testing using the Dynamic Cone Penetration Test (DCP), the Falling Weight Deflectometer (FWD), the road profiler, and conducting visual pavement surface distress survey. A survey of state highway agencies on the use and performance of RCA in base layers will be conducted with focus on the Midwest states. In addition, laboratory testing on RCA and CA base materials retrieved from pavement test sections is limited to particle size distribution, specific gravity, absorption, and Micro-Deval abrasion test.

1.3 Background

In flexible pavement systems, the base course layer acts to distribute traffic loads to the underlying sub-base and subgrade layers, as well as to facilitate drainage. The base course must also provide support to the wearing surface to prevent tensile fatigue cracking. Base course aggregate must have adequate permeability, durability, and angularity. Pertinent properties of unbound aggregate are characterized by parameters such as resilient modulus (M_R), saturated hydraulic conductivity (k_{sat}), strength in terms of California Bearing Ratio (CBR), maximum dry density ($\gamma_{d,max}$), optimum water content (w_{opt}), etc.; these parameters are critical for a mechanistic-empirical based pavement design method.

Around two billion tons of aggregate are produced in the United States annually, and aggregate production is projected to exceed 2.5 billion tons by the year 2020 (Ceylan, 2014). These figures raise issues related to sustainability, as quarries gradually become depleted and environmental regulations become more stringent. With high demand for construction aggregate

and an increasing public desire to manage waste materials in a responsible manner, there has been increasing interest in the prospect of utilizing by-products and reclaimed material for pavement construction purposes. For base courses in flexible pavement systems, the use of RAP and RCA has been the subject of increased research in recent years (Gabr and Cameron, 2012).

RCA is produced by crushing concrete demolition waste from existing concrete structures, ensuring the removal of any reinforcing steel. RCA contains residual cement paste and mortar, which results in higher water absorption capacity as well as lower density compared to natural aggregate, as well as lowering abrasion resistance (e.g. LA abrasion test). Due to the crushing processing method, RCA tends to show more angularity than virgin aggregate (Butler et al., 2013). Ceylan (2014) reports that pavement sections with RCA base courses showed pavement condition index (PCI) values and international roughness index (IRI) values that were slightly higher than sections with natural aggregate base courses; however, these differences were not found to be significant at the 95% confidence level. Edil et al. (2012) reported a 30% LA abrasion loss for RCA material, compared to a loss of 23% for class 5 natural aggregate. Edil et al. (2012) conducted micro-deval trials on RCA samples sourced from Texas and California with varying (5, 10, and 30) wet/dry cycles. California RCA showed losses of 16% over all cycles, Texas RCA showed 17%, 19% and 21% losses at 5, 10, and 30 wet/dry cycles respectively, and class 5 aggregate showed losses of 12% for 5 and 10 wet dry cycles, and 11% after 30 cycles. No clear trends in micro-deval losses were observed with respect to varying wet/dry cycles.

RCA shows unique behavior due to the presence of cement paste. RCA base course may show an increase in strength due to hydration and pozzolanic reactions that produce Calcium - Silica-Hydrate (C-S-H) (Jayakody, 2014). Complications related to drainage may occur due to the cement paste. Tufa is the formation of precipitates from water supersaturated with calcite. Tufa acts to block drainage paths, resulting in accumulation of moisture in base layers. Ceylan (2014) found that tufa formation appears to be directly related to the proportion of fines (smaller than #4 sieve). Reducing the amount of fines in the RCA reduced tufa formation, but potential for tufa formation could not be completely eliminated. Ceylan (2014) points out the need for additional research in the area of tufa formation.

1.4 Organization of the Manuscript

This manuscript is organized in six chapters. Chapter One introduces the problem statement, objective, and scope of the research. The RCA base layer survey is presented in Chapter Two, and the research methodology is discussed in Chapter Three. Chapters Four and Five present a detailed analysis of laboratory and field testing programs, respectively, with critical analysis of the outcome. The conclusions and recommendations are provided in Chapter Six.

Chapter 2

Recycled Concrete Aggregate Base Layer Materials Survey

A survey was designed with various questions to obtain the current information on RCA base layer performance and distributed to a number of highway agencies in the U.S. The research team conducted the survey by e-mail and found it challenging to get people to answer the survey questions. Out of the contacted state DOTs, only 20 replies were obtained. The most important survey questions and answers are presented below.

Performance of Recycled Concrete Aggregate (RCA) and Reclaimed Asphalt Pavement (RAP) as Base Layers in HMA Pavements:

1- *Question: What is the most commonly used material in base course layers for HMA pavement??*

Answers:

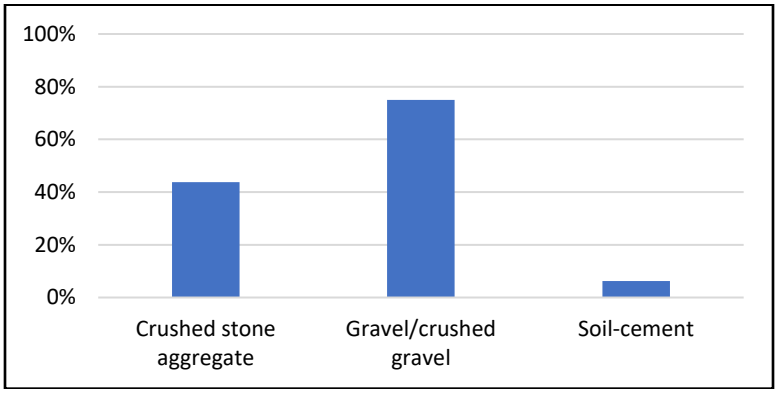

Figure 2.1: Most commonly used material in base course layers

Comments:

1) Crushed stone in 75% and crushed gravel in 25% of state
2) Florida has a widely available source of unique unconsolidated limestone, that we refer to as limerock. We do not consider this unbound aggregate.
3) New HMA pavement typically isn't constructed over a base layer and is built on either chemically stabilized (lime, fly ash, or cement) soil or just prepared subgrade soils.
4) 50% Recycled HMA/Concrete 30% In place Reclamation, i.e. in place recycled HMA and base 15% Gravel 5% crushed carbonates

2- *Question: Does your department allow the use of Recycled Concrete Aggregate (RCA) materials in HMA pavement as:*

Answers:

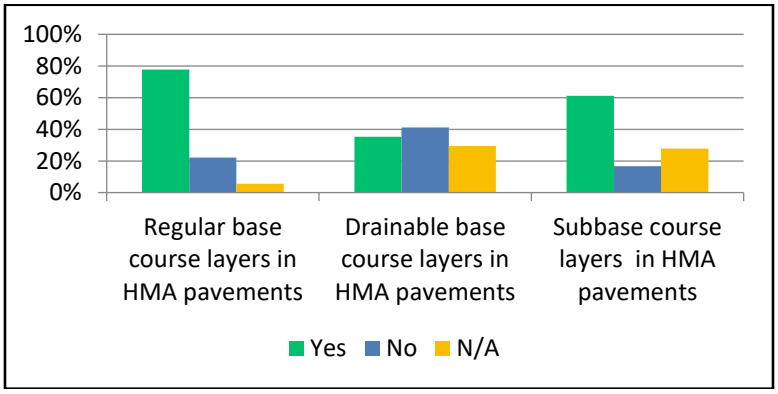

Figure 2.2: Allowable use of RCA as regular, drainable, and subbase layers

Comments:

1) We allow up to 50% RCA by weight in our base courses.
2) WYDOT will implement a new specification for the 2020 construction season
3) Allowed up to 50%. Must be blended with virgin aggregate base or subbase.
4) Its use is not allowed in HMA.
5) Subbase use is generally acceptable, but not part of our standard specifications and requires a special provision or a change order. Some RCA has been blended with our untreated base course on some projects by change order or special provision, as long as the material meets the same requirements we have for an aggregate base.
6) The conditions when RCA is used is typically during concrete pavements reconstruction, really no experience under HMA.
7) As mentioned in previous question base course materials are rarely used for HMA but we do construct them occasionally. We only have one layer of base materials when used that we call "Foundation Course"
8) Not used for our best drainable aggregate, but we do have a moderate drainable base, where concrete is allowed.
9) SDDOT only allows RCA that is obtained from a SDDOT project/pavement. Therefore, although RCA is allowed as base for HMA, not many projects create RCA and use HMA as the new pavement.

3- *Question: Does your department allow the use of Reclaimed Asphalt Pavement (RAP) materials in HMA pavement as:*

Answers:

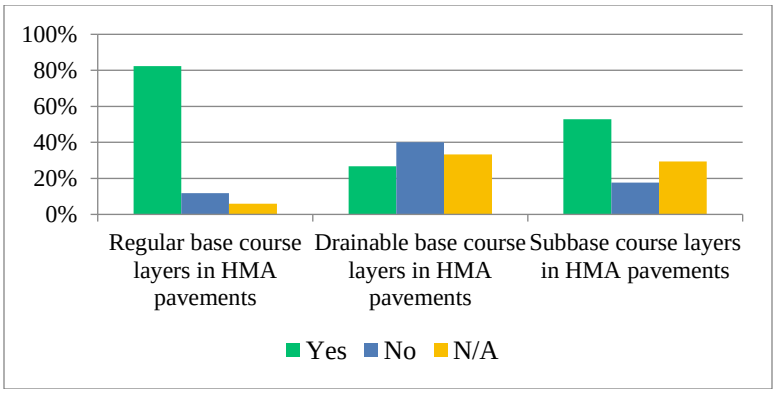

Figure 2.3: Allowable use of RAP as regular, drainable, and subbase layers

Comments:

1) We allow up to 40% by weight of RAP in our base courses.
2) RAP only allowed as a top 3" surcharge on top of base course gravels
3) Allowed up to 50%. Must be blended with virgin aggregate base or subbase.
4) RAP is not allowed in HMA surface courses. It is allowed in subbase courses as FDR.
5) Though deviations have occurred on some projects, this is not our standard approved practice.
6) Its use is typically blended with the top two inches of existing base course.
7) Must be blended with crushed stone/gravel, maximum 25% and 30% respectively
8) GDOT has placed a very limited test section using 100% recycled base via cold central plant recycling.
9) Same comment as in question #3.
10) Not used for our best drainable aggregate, but we do have a moderate drainable base, where concrete is allowed.
11) RAP is typically blended about 50/50 with virgin granular base when used as a base course under HMA pavement.

4- *Question:* Compared with the most commonly used material as base course, what is the approximate percentage of RCA use?

Answers:

1) 1%
2) 0% in Preservation projects, 75% for Reconstruction projects
3) NA
4) 10%
5) 5%
6) N/A
7) 7) Approximately 1% or less. Not aware of any used in last 15 years.
8) 0.1%
9) Negligible.
10) 5%
11) 60%
12) Not exactly sure but it is very low.
13) 1%, recently allowed for use, but little interest as of now

14) 15%
15) 1 (one) percent (Most RCA is used in commercial developments and County work)
16) 10% for HMA pavements
17) RAP is the most commonly used material, whether in reclamation or milling are used along with RCA to make base. So millings/reclamated HMA about 50% of all base and RCA about 25% of all base.
18) very small percent used as base under HMA

5- *Question:* Compared with the most commonly used material as base course, what is the approximate percentage of RAP use?

Answers:

1) 99%
2) 35
3) Not often
4) 1%
5) 1%
6) N/A
7) Approximately 30%
8) 5% as FDR
9) Negligible.
10) 0
11) 30
12) < 25%
13) 0%, RAP not used in bases, only in HMA
14) N/A
15) 5%
16) RAP is the most commonly used material, whether in reclamation or milling are used along with RCA to make base. So millings/reacclimated HMA about 50% of all base and RCA about 25% of all base.
17)
18) Using a 50/50 blend of RAP with virgin granular base under HMA, most projects (guess 60%) use RAP as base.

6- *Question:* What are your agency's current goals regarding the use of RCA and RAP?

Answers:

1) We have no established goals. It's allowed as a convience to the contractor.
2) Increase the use of RCA and RAP in future projects
3) 40% RAP Blend
4) RCA for base and RAP as a % mix in asphalt pavement
5) No target established
6) N/A
7) Do not have any set goals.
8) N/A
9) The general goal is reuse in construction of reclaimed materials, but the goals are not quantified. Not much concrete is removed for recycling. There are large amounts of RAP milled, but virtually all of it goes back into the asphalt mix itself.
10) Use RCA as an economically driven option for subbase. Utilize, manage, encourage, and allow RAP in HMA courses. Pay attention to current research and information for adaptation.

11) continue to use as is, RCA is restricted within 100 feet of a watercourse
12) We continue to allow the use of recycled materials in our gravel materials and HMA mixtures. We are looking for other uses as long as the benefits outweigh the costs.
13) To have specificications to alllow its use and let economics dertermine its use.
14) Increase use of RCA; develop specifications for RAP for base courses.
15) The State of Florida's goal is for 100 % use of RCA by any user.
16) Maintain its use specifically for PCC pavements.
17) I think that they close to being met. We are liberal in allowing both both HMA and RCA in base and surfacing. FY!, RCA not allowed for surfacing except for shoulders for two reasons: dust and wire mesh (tires destroying potential).
18) SDDOT makes effort to use all RCA and RAP generated from our pavements. SDDOT does not allow contractor furnished (tipping piles) RAP and RCA sources.

7- *Question:* Does your department have any of the following specifications for Recycled Concrete Aggregate (RCA) use as base layer materials :

Answers:

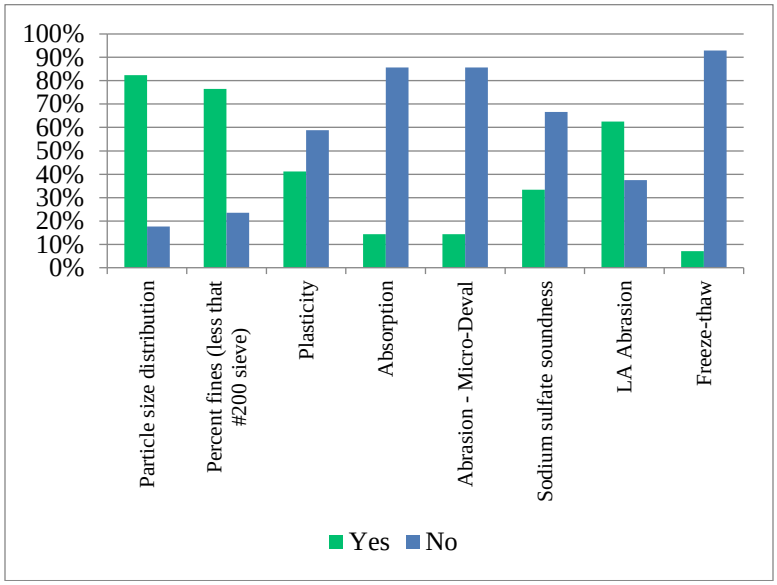

Figure 2.4: Specific specifications for RCA material

Comment:

1) When blending recycled materials into our base courses, the blend must meet the same requirements of our standard crushed aggregate base course materials.
2) Also include R-Value
3) RCA may be used as 12" - 18" thick 'rock base', per Missouri Standard Spec Section 303. The spec has basic deleterious material, particle size distribution and shape factor requirements, and does not differentiate between RCA and crushed stone. Maximum particle size is large and may be up to 6" less than the base thickness. RCA may also be used for conventional 'aggregate base course, placed in a 4" or 6" layer, as defined in Missouri Standard Spec Section 304. The spec does not differentiate between RCA and crushed stone in material requirements.
4) also specify minimum percent of crushed material, 40 to 50% depending on application
5) We allow RCA in our Reclaimed Pavement Borrow Material.
6) Percent fine on the -100 screen (5-18% passing) Spec that require it to be free of hazardous materials
7) Section 815 of our Standard Specifications.
8) Florida has a Limerick Bearing Ratio (LBR) test modeled on the California Bearing Ratio (CBR) test. Some differences: LBR - reference pressure is 800 psi, soak time 48 hours, penetration measurement at 0.1 inch (2.54 mm) (corrected for curve inflection); CBR - reference pressure is 1,000 psi, soak time 96 hours, penetration measurement at 2.5 mm and 5 mm (corrected for curve inflection)

8- *Question*: Does your department have any of the following specifications for Reclaimed Asphalt Pavement (RAP) use as base layer materials:

Answers:

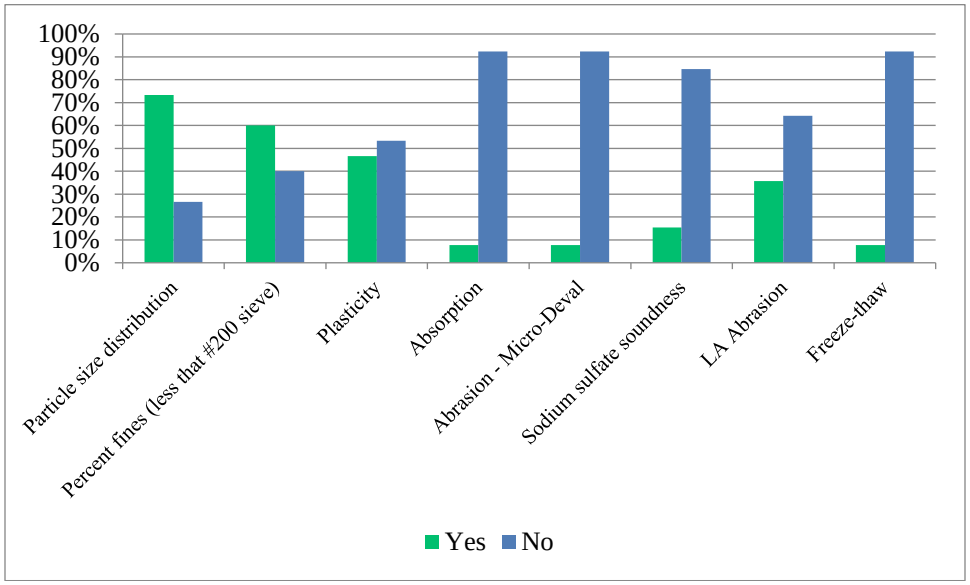

Figure 2.5: Specific specifications for RAP material

Comment:

1) Same comment as for RCA, the blended material must meet the same requirements of our crushed aggregate base courses.
2) RAP is only used as a base for emergency or unique cases.
3) RCA may be used for conventional 'aggregate base course', placed in a 4" or 6" layer, as defined in Missouri Standard Spec Section 304. The spec does not differentiate between RCA and crushed stone in material requirements.
4) RAP is not used exclusively for base course. The existing HMA is milled and blended with the top two inches of existing aggregate base course then graded, compacted and tested for acceptance.
5) We allow RCA in our Reclaimed Pavement Borrow Material.
6) GDOT has a draft special provision for use with 100% recycled asphalt pavement.
7) Since SDDOT only allows recycled pavements from our existing pavements, we assume the quality of the RCA and RAP are acceptable.

9- *Question*: Do you have issues/problems related to RCA performance as base layers?

Answers:

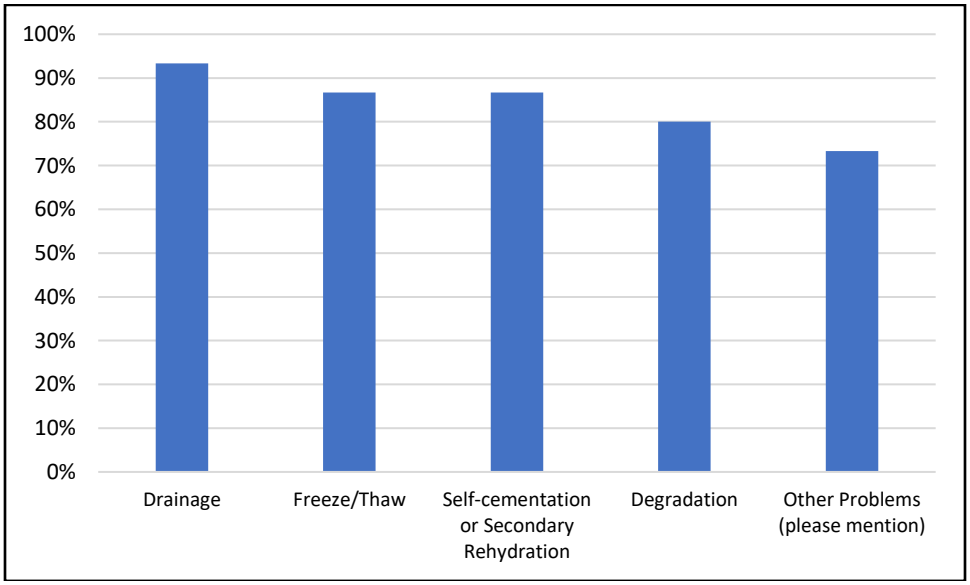

Figure 2.6: Issues or problems with RCA performance as base layers

Comments:

1) No problems have been identified.
2) NA
3) No
4) No
5) No
6) RCA is used infrequently, so we are not aware of problems related specifically to its use.
7) Tufa clogs rodent screens and backs up water in the pavement structure
8) N/A
9) No
10) No issues to date unless it has been placed out of tolerance of gradation requirements.
11) No

10- *Question*: Do you have issues/problems related to RAP performance as base layers?

Answers:

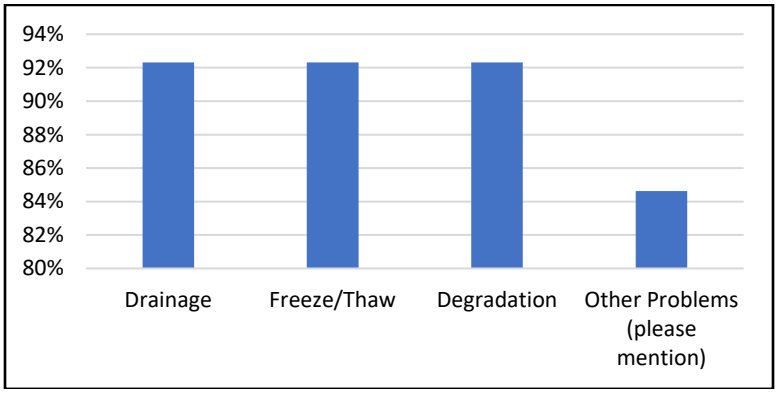

Figure 2.7: Issues or problems with RAP performance as base layers

Comments:

1) No problems have been identified.
2) Unknown
3) No
4) No
5) No

6) RAP is virtually never used as a base layer, because of its greater value in asphalt mix, therefore we are not aware of problems related specifically to its use.
7) Environmental
8) No
9) N/A
10) No
11) No

11- *Question*: Do you have a case history or example on performance issues of:

Answers:

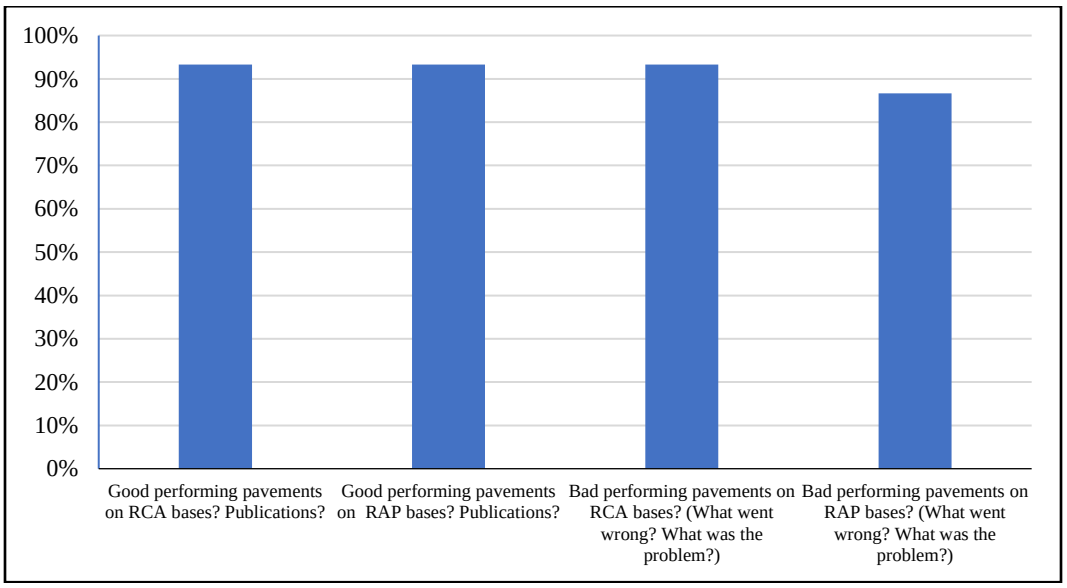

Figure 2.8: Case history on performance issues

12- *Question*: Do you have any of the following HMA pavement performance issues when using RCA base layer?

Answers:

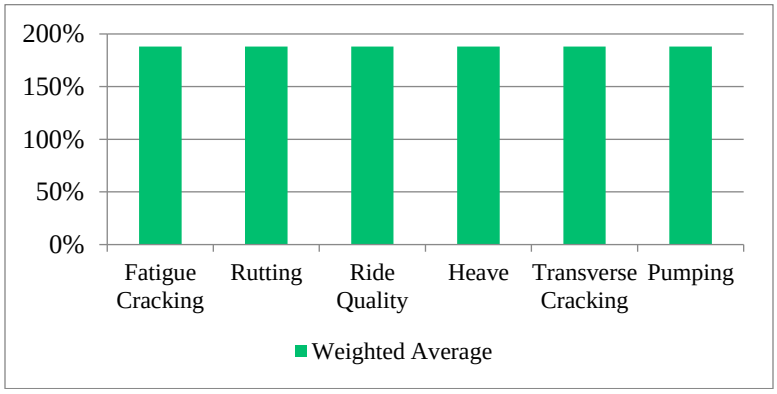

Figure 2.9: HMA pavement performance issues when using RCA base layers

Comments:

1) No problems have been identified or linked to using RCA in our base courses, but we don't see this very often, if at all.
2) NA
3) Although allowed if blended at a ratio of 50:50 with virgin aggregate base, I am not aware of any RCA used in base layers under HMA pavements
4) N/A
5) If we have any problems with pavements incorporating RCA in the base layer, we are not aware of it.
6) These pavement performance issues all occur but it may or may not be caused by the base course.
7) It is not used often enough to know.
8) As noted earlier, TDOT has just started to allow the use of RCA and we do not have any experience with performance at this time
9) No, no history of RCA use under HMA.
10) Again, we rarely use a base layer for HMA so these do not apply
11) We have had HMA roads experience early failure, not sure of the mechanism, but I believe that it may be from secondary cementation. This is why if RCA > 75% our gradation must be coarser.
12) Not many/or any HMA pavements place on RCA base

13- *Question*: Do you have any of the following HMA pavement performance issues when using RAP base layer?

Answers:

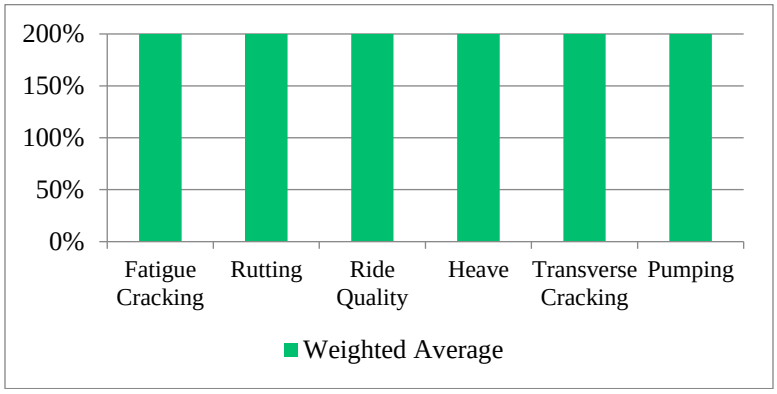

Figure 2.10: HMA pavement performance issues when using RAP base layers

Comments:

1) No problems have been identified relating specifically to the use of RAP in base courses.
2) Performance studies have not been done on these issues.
3) When used as FDR.
4) If we have any problems with pavements incorporating RAP in the base layer, we are not aware of it.
5) As previously stated RAP is not used exclusively for the base course.
6) It is not used often enough to know.
7) HMA base not utilized
8) No history of use.
9) Same comment as in #12
10) In the past I have heard of rutting issues with reclaimed bases, not sure whether this has been from (poor subgrade, under compacted base, or lack of crushing in the base. Have not heard of recent projects with this issue. We now regulate a maximum lift thickness of 6", have equipment requirements for HMA base, and test roll all base.

14- *Question*: What construction control method do you use for RCA and RAP bases?

Answers:

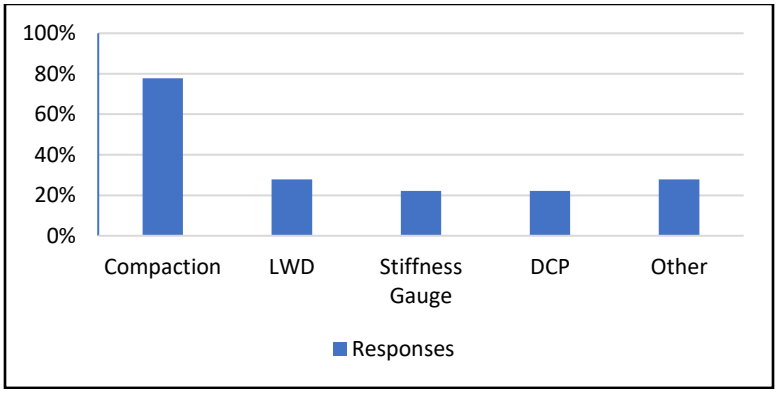

Figure 2.11: Construction control method for RCA and RAP

Comments:

1) Unknown
2) N/A
3) Nothing specifically for these materials other than the standard specs referenced earlier.
4) considering investigating the Troxler E-Gauge
5) Spot test have to meet quality compaction (the eye ball test) and either the DCP, specified density or LWD. Then finally the base is test rolled (the final 100% coverage eyeball and depression test)

15- *Question*: Do you allow the sole use of RCA or RAP? Or do you blend/mix with other materials (such as RAP + RCA mixture or RCA + Virgin Aggregate mixture)?

Answers:

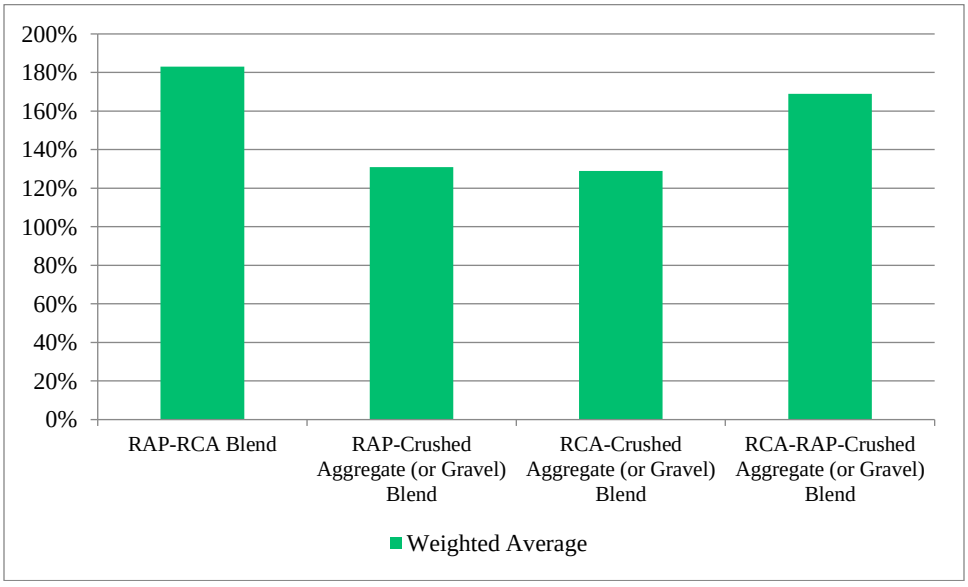

Figure 2.12: Mixed blends for RCA and RAP

Comments:

1) 40% max (by weight)
2) up to 50% blend
3) max 50% RAP blended with virgin aggregate base / subbase
4) As FDR.
5) Theoretically, by standard spec, this combination would be allowed for an aggregate base course.
6) Local evidence and a local BYU study has convinced us that the combined properties are inferior to either on their own.
7) existing HMA pavement is blended with the top two inches of aggregate base course.
8) Reclaimed Pavement Borrow Material
9) Combination of the two is capped at 50% max (by weight)
10) Theoretically, by standard spec, this combination would be allowed for an aggregate base course.
11) not typical

16- *Question*: Rate the importance (or magnitude) of the following the potential barriers within your agency to using RCA in pavement foundations on a scale of 0-5:

Answers:

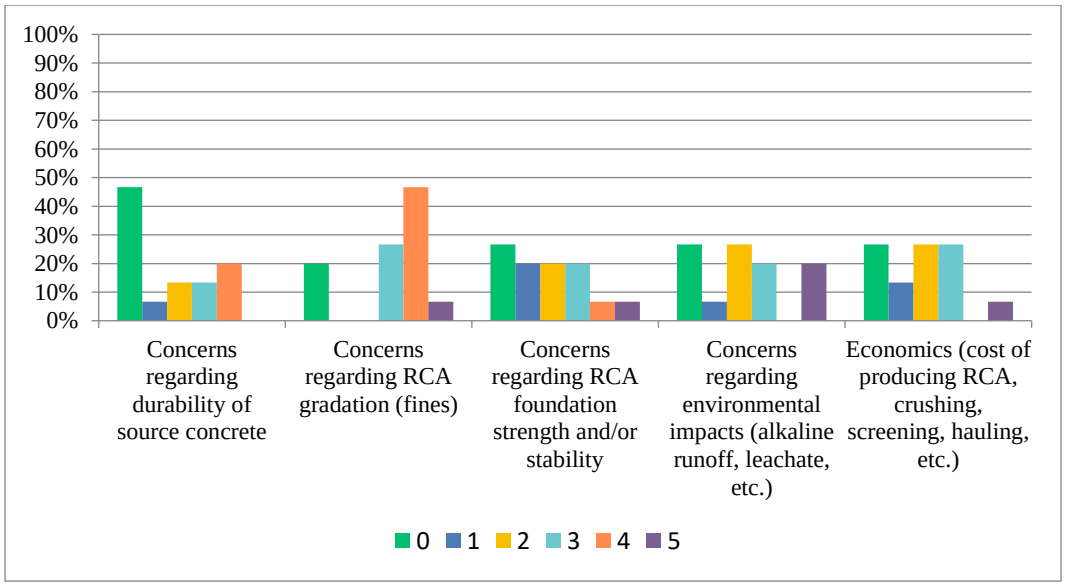

Figure 2.13: Importance scale for RCA material

Comments:

1) RCA is not widely used for this purpose.
2) NA
3) No major concerns if blending at max of 50%
4) I don't envision ever not using RCA for aggregate base course as there is an abundant source.
5) We have been using RCA for foundation course for PCC pavements fo 20+ years and don't feel like we have any current barriers.

17- *Question*: Rate the importance (or magnitude) of the following the potential barriers within your agency to using RAP in pavement foundations on a scale of 0-5:

Answers:

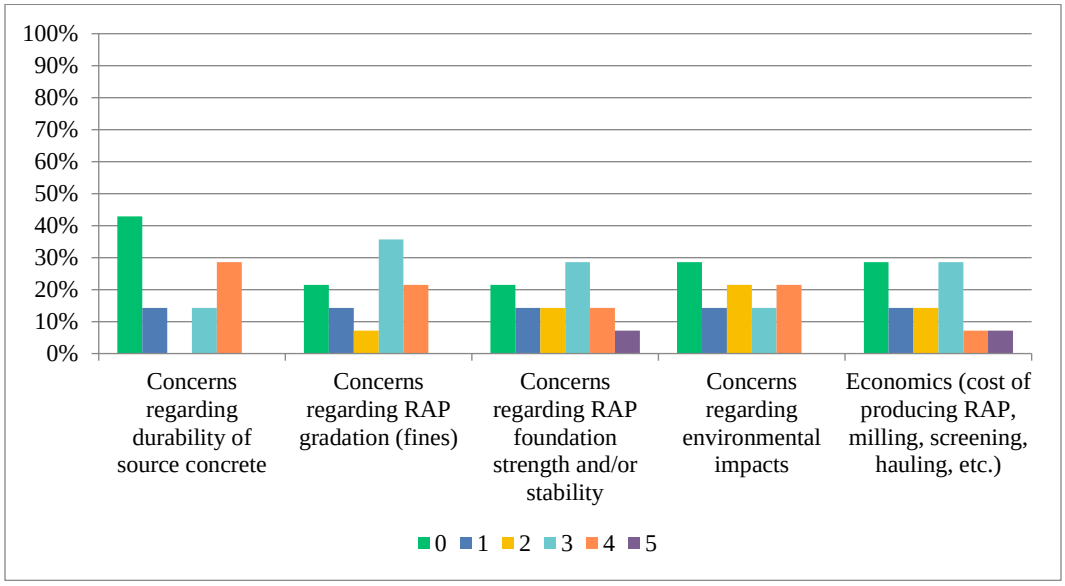

Figure 2.14: Importance scale for RAP material

Comments:

1) No major concerns if blending at max of 50%
2) When used as FDR.
3) RAP is not used exclusively for base course.
4) We have found that the RAP used as foundation course provides better drainage than RCA and some of our natural aggregates. We have no concerns but currently the RAP is more valuable if use in the Asphalt Mix Design.

18- *Question*: Do you have any structural capacity issues with HMA pavements on RCA bases? RAP bases?

Answers:

1) None that have been identified.
2) none
3) Yes
4) No
5) No
6) N/A
7) No
8) No and no.
9) None we're aware of.
10) Not that we are aware of.
11) Not for RCA, RAP is not used

12) No that I'm aware of.
13) N/A
14) No solid structural coefficient at this time.
15) No
16) No
17) No

19- *Question*: How do you compare HMA pavement performance with RCA or RAP base versus the most common base (e.g., versus similar pavements with virgin aggregate base layers)?

Answers:

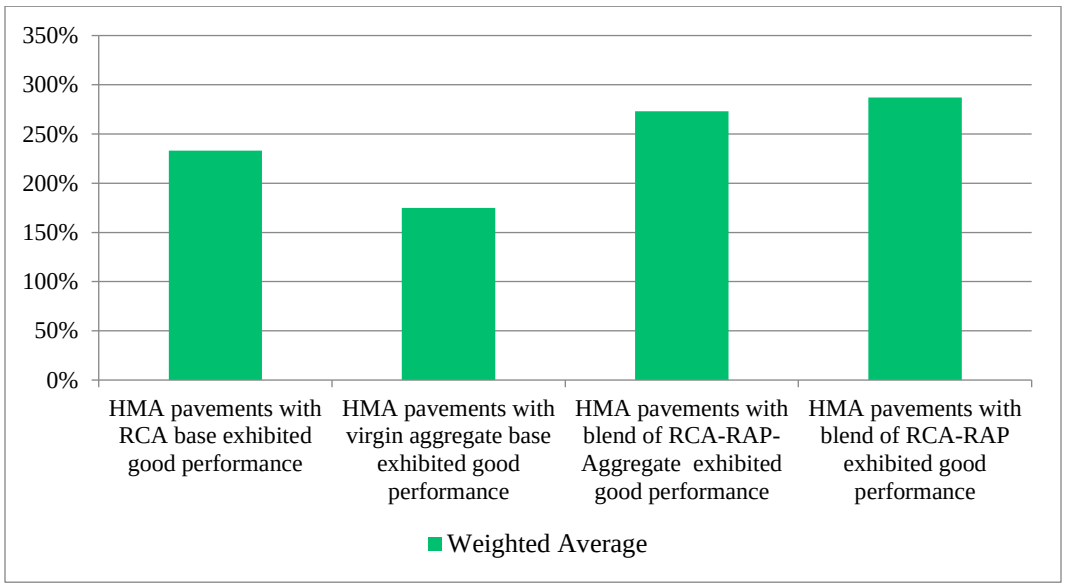

Figure 2.15: Comparison of RCA/RAP vs Virgin Aggregate

20- *Question*: When RAP is used as base layers do you have any issues with HMA performance compared with similar pavements with virgin aggregate base layers?

Answers:

1) *Not large enough sample size, however no issues have ever been documented.*
2) *Drainage can become an issue*
3) *NA*
4) *no*
5) *No*
6) *No*
7) *No*
8) *None we're aware of.*
9) *Insufficient experience. No problems observed.*
10) *no*
11) *We don't have enough information to make a judgement.*
12) *N/A*

13) *No history.*
14) *No concerns*
15) *Yes, when RCA too fine. Would rather have a mixture of no more than 75% RCA. But we think that we are lessoning potential of degradation by our gradation changes, making coarser with RCA > 75%.*
16) *not typical in SDDOT projects*

21- *Question*: When RCA is used as base layers do you have any issues with HMA performance compared with similar pavements with virgin aggregate base layers?

Answers:

1) *No*
2) *None*
3) *No*
4) *No*
5) *No*
6) *No when used as FDR.*
7) *None we're aware of.*
8) *No experience.*
9) *RAP is not used exclusively.*
10) *We don't have enough information to make a judgement.*
11) *N/A*
12) *Only one very limited test section.*
13) *No concerns*
14) *As long as material is compacted well, in lifts 6" or less with the right equipment and test rolled, then no problem.*
15) *performs well at 50/50 blend.*

22- *Question*: *Do you have any comment on RCA and or RAP that you believe is important to this issue? Please specify*?

Answers:

1) *No*
2) *No*
3) *Lack of material availability to be used as base layer.*
4) *FDR base has much higher modulus than gravel making it desirable.*
5) *No.*
6) *RCA should not be used in direct contact or directly above sock wrapped underdrain as the concrete fines will plug it up.*
7) *N/A*
8) *It is important that the processing of the RCA or RAP is done correctly, and the fines are removed from the material that is to be used for the base course. The gradation and material passing the #200 sieve are key.*
9) *Make sure high RAP is compacted well. For high RCA, make gradation coarser. Do not allow concrete brick to be use, or have an upper limit, say 10% in base (Higher cement content, finer, therefore secondary re-cementation potential).*

Chapter 3

Research Methodology

This chapter describes the field and laboratory testing program conducted to investigate RCA and CA base materials. Identified test sections at the selected pavement sites were subjected to nondestructive testing using the Falling Weight Deflectometer, pavement surface profile measurements, visual pavement distress surveys and Dynamic Cone Penetrometer. RCA and CA base layer aggregate samples were collected and subjected to a comprehensive laboratory testing program. Laboratory tests included particle size analysis, Micro-Deval (MD), absorption, and specific gravity.

3.1 Selection of Pavement Test Sites

The selected HMA pavement sites for field testing were identified based on presence of the RCA base layer materials used in construction. Figure 3.1 depicts the locations of the investigated pavements in Wisconsin.

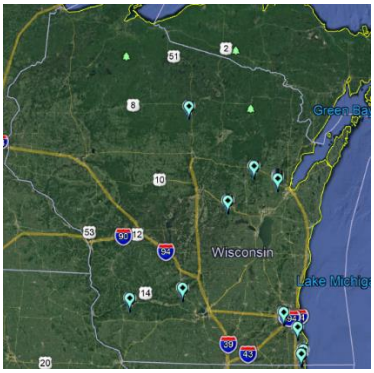

Figure 3.1: Locations of the investigated pavements in Wisconsin.

3.2 Non-Destructive Field Testing at Selected Pavement Sites

The field testing program for the selected pavement sites was conducted by UWM research team and WisDOT personnel. The testing program consisted of Falling Weight Deflectometer, visual distress surveys, and Dynamic Cone Penetration.

3.2.1 Falling Weight Deflectometer Tests

The FWD testing was conducted by WisDOT and required extensive efforts by the WisDOT team and UWM researchers. This included travel to various pavement sites across Wisconsin, implementing full traffic control and lane closure, selecting test sections, and executing the testing program. Once at the pavement site, the research team conducted a windshield visual distress survey/evaluation of the whole length of the site to identify representative test section(s).

The FWD test was conducted according to ASTM D4694: Standard Test Method for Deflections with a Falling-Weight-Type Impulse Load Device. The WisDOT KUAB FWD was used with three different load drops of 5,000, 9,000, and 12,000 lb Seven geophones were used to record pavement surface deflection located at the center of the loading plate and at 12, 24, 36, 48, 60, and 72 inches behind the loading plate. In another configuration, nine geophones were used to record pavement surface deflection with two additional geophones located at 12 inches in front of and to the left of the loading plate. Pavement surface and air temperatures and GPS coordinates were acquired at each test point. Figure 3.2 shows the FWD during testing at various pavement sites.

The total length of the FWD test section for each pavement site varied between 528 ft ($\frac{1}{10}$ of a mile) and more than 5,000 ft depending on field conditions and availability of equipment. The FWD test point spacing ranged from 10 to 100 ft. The majority of the FWD tests were conducted at the outside wheel path of the outside lane of the pavement section. For a limited number of pavement test sections, FWD testing was conducted on both the outside and inside wheel paths.

(a) FWD plate and sensors on pavement surface (b) FWD plate and sensors on pavement surface

Figure 3.2: Nondestructive testing using the WisDOT FWD KUAB/GSSI GPR unit at various HMA pavement sites.

3.2.2 Visual and Automated Pavement Surface Distress Surveys and Profile Measurements

Visual surveys were conducted (as shown in Figure 3.3) to identify and quantify the various types of pavement surface distress exhibited at the investigated pavements and to obtain data needed to evaluate pavement performance in terms of a Pavement Condition Index (PCI).

Each distress survey was conducted for one 528 ft section at each pavement site. The section was selected to be representative of the overall pavement condition.

(a) Visual distress survey (b) Measuring distresses

Figure 3.3: Visual pavement surface distress surveys conducted by the research team.

At the investigated pavement sites, surface distresses were visually identified, quantified, and recorded. Pavement distress types, extent, and levels of severity were identified and quantified according to the FHWA distress identification manual. Pavement surface profile measurements were conducted using a walk behind using SSI-CS800 Walking Profiler.

3.3 Sampling of Base Layer Aggregates and Field Testing

3.3.1 Sampling of RCA and CA Base Materials

UWM research team coordinated efforts to obtain RCA and CA base samples from the selected pavement sites. RCA and CA base materials samples with a volume of approximately three 5-gallon buckets were collected from these sites using three different methods via coring pavement surface by a drilling company hired by UWM.

Figure 3.4 depicts pictures of the various efforts involved in base aggregate sampling. The aggregate samples were collected with the aid of basic tools such as small size shovels and hand-held pickaxes to dig down to the bottom of base course aggregate layers. The collected samples were placed in 5-gallon buckets, covered, and transported to the Pavement and Geotechnical Research Laboratory at UW-Milwaukee for testing and evaluation.

3.3.2 Dynamic Cone Penetration Test

The field testing program included aggregate base course layer and subgrade testing using the DCP. A dynamic cone penetrometer with a single-mass hammer was used to perform tests on the project sites. The DCP was driven into the aggregate base layer by the impact of a single-mass 17.6 lb hammer dropped from a height of 22.6 in. The test was conducted according to the standard test procedure described by ASTM D6951: Standard Test Method for Use of the Dynamic Cone Penetrometer in Shallow Pavement Applications. For all pavement test sites, two or more tests were conducted at wheel path location as well as at the center of the lane. Figure 3.5 depicts the DCP test conducted on selected pavement sites.

(a) WisDOT coring rig at STH 32 (b) Sampling Base materials (c) Exposed RCA base material

Figure 3.4: Coring of pavement surface to retrieve base aggregate samples.

Figure 3.5: Dynamic cone penetration test on aggregate base course layers.

3.4 Laboratory Testing of Base Aggregate

Representative aggregate samples were collected from the investigated pavement sites as described earlier. Table 3.1 presents the ASTM and AASHTO standard test procedures conducted on the RCA and CA base materials from each investigated pavement site.

3.4.1 Particle Size Analysis

Sieve analysis was used to determine the particle size distribution of the base course aggregate specimens. First, the sample was oven-dried to constant mass at 230 °F. Then quartering was used to reduce the sample into a test sample that was at least 15 kg. The purpose

was to prepare a test sample that was representative of the sampled project site location. Next, the sample was washed over a No. 200 sieve so that material finer than the No. 200 sieve would pass through the opening of the sieve. Then the sample was oven-dried to constant mass once again.

Afterwards, the following set of sieves were stacked: 1.25″, 3/4″, 3/8″, No. 4, No. 10, No. 40, No. 200, and a pan. These sieve sizes are in compliance with the WisDOT specifications for the particle size distribution of 1 ¼ in dense graded base course aggregate layers described in Section 305.2.2.1 of WisDOT Standard Specifications for Highway and Structure Construction (2018). The stacked sieves were then placed onto an automatic sieve shaker and were agitated according to the standard procedures. The retained masses on each sieve were weighed and used to calculate the percentage of material passing each sieve and subsequently plot the particle size distribution curves.

Table 3.1: ASTM and AASHTO standard test methods employed.

Standard Test Procedure	Standard Designation	
	ASTM	AASHTO
Standard Test Method for Materials Finer than 75-µm (No. 200) Sieve in Mineral Aggregates by Washing	C117 -17	T 11-05 (13)
ASTM: Standard Test Method for Relative Density (Specific Gravity) and Absorption of Coarse Aggregate AASHTO: Standard Method of Test for Specific Gravity and Absorption of Coarse Aggregate	C127 - 15	T 85-14
Standard Practice for Reducing Samples of Aggregate to Testing Size	C702 - 11	T 248 - 14
Standard Practice for Sampling Aggregates	D75 - 14	T 2 - 91 (15)
Standard Test Method for Resistance of Coarse Aggregate to Degradation by Abrasion in the Micro-Deval Apparatus	D6928 - 17	T 327 - 12

3.4.2 Specific Gravity and Absorption

The absorption of aggregates is significant especially with respect to durability and resistance to harsh freeze-thaw deterioration. The specific gravity and absorption tests were used to measure the oven-dry specific gravity, saturated-surface-dry specific gravity, apparent specific gravity, and absorption of the aggregate specimens. Aggregate samples consisted of particles larger than the No. 8 sieve and were submerged in water for 24 hours so that they reached saturation. The aggregate samples were removed from the water and an absorbent towel was used to dry the surface of the aggregate particles so that they were in the saturated-surface-dry condition. The aggregate sample was then weighed to get the saturated-surface-dry weight. Next, the sample was placed into a wire basket and weighed while submerged in water to obtain the weight of the sample while in water. The sample was then dried to constant mass in the oven at 230 °F and the weight of the dry sample was recorded. The oven-dry specific gravity, G_s (OD), the saturated-surface-dry specific gravity, G_s (SSD), and the apparent specific gravity, G_s (Apparent), were then calculated. Absorption was also calculated from these measurements.

3.4.3 Micro-Deval Abrasion Test

The Micro-Deval abrasion test measures the resistance of aggregates to abrasion. As a brief overview of the test, a specimen is placed into a container that also includes stainless steel balls and water. The container is placed into the Micro-Deval apparatus and revolved to produce an abrasive charge (shown in Figure 3.6). Because of the impact of the abrasive charge, the sample degrades. Water is used in the test because many aggregates are more susceptible to

abrasion when wet than dry. The Micro-Deval abrasion test was run on both coarse aggregates and fine aggregates. The steps for the Micro-Deval abrasion test are explained for the coarse aggregate specimens. The steps for the fine aggregate specimens are the same except that the sieve sizes and masses retained, volume of water, mass of the steel balls, and number of revolutions are different from those used for coarse aggregates.

(a) Soaking Micro-Deval test specimen

(b) Micro-Deval test container and charge

(c) Loading aggregate and charge

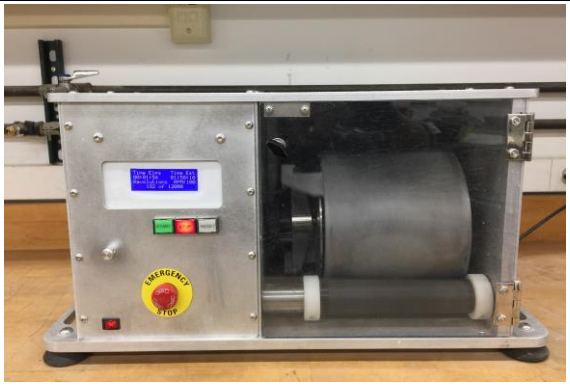

(d) Running Micro-Deval test

Figure 3.6: Micro-Deval abrasion test apparatus.

Chapter 4

Analysis of Laboratory Test Results on Base Aggregate Materials

This chapter presents the results of the laboratory testing program on the base layer aggregate materials collected from the investigated pavement sections. Laboratory test results are analyzed and critically evaluated.

4.1 Particle Size Distribution

Figure 4.1 depicts the particle size distribution of the investigated RCA and CA base materials as well as the historical WisDOT base course layer specifications, including the current lower and upper WisDOT specifications for the particle size distribution of 1¼ in dense graded base course aggregate layers (Section 305.2.2.1 of WisDOT Standard Specifications for Highway and Structure Construction, 2108). Visual examination of Figure 4.1 shows that the particle size distributions of the aggregate samples are generally within WisDOT specification limits, but partly cross the lower limit boundary towards the fine aggregate fraction. The amount of gravel size particles, sand size fraction, and percent fines of all investigated RCA and CA base materials are summarized in Table 4.1. In order to further evaluate and compare both the RCA and the CA base materials, the fineness modulus (FM) was calculated according to ASTM C125. The larger the FM, the coarser the aggregate is. Another way to evaluate the base aggregate particle size distribution is by using the Grading Number (GN), which is an index introduced to represent the effect of gradation on DCP test results (Dai and Kremer, 2006).

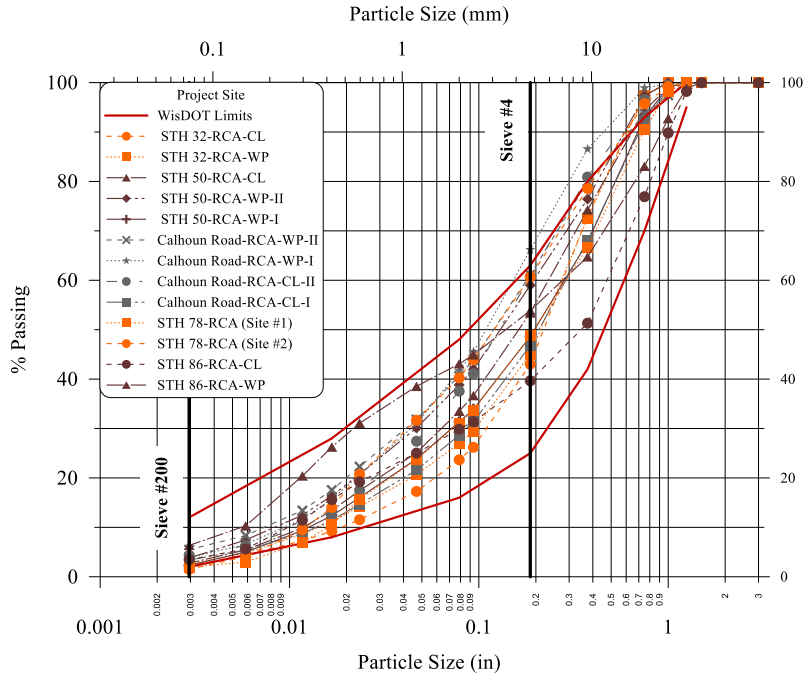

(a) RCA base materials

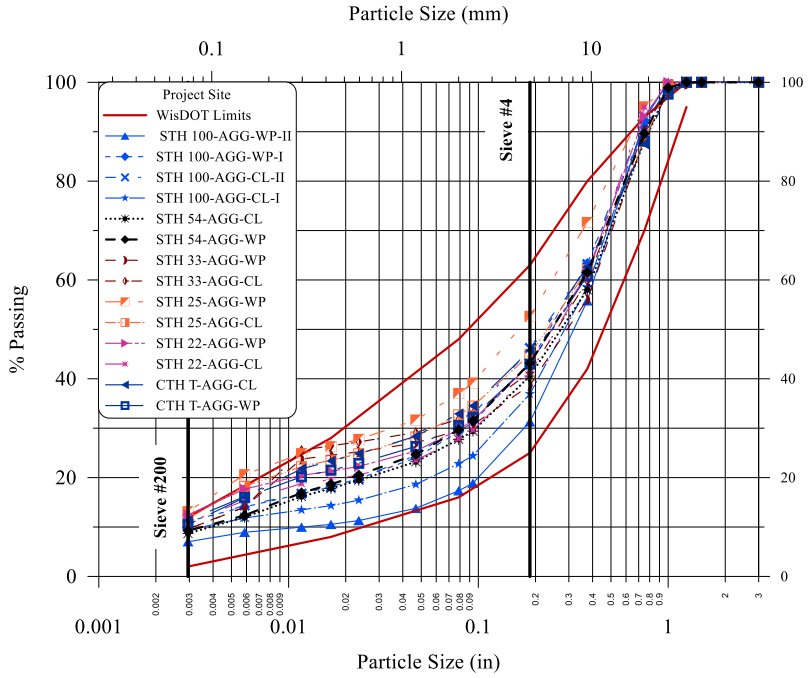

(b) CA base materials

Figure 4.1: Particle size distribution of the investigated RCA and CA base course and the current WisDOT gradation specification limits for the 1¼″ dense graded base course materials.

Table 4.1 presents the fractions of gravel, sand, and fines and the FM of the investigated aggregates. The results are also depicted in Figures 4.2 and 4.3. Inspection of the data presented shows that the RCA base materials contain lower percentages of fines ranging from 1.49 to 6.36 compared with the CA base materials range between 7.02 and 13.1%. On the other hand, the RCA base materials contain larger sand size fraction (30.2 to 62.36%) compared with the CA base materials (24.26 to 39.53%). Such larger amount of fine could allow the RCA base materials to absorb and maintain larger than normal moisture content leading to potential issues and problem in freezing temperatures. With regard to the gravel fraction, the RCA base materials have smaller amount (33.83 to 60.36%) compared with the CA base materials (47.36 to 68.72%). Figure 4.3 presents the calculated Fineness Modulus (FM) and Grading Number (GN) RCA and CA base materials along with the WisDOT limits of 3.96 to 6.1 for FM and 2.5 to 4.2 for GN. The higher the FM values the coarser the material is. Inspection of Table 4.1 and Figure 4.3 shows that the RCA base materials exhibited values ranging from 4.18 to 4.93% with an average of 4.55% compared with range between 4.08 and 5.13% with an average of 4.56% for the CA base materials. The calculated GN for the investigated aggregates are presented in Table 4.1 and Figure 4.3. The maximum value of GN is 7 when 100% of the material passes the sieve No. 200. This represents an extremely fine material (all silt and clay particles). On the other hand, the minimum value of GN is 0 when 0% of the material passes the largest sieve. This indicates a very coarse material. The GN for the RCA base materials varies between 3.07 and 4.13 with an average of 4.13 while the GN for the CA base materials ranges from 3.14 and 3.95 with an average of 3.53. The variation in the FM and GN are depicted in Figure 4.4. In general, both FM and GN values for RCA and CA base materials fell within WisDOT specification limits but the

CA base materials can be characterized as “coarser” when compared with the RCA base materials.

Table 4.1: Particle size characteristics of the investigated base RCA and CA base course.

Aggregate Source		Gravel (%)	Sand (%)	Fine (%)	Fineness Modulus	Grading Number
RCA	STH 78 (Site #1)	51.25	46.84	1.91	4.78	3.48
	STH 78 (Site #2)	39.34	59.17	1.49	4.34	3.90
	STH 32 CL	56.99	40.78	2.23	4.93	3.49
	STH 32 WP	54.94	42.44	2.62	4.80	3.56
	STH 50 CL	46.59	50.66	2.74	4.58	3.71
	STH 50 WP-1	51.39	46.28	2.34	4.70	3.54
	STH 50 WP-2	41.00	55.19	3.81	4.31	3.92
	Calhoun Rd WP I	33.83	62.36	3.81	4.20	4.13
	Calhoun Rd WPII	38.91	55.60	5.49	4.25	3.96
	Calhoun Rd CL I	53.22	43.41	3.37	4.79	3.49
	Calhoun Rd CL II	39.26	56.44	4.31	4.40	3.93
	STH 86 CL	60.36	36.18	3.46	4.91	3.07
	STH 86 WP	46.13	47.51	6.36	4.18	3.70
CA	STH 22 Shawano CL	58.90	30.20	10.90	4.56	3.55
	STH 22 Shawano WP	57.06	30.49	12.46	4.47	3.61
	STH 25 CL	55.11	33.17	11.72	4.39	3.63
	STH 25 WP	47.36	39.53	13.10	4.08	3.95
	STH 33 CL	58.71	31.64	9.65	4.40	3.59
	STH 33 WP-II	61.29	29.15	9.56	4.52	3.45
	STH 54 CL	59.44	31.88	8.68	4.71	3.39
	STH 54 WP	56.85	33.93	9.22	4.61	3.51
	STH 100 CL I	63.06	27.55	9.39	4.88	3.33
	STH 100 CL II	53.78	35.35	10.88	4.53	3.62
	STH 100 WP I	56.73	32.13	11.14	4.60	3.54
	STH 100 WP II	68.72	24.26	7.02	5.13	3.14
	CTH T CL	54.24	34.40	11.40	4.41	3.62
	CTH T WP	57.01	32.51	10.48	4.51	3.52

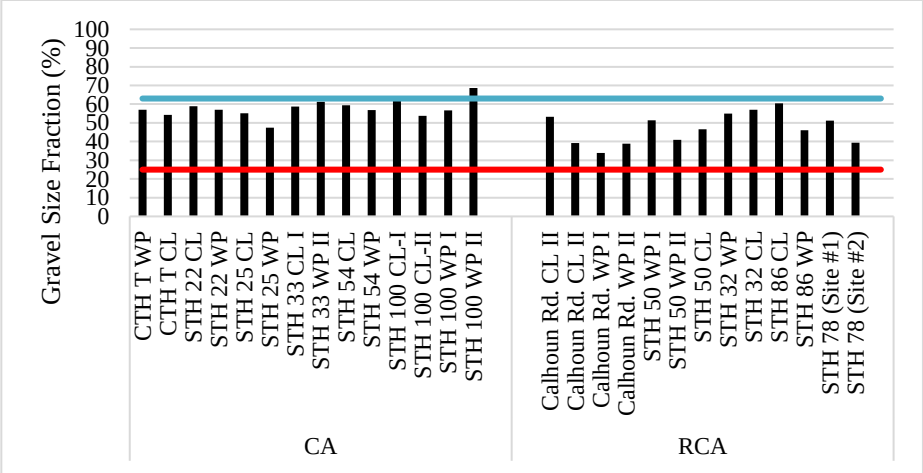

(a) Gravel fraction composition

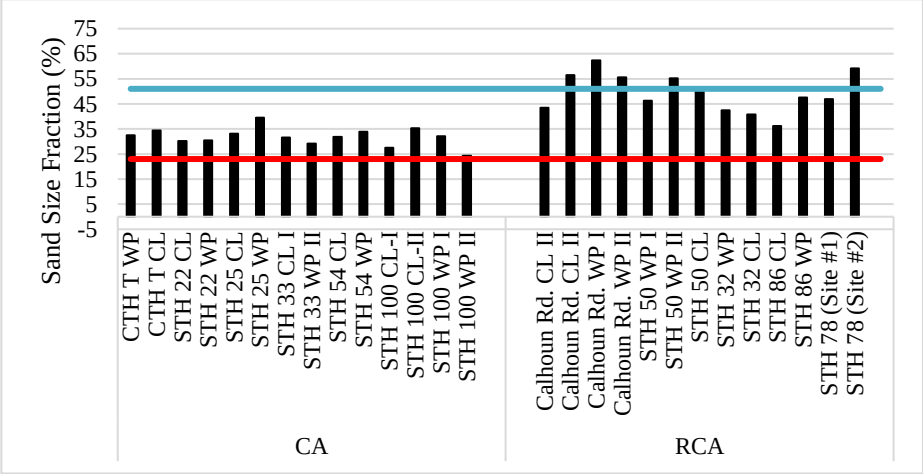

(b) Sand fraction composition

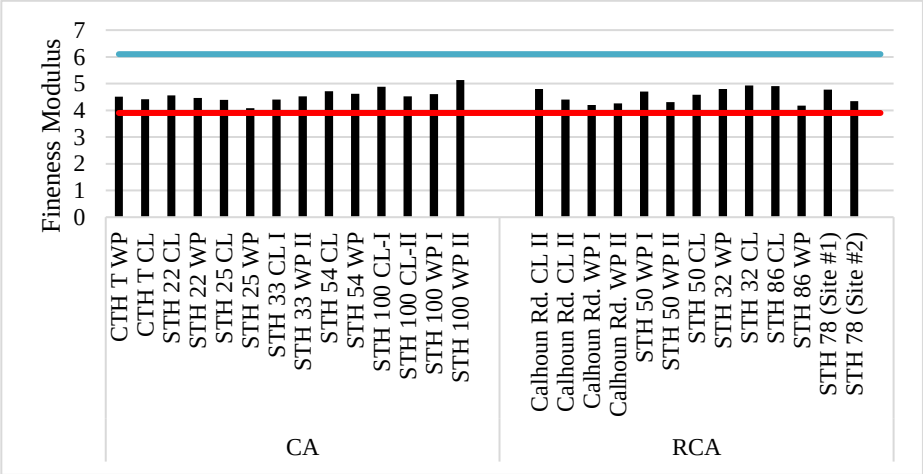

(c) Fines fraction composition

Figure 4.2: Particle size characteristics the investigated RCA and CA base materials.

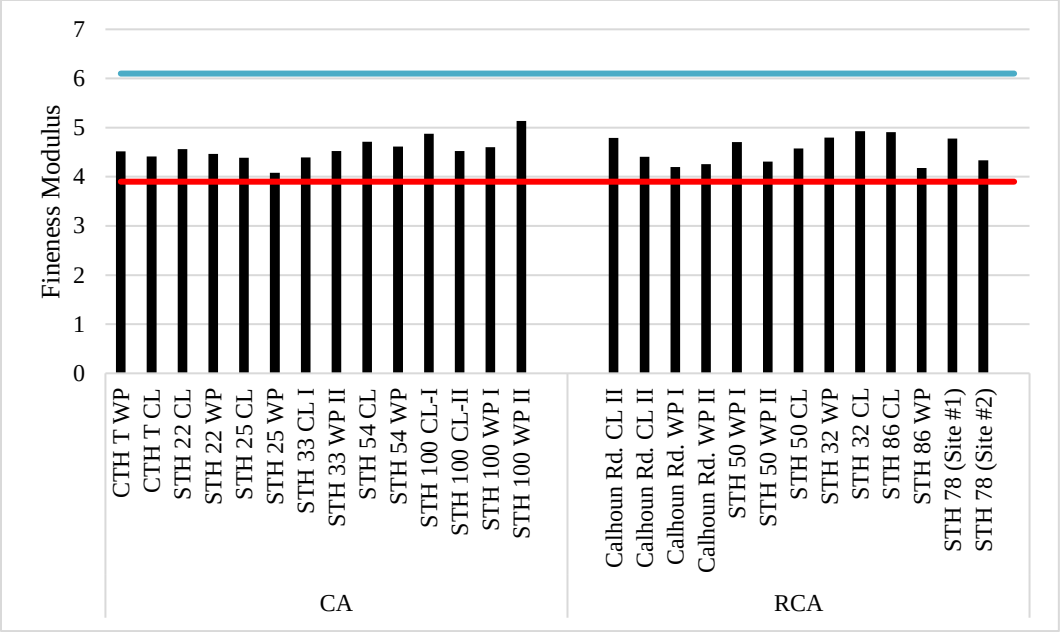

(a) Fineness Modulus (FM) of the investigated aggregates (WisDOT limits are 3.96 to 6.1)

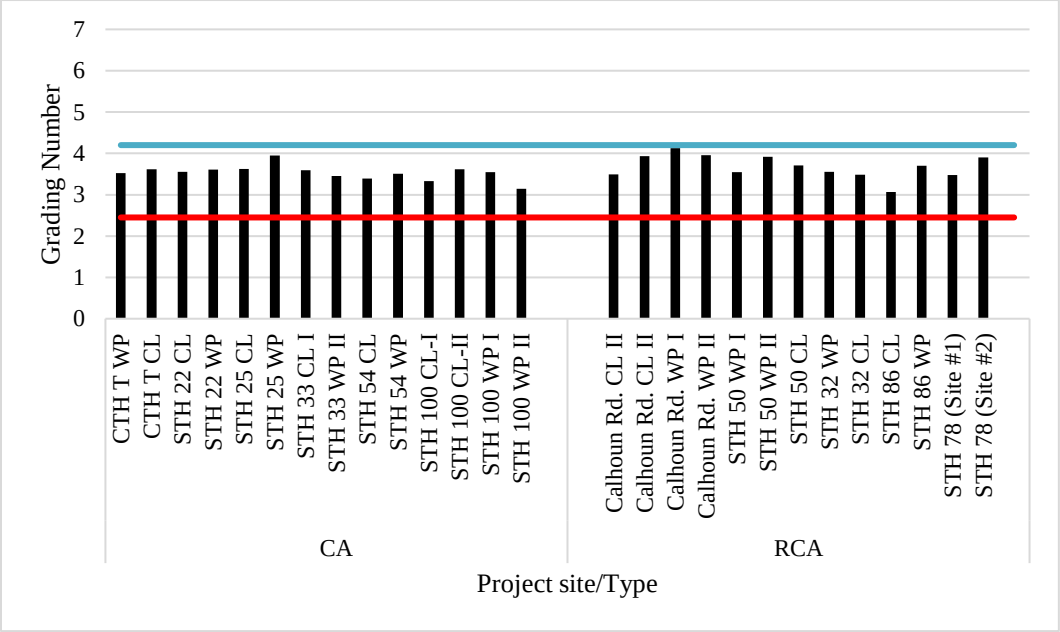

(a) Grading Number (GN) of the investigated aggregates (WisDOT limits are 2.5 to 4.2)
(b)

Figure 4.3: FM and GN of the investigated RCA and CA base materials.

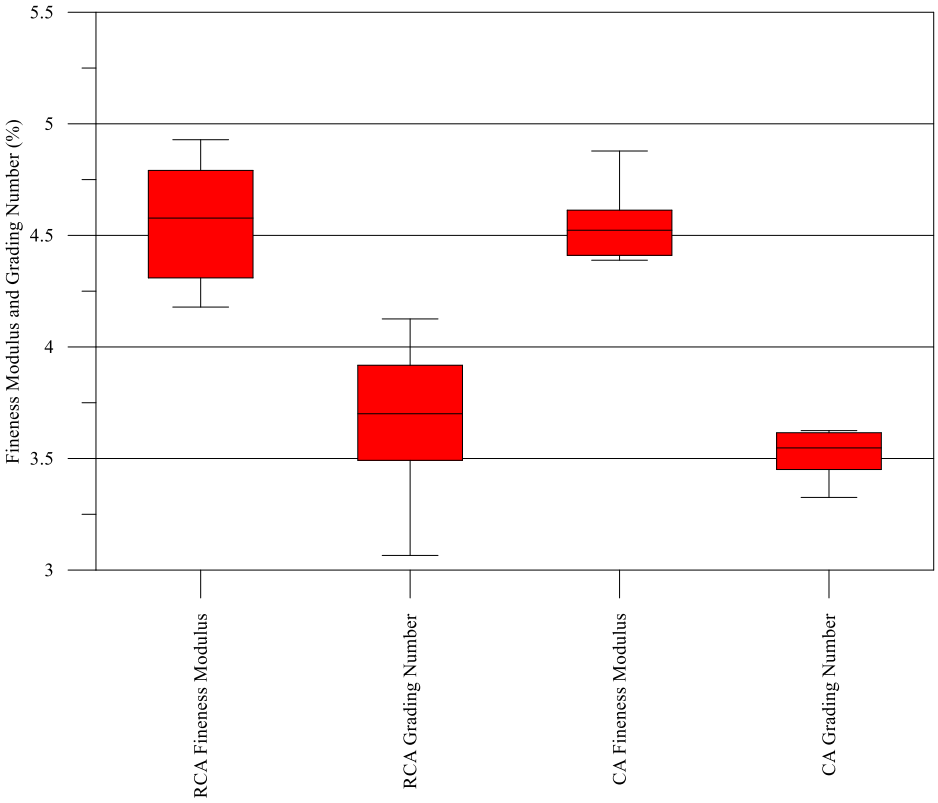

Figure 4.4: Box-Whisker plot of the FM and GN for RCA and CA base layer materials.

4.2 Durability Tests of the Investigated Aggregates

4.2.1 Specific Gravity and Absorption

The oven-dry (OD) specific gravity, saturated-surface dry (SSD) specific gravity, and apparent specific gravity of the coarse fraction of the investigated RCA and CA are summarized in Table 4.2 and depicted in Figures 4.5 and 4.6. The results of the oven dry specific gravity ranged from 2.12 to 2.44 with an average of 2.30 for the RCA base materials and from 2.49 to

2.69 for the CA base materials with an average of 2.62. In general, RCA base materials possessed low specific gravity values when compared with CA base materials.

The absorption test results summarized in Table 4.2 and Figures 4.6-4.7 showed the investigated RCA base materials exhibited a range from 2.7% to 8.2% with an average of 4.6% indicating relatively high absorption characteristics. On the other hand, the CA base materials showed an absorption range from 1.41 to 3.43% with an average of 2.13%. The analysis by Tabatabai et al. (2013) of various Wisconsin coarse aggregates indicated that the mean absorption value is 1.71%.

Table 4.2: Results of specific gravity and absorption tests on the investigated RCA and CA base materials (coarse fraction).

Aggregate Source		Specific Gravity			Absorption
		OD	SSD	Apparent	
RCA	STH 78 (Site #1)	2.19	2.37	2.67	8.20
	STH 78 (Site #1) CL	2.27	2.42	2.67	6.63
	STH 78 (Site #1) WP	2.24	2.40	2.67	7.19
	STH 78 (Site #2)	2.32	2.42	2.58	4.40
	STH 32 CL	2.12	2.23	2.39	5.36
	STH 32 WP	2.20	2.34	2.58	6.83
	STH 50 CL	2.38	2.47	2.61	3.80
	STH 50 WP	2.26	2.34	2.46	3.60
	Calhoun Rd WP I	2.40	2.47	2.57	2.67
	Calhoun Rd WPII	2.42	2.49	2.59	2.76
	Calhoun Rd CL I	2.34	2.41	2.51	3.04
	Calhoun Rd CL II	2.21	2.28	2.38	3.22
	STH 86 CL	2.44	2.51	2.62	2.80
	STH 86 WP	2.42	2.50	2.63	3.27
CA	STH 22 Shawano CL	2.69	2.74	2.82	1.61
	STH 22 Shawano WP	2.69	2.74	2.82	1.61
	STH 25 CL	2.51	2.58	2.71	3.02
	STH 25 WP	2.56	2.64	2.76	2.80
	STH 33 CL	2.49	2.58	2.73	3.43
	STH 33 WP	2.53	2.61	2.75	3.12
	STH 54 CL	2.69	2.73	2.81	1.61
	STH 54 WP	2.69	2.73	2.80	1.41
	STH 100 CL I	2.63	2.68	2.78	2.11
	STH 100 CL II	2.63	2.69	2.79	2.11
	STH 100 WP I	2.64	2.69	2.78	1.86
	STH 100 WP II	2.65	2.70	2.79	1.90
	CTH T CL	2.65	2.69	2.76	1.50
	CTH T WP	2.64	2.68	2.76	1.70

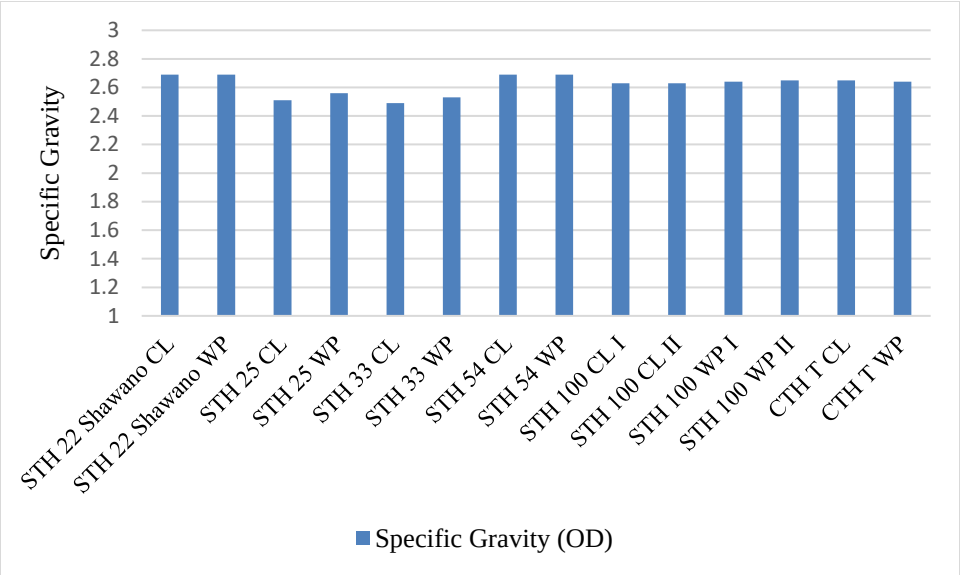

(a) Specific gravity

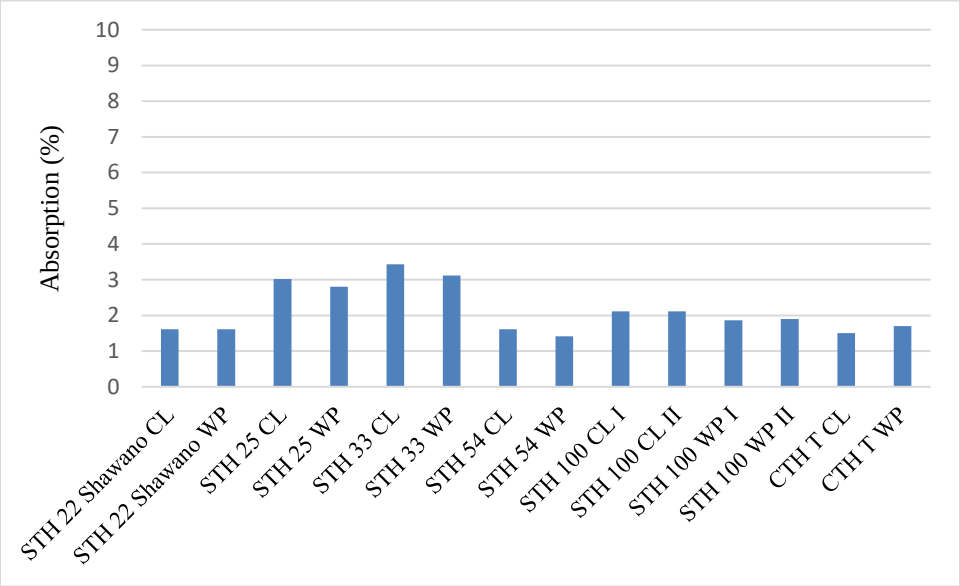

(b) Absorption

Figure 4.5: Specific gravity and absorption test results for investigated CA base Materials.

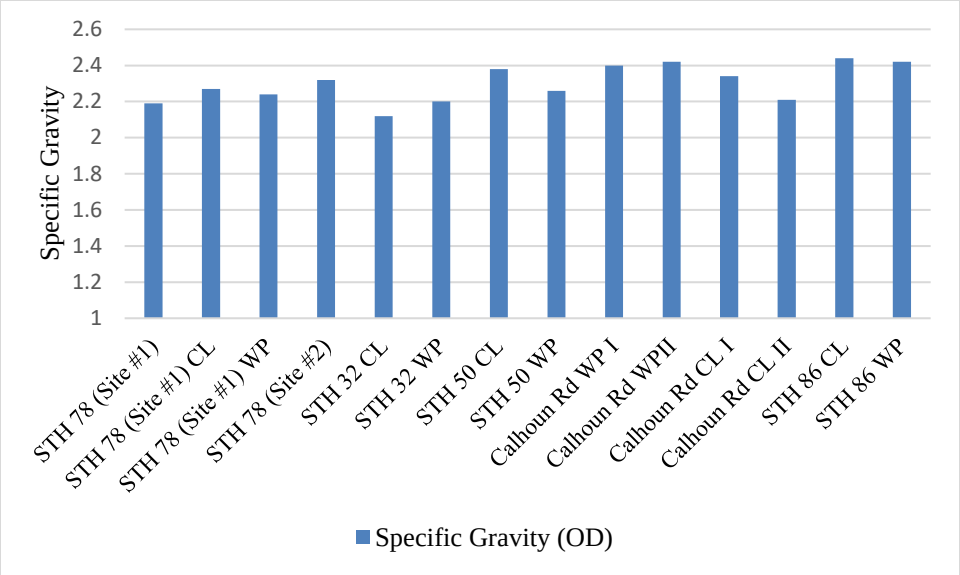

(a) Specific gravity

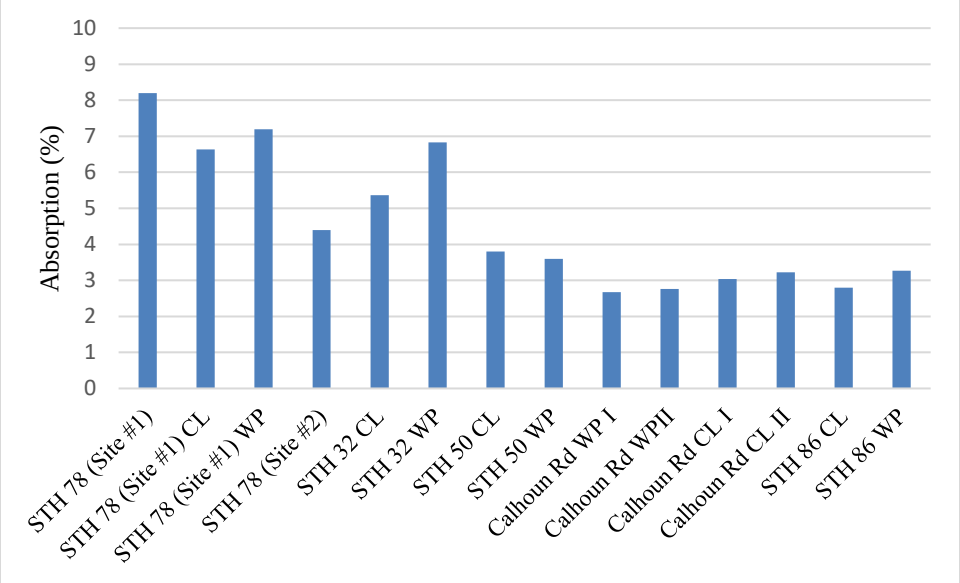

(a) Absorption

Figure 4.6: Specific gravity and absorption test results for investigated RCA base Materials.

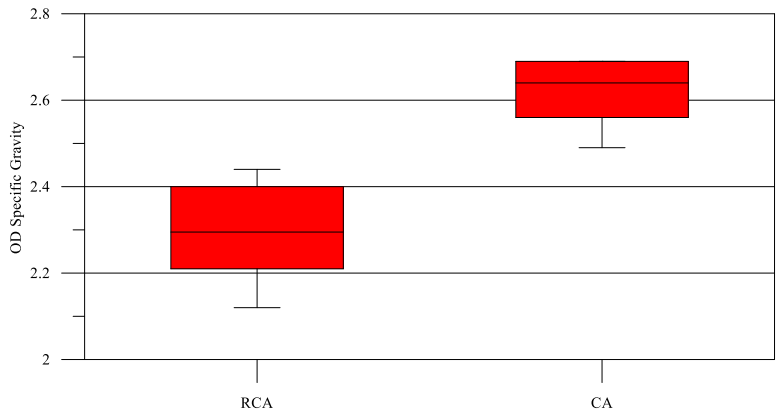

(a) Specific gravity

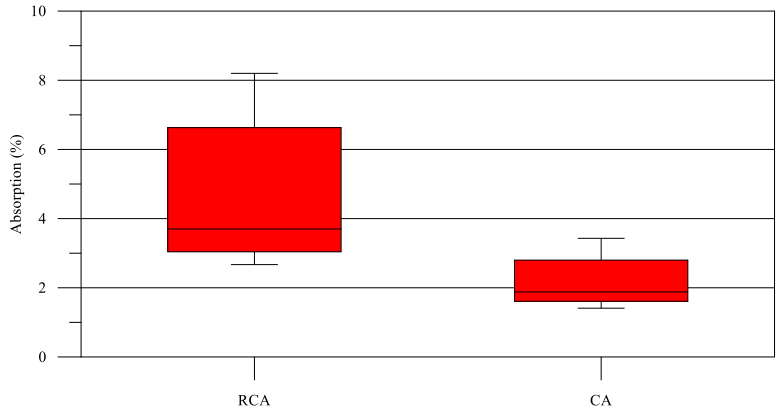

(b) Absorption

Figure 4.7: Box-Whisker plot of specific gravity and absorption test results for investigated RCA and CA base Materials.

4.2.2 Micro-Deval Abrasion

The mass loss (expressed as a percentage) by Micro-Deval abrasion of the investigated RCA and CA base materials are summarized in Table 4.3 and depicted in Figures 4.8 and 4.9. Inspection of test results shows that the RCA base materials exhibited mass loss, in general, comparable with that exhibited by the CA base materials. The mass loss exhibited by the RCA base materials varies between 13.42% and 24.85% with an average of 18%. On the other hand,

the mass loss for the CA base materials ranged from 13.73% to 26.76% with an average of 18.58%

Table 4.3: Mass loss of coarse and fine aggregates from the Micro-Deval abrasion test.

Base Layer Aggregate Source		Mass Loss (%)
RCA	STH 78 (Site #1)	24.85
	STH 78 (Site #2)	24.19
	STH 32 CL	17.84
	STH 32 WP	16.73
	STH 50 CL	16.97
	STH 50 WP	19.53
	Calhoun Rd Wheel Path I	13.42
	Calhoun Rd Wheel Path II	16.74
	Calhoun Rd Centerline I	19.25
	Calhoun Rd Centerline II	17.96
	STH 86 CL	14.11
	STH 86 WP	14.46
CA	STH 22 Shawano CL	17.86
	STH 22 Shawano WP	17.60
	STH 25 CL	18.26
	STH 25 WP	19.33
	STH 33 CL	26.72
	STH 33 WP	26.76
	STH 54 CL	13.73
	STH 54 WP	14.91
	STH 100 CL I	20.95
	STH 100 CL II	17.13
	STH 100 WP I	16.53
	STH 100 WP II	15.07
	CTH T CL	17.82
	CTH T WP	17.45

Tabatabai et al. (2013) conducted an analysis on Micro-Deval test results of various Wisconsin coarse aggregates. The mean Micro-Deval mass loss was found to be 15.05% for coarse aggregates. Eight of the RCA and eleven of the CA investigated base materials exhibited mass loss that exceeded this average.

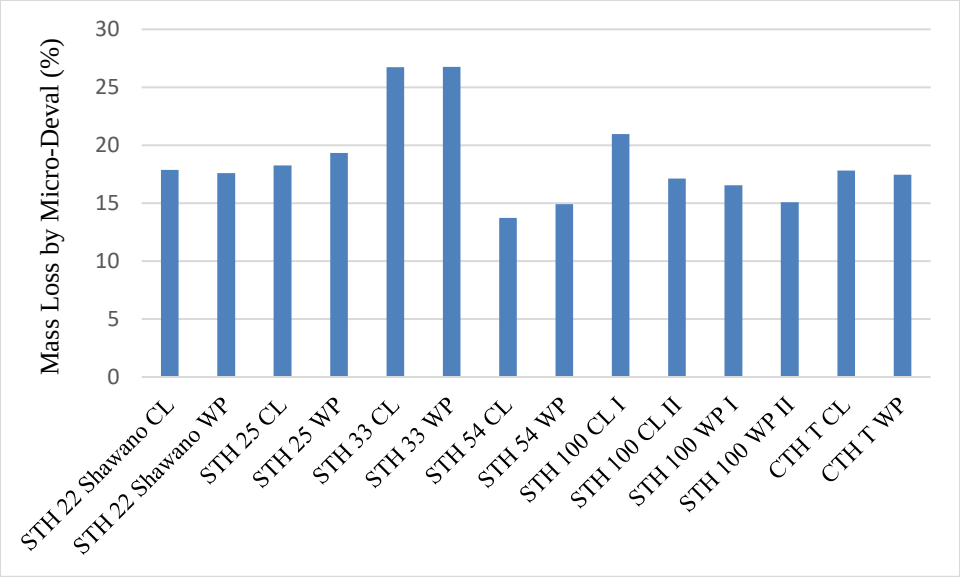

(a) CA base materials

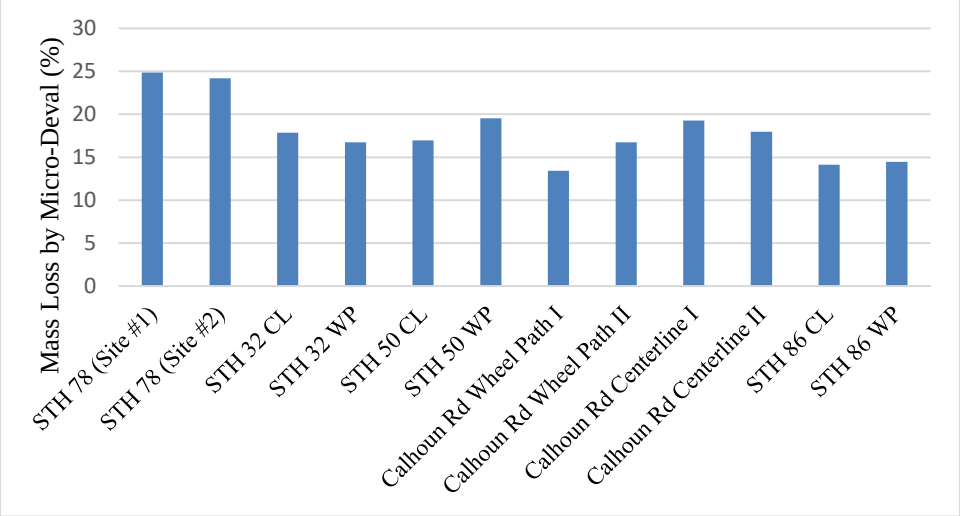

(b) RCA base materials

Figure 4.8: Mass loss of the RCA and CA base materials to the Micro-Deval test.

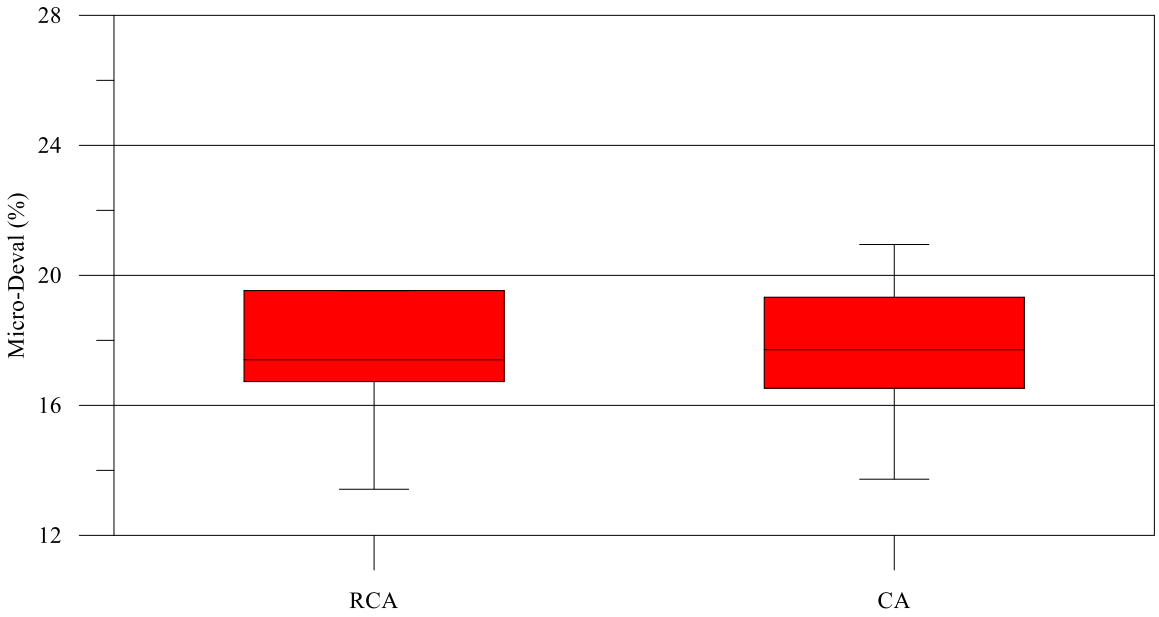

Figure 4.9: Box-Whisker plot of the mass loss of the RCA and CA base materials to the Micro-Deval test.

Chapter 5

Analysis of Field Test Results on RCA and CA Base Layers

This chapter presents the results of the field testing program on the RCA and CA base layers of the investigated pavement sections. Field test results are analyzed and critically evaluated.

5.1 Dynamic Cone Penetration Test

Multiple DCP tests were conducted at each pavement test site on both the wheel path and the lane center whenever possible. DCP test results were not possible to obtain from the RCA base layer at STH 78 between Merrimac and Prairie du Sac due to refusal. Significant number of drops (~270 drops per test) were performed during few attempts with on penetration recorded. No DCP tests were performed on the RCA base layer of STH 86 in Tomahawk due to field conditions. The results of the DCP tests on the investigated RCA base layer of STH 50 in Kenosha are shown in Figure 5.1. The penetration rate profile in in/blow is presented with depth. Figure 5.1a indicates a very high resistance to penetration (<0.16 in/blow) through the 10-inch RCA base layer (at the lane center) followed by less penetration resistance (> 1.25 in/blow) when the DCP went through the subgrade soil. The DCP test was stopped at about 5 inches of depth due to penetration refusal at the wheel path of the RCA base layer.

The DCP tests on the RCA and CA base layers were used to estimate the CBR variation with depth using Webster et al. (1992, 1994) formula:

$$CBR = \frac{292}{DCPI^{1.12}}$$

where DCPI is penetration index in mm/blow. The estimated CBR are then averaged over one inch of base layer thickness to provide profiles of CBR with depth, as shown in Figure 5.1c for

the RCA base layer of STH 50 in Kenosha. Inspection of this figure demonstrates the variability in RCA base material strength with depth as well as between wheel path and lane center locations. The average estimated CBR values for the 10-inch RCA base layer ranges from 93.9% for lane center to 98% for wheel path, indicating high strength base. Such good strength was experienced by the researchers during the penetrations tests and the removal of the RCA samples from the base layer through HMA surface layer coring.

Moreover, the DCP test results are used to predict the distribution of the base layer modulus with depth using the Powell et al. (1984) formula:

$$M_r = 17.58 CBR^{0.64}$$

where Mr is the resilient modulus in MPa. Figure 5.1d depicts the distribution with depth of the estimated RCA base layer modulus for STH 50 in Kenosha. The average estimated layer modulus values for the 10-inch RCA base layer varies between 46.7 ksi for lane center and 48 ksi for wheel path, indicating relatively high layer moduli values.

The results of the DCP tests the corresponding estimated distributions of CBR and layer modulus for the CA base of STH 25 in Maxville are presented in Figure 5.2. Examination of the figure shows lower penetration resistance at the top 2 inches (>0.25 in/blow) of the CA base layer followed by higher penetration resistance (<0.1 in/blow). The average estimated CBR values ranged from 88.5% for lane center to 91.9% with for wheel path. The variation of the corresponding average estimated layer modulus ranged from 44.9 to 46 ksi. The results of the DCP tests and corresponding estimated CBR and layer modulus values for the investigated RCA and CA base layers are presented in Appendix A.

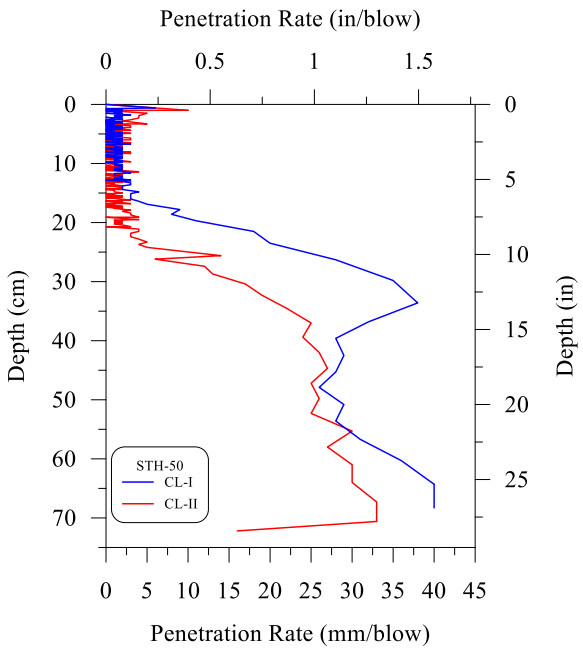

(a) DCP tests STH 50, CL-I, CL-II

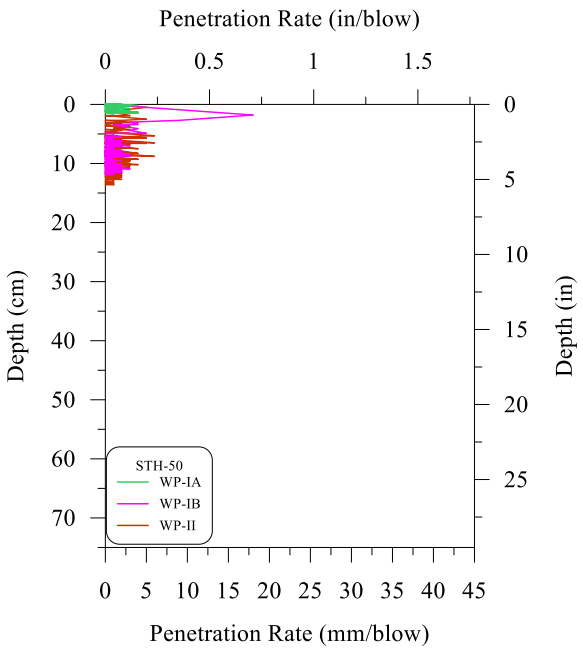

(b) DCP tests STH 50, WP-IA, WP-IB, WP-II

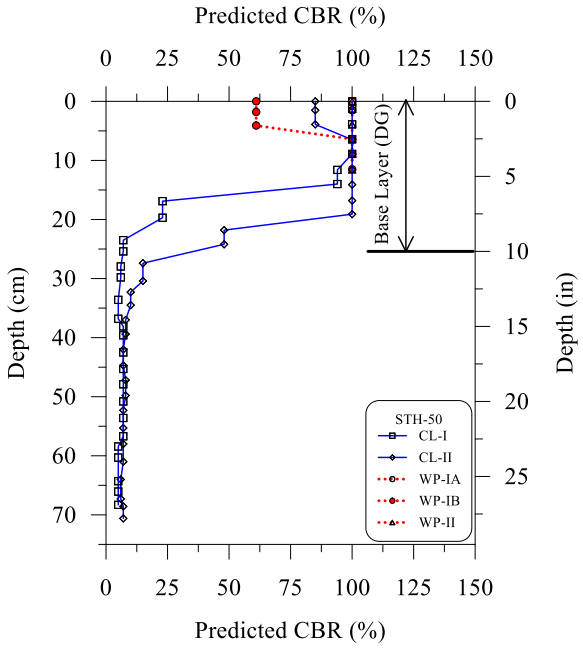

(c) Predicted CBR (%) STH 50

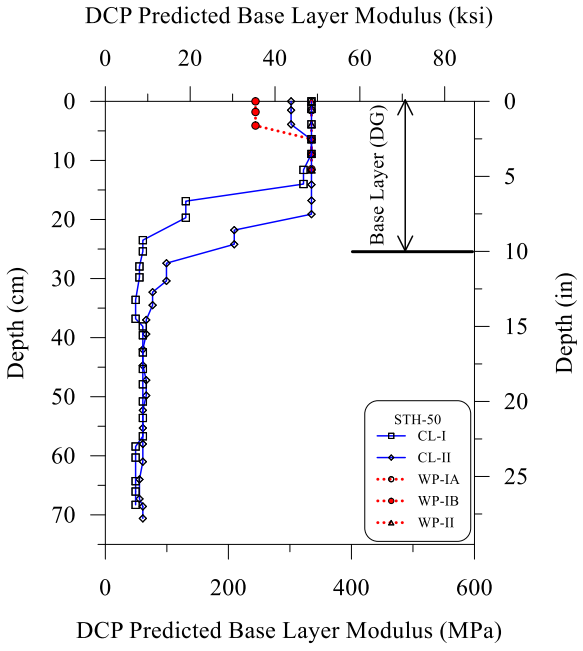

(d) Base layer modulus by DCP test STH 50

Figure 5.1: Penetration resistance with depth from DCP test and distribution with depth of the corresponding estimated CBR and base layer modulus for the RCA Base at STH 50, Kenosha.

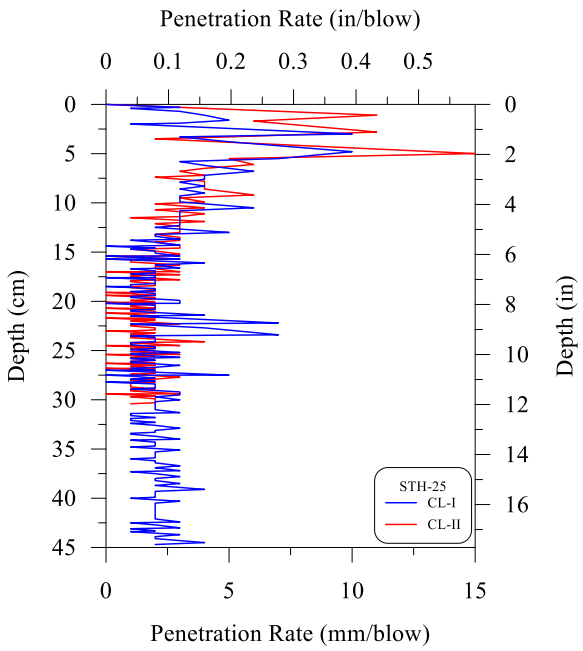

(a) DCP tests STH 25, CL-I, CL-II

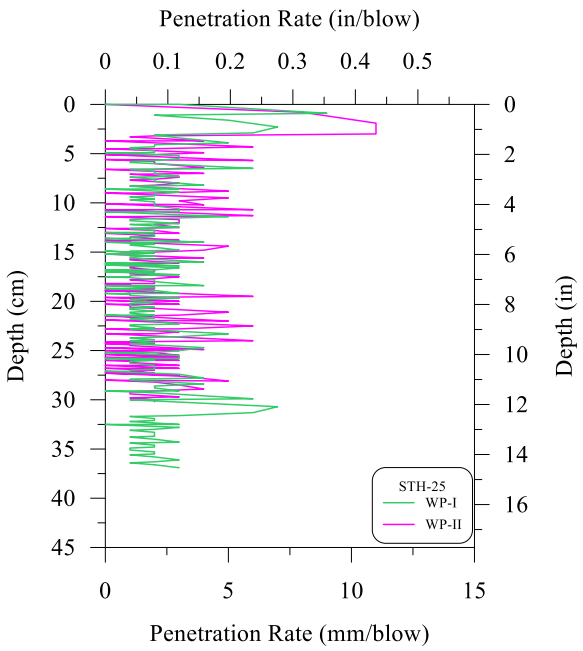

(b) DCP tests STH 25, WP-I, WP-II

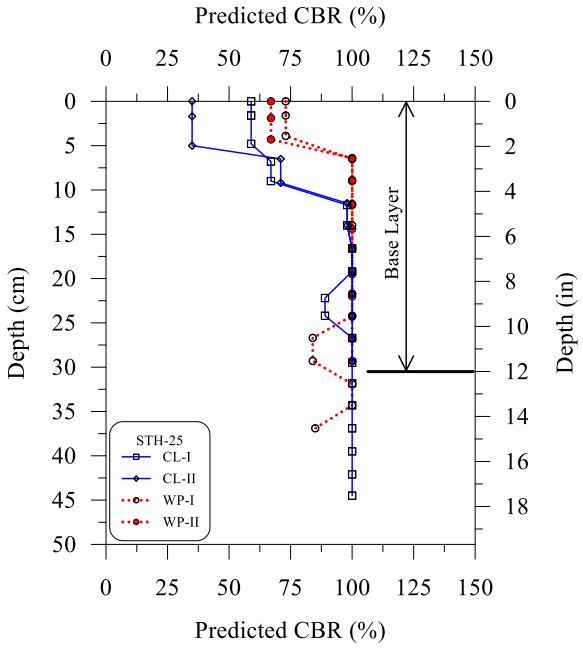

(c) Predicted CBR (%) STH 25

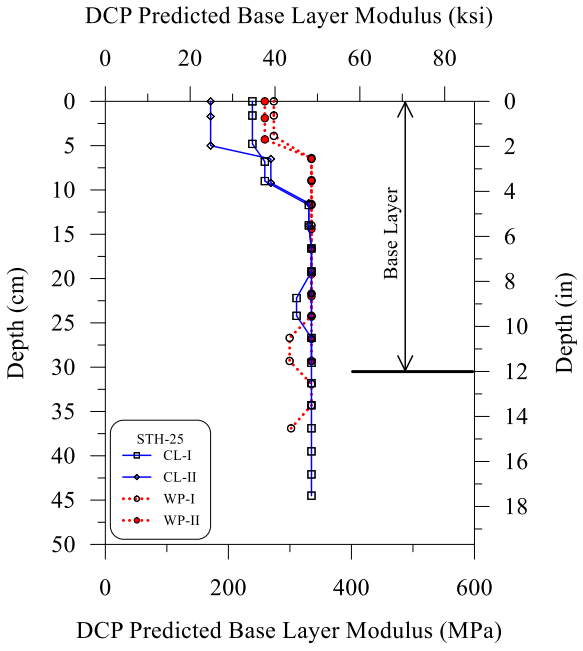

(d) Base layer modulus by DCP test STH 25

Figure 5.2: Penetration resistance with depth from DCP test and distribution with depth of the corresponding estimated CBR and base layer modulus for the CA Base at STH 25, Maxville.

Saeed (2008) investigated the performance related tests of recycled aggregates including RCA for use in unbound pavement layers. In his NCHRP report, Saeed (2008) identified the resilient or compressive strength and California Bearing Ratio among other properties that are relevant to the use of the recycled aggregates in base layers as unbound materials. Therefore, summary and evaluation of the results of the CBR and layer modulus estimated from DCP test on RCA and CA is presented herein. Tables 5.1 and 5.2 present layer thicknesses, layer type (open graded versus dense graded), number of layers, average predicted CBR, and average predicted layer modulus for the investigated RCA and CA base layer, respectively. The test results summarized in Tables 5.1 and 5.2 are presented also in Figures 5.3 and 5.4 for performance comparison between RCA and CA base layers. Visual examination of Figure 5.3 and 5.4 shows that the CBR and layer moduli values of both base layer types are comparable. In order to express this comparison in number, simple statistical analysis was conducted to calculate averages, identify ranges, and determine variation. The results of the statistical analysis are presented in Table 5.3 and Figures 5.5 and 5.6. Examination of the statistical summary shows that the average predicted CBR ranged from 65 to 96% for the RCA bases and between 58% to 90% for the CA bases. The coefficient of variation was higher for the CA bases (from 2 to 46) compared with RCA bases (from 2 to 16). Similar trend is exhibited by average predicted layer modulus with the average range for the RCA bases between 37 and 47 ksi and for the CA bases from 34 and 45 ksi. The CBR and base layer modulus values obtained from the results of the DCP tests indicated in general good properties of the investigated bases. It should be noted that the RCA base layer at STH 100 exhibited low values at localized locations. In general, there was difficulties in retrieving RCA base materials from STH 78 (with higher than normal moisture content), STH 32, and STH 50. The researcher believes that was due to the tufa effect where the

process and formation of Calcium Silicate Hydrates (C-S-H) or secondary rehydration from the fine cementitious material is found on the RCA.

Table 5.1: Summary of RCA base layer thicknesses and the corresponding estimated CBR and layer modulus for the investigated pavements.

Pavement Test Section and Location	Base Course and Subbase Layers							
	WisDOT Plans				Predicted CBR (%)		Predicted M_r (ksi)	
	Pavement Age (year)	Base Layer Thickness (in.)						
		Layer 1	Layer 2	Layer 3	Layer 1	Layer 2	Layer 1	Layer 2
Calhoun CL-I	13	15 RCA (DG)	18 (GB)	NA	49.5	-	31.0	-
Calhoun CL-II					71.2	-	39.1	-
Calhoun WP-I					72.2	-	39.5	-
Calhoun WP-II					65.7	-	37.1	-
STH-32-CL-I	13	4 (OG)	10 (DG)	12-16 (BR)	90.1	98.9	45.5	48.3
STH 32-CL-II					94.2	99.7	46.7	48.5
STH 32-WP-I					93.5	98.1	46.5	48.0
STH 32-WP-II					56.0	94.2	33.5	46.8
STH 50-CL-I	13	10 (DG)	NA	NA	93.9	-	46.7	-
STH 50-CL-II					94.9	-	47.0	-
STH 50-WP-I					96.1	-	47.4	-
STH 50-WP-IB					98.0	-	48.0	-
STH 50-WP-II					96.3	-	47.4	-
STH 78-Site 1	9	4-6 RCA (DG)	8 RCA (3” DG)	NA	DCP Refusal			
STH 78-Site 2	9	4-6 RCA (DG)	8 RCA (3” DG)	NA				
STH 86	14	11	NA	NA	N/A			
STH-100-CL	12	4 (OG)	8.5 RCA (DG)	18 (SC)	36.6	90.5	25.5	45.6
STH-100-WP					35.0	68.4	24.8	38.1

DG = 1 ¼″ Dense Graded, OG = Open Graded, BR = Breaker Run, SC = Select Crushed, GB = Granular Backfill
WP = Wheel Path, CL = Center of Lane

Table 5.2: Summary of CA base layer thicknesses and the corresponding estimated CBR and layer modulus for the investigated pavements.

Pavement Test Section and Location	Base Course and Subbase Layers							
	WisDOT				Predicted CBR (%)		Predicted M_r (ksi)	
	Pavement Age	Base Layer Thickness (in.)						
		Layer 1	Layer 2	Layer 3	Layer 1	Layer 2	Layer 1	Layer 2
CTH-T-CL-I	11	6	8 (BR)	NA	49.6	53.9	31.0	32.7
CTH-T-CL-II					65.3	60.9	37.0	35.4
CTH-T-WP-I					67.3	53.1	37.7	32.4
CTH-T-WP-II					73.2	84.7	39.8	43.7
STH-25-CL-I	14	12 (DG)	NA	NA	88.5	-	44.9	-
STH-25-CL-II					90.8	-	45.7	-
STH-25-WP-I					91.9	-	46.0	-
STH-25-WP-II					89.3	-	45.2	-
STH-33-CL-I	11	9 (DG)	12 (SC)	NA	77.1	65.1	41.1	36.9
STH-33-CL-II					84.8	66.6	43.7	37.5
STH-33-CL-III					76.0	60.4	40.8	35.2
STH-33-WP-I					67.6	68.8	37.8	38.2
STH-33-WP-II					74.5	68.2	40.2	38.0
STH-33-WP-III					59.8	57.2	35.0	34.0
STH-22-Shawano-CL-I	22	13 (DG)	NA	NA	85.7	-	44.0	-
STH-22-Shawano-CL-II					78.3	-	41.5	-
STH-22-Shawano-WP-I					70.1	-	38.7	-
STH-22-Shawano-WP-II					78.2	-	41.5	-
STH-54-CL-I	10	14 (DG)	30 (SC)	NA	81.2	-	42.5	-
STH-54-CL-II					86.0	-	44.1	-
STH-54-WP-I					83.6	-	43.3	-
STH-54-WP-II					37.7	-	26.0	-
STH-100-CL	12	4 (OG)	8.5 (DG)	18 (SC)	36.6	90.5	25.5	45.6
STH-100-WP					35.0	68.4	24.8	38.1
STH 59	16	8	15 (BR)					

DG = 1 ¼″ Dense Graded, OG = Open Graded, BR = Breaker Run, SC = Select Crushed, GB = Granular Backfill, SB = Select Borrow, WP = Wheel Path, CL = Center of Lane

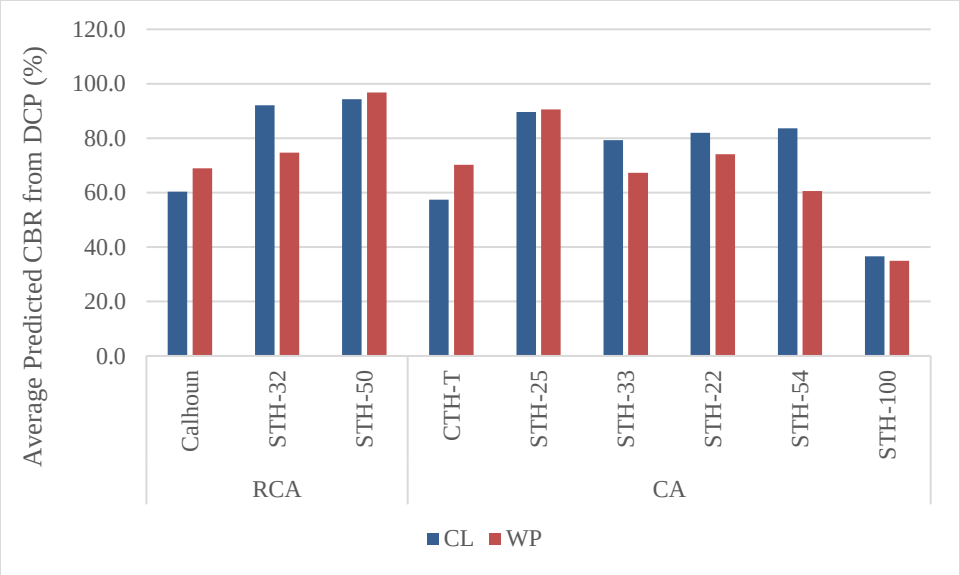

Figure 5.3: Comparison of the average predicted CBR from DCP for the RCA and CA base layers of the investigated pavements.

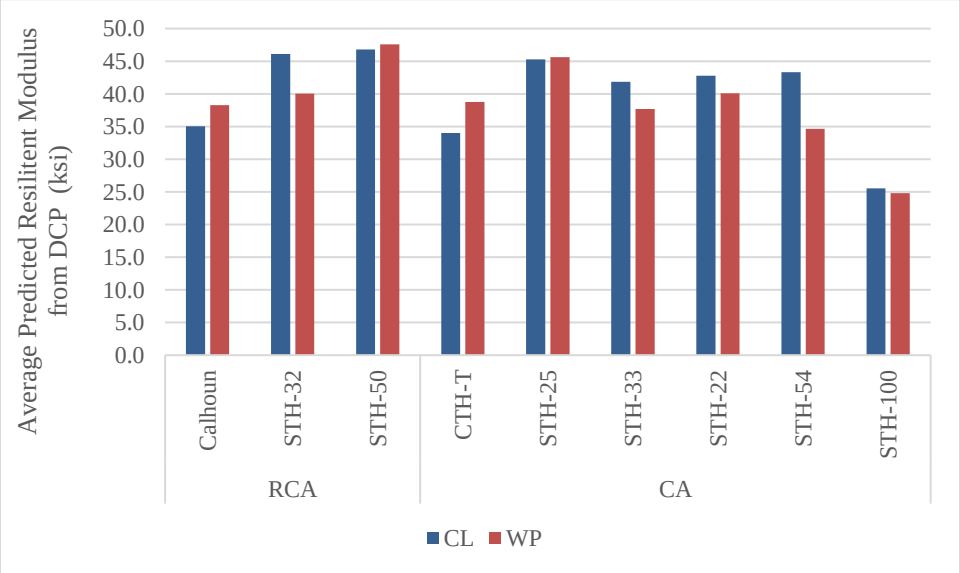

Figure 5.4: Comparison of the average predicted layer modulus from DCP for the RCA and CA base layers of the investigated pavements.

Table 5.3: Statistical summary of predicted CBR and layer modulus of the RCA and CA base layer materials

Base Layer Material	Test Pavement Location	Predicted CBR (%)				Layer Modulus (ksi)			
		Average	Min.	Max.	COV (%)	Average	Min.	Max.	COV (%)
RCA	Calhoun	65	50	72	16	37	31	39	11
	STH-32	91	56	100	16	45	34	49	11
	STH-50	96	94	98	2	47	47	48	1
	STH-78	Refusal							
	STH-86	N/A							
CA	CTH-T	64	50	85	18	36	31	44	12
	STH-25	90	88	92	2	45	45	46	1
	STH-33	69	57	85	12	38	34	44	7
	STH-22	78	70	86	8	41	39	44	5
	STH-54	72	38	86	32	39	26	44	22
	STH-100	58	35	91	46	34	25	46	30

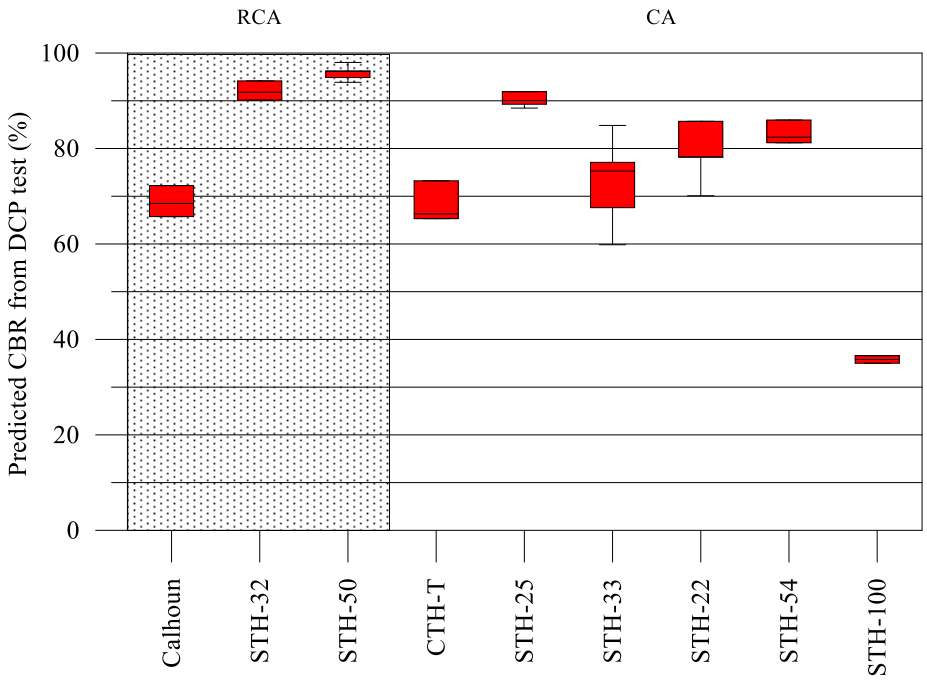

Figure 5.5: Box-Whisker comparison of the average predicted CBR values from DCP tests for RCA and CA base layers for the investigated pavement.

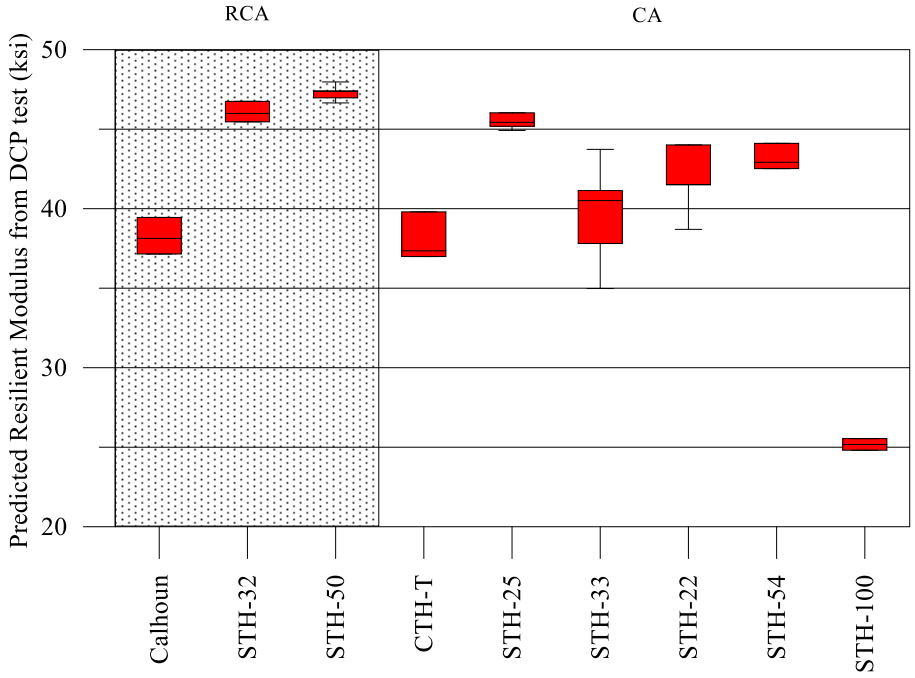

Figure 5.6: Box-Whisker comparison of the average predicted layer modulus values from DCP tests for RCA and CA base layers for the investigated pavement.

5.2 Falling Weight Deflectometer

The FWD test data was analyzed using the pavement layer moduli back-calculation software from ERI, Inc. The back-calculation program is widely used to estimate pavement layer moduli from FWD test results, specifically with KUAB FWD machines. In the analysis, the investigated pavements typical sections with the layer thicknesses were obtained from WisDOT project plans, existing soils reports/pavement, and HMA pavement coring by UWM Pavement and Geotechnical Research team. Typical sections of all investigated pavements are presented in Appendix B. All analysis steps necessary to predict layer moduli values were executed. For example, pavement deflections were normalized to the 9,000 lb load and then adjusted for temperature variations measured in the field.

Figure 5.7 depicts the results of the FWD test on 150 ft section on STH 50 in Kenosha with RCA base course layer. The figure presents the variation with distance of the adjusted normalized D_0, the back-calculated layer moduli of the HMA (E_{HMA}) and base layers (E_{base}), and the back-calculated subgrade modulus ($E_{Subgrade}$). Inspection of this figure indicates that D_0 values showed medium variability with distance, with D_0 values ranging between 6.7 and 16.9 mils (COV of 26.6%) with an average of 9.6 mils. The RCA base back-calculated layer modulus (E_{base}) exhibited variability ranging from 22.5 to 42.4 ksi (COV of 19.8%) with an average of 27.3 ksi. For the sake of comparison, Figure 5.8 presents the results of the FWD test on a 170 ft section on STH 25 in Maxville with CA base course layer. The FWD test was conducted every 10 ft on the right wheel path and on the lane center. The results of Figure 5.8 show that D_0 variability with distance is comparable with that measured on STH 50 with RCA base layer, with D_0 values ranging between 7.7 and 13 mils (COV of 15.8%) with an average of 10.2 mils. The

CA base back-calculated layer modulus (E_{base}) exhibited variability ranging from 19.6 to 93.9 ksi (COV of 39.4%) with an average of 46 ksi. The CA back-calculated base layer modulus for STH 25 showed higher average (46 ksi) compared with the RCA back-calculated base layer modulus for STH 50.

The variation of the deflection under the loading plate (D_0) for all investigated HMA investigated pavements with RCA and CA base layers is presented in Table 5.4 and depicted in Figures 5.9 and 5.10. The summary of test results is for all test sections performed for the same pavement since there are more than one test section conducted per pavement. The variation of the adjusted normalized, D_0 average range was between 5.5 and 9 mils (COV from 20.5 to 36.7%) for the pavements with RCA base layer compared with 8.5 and 13.8 (COV from 15.4 to 21.4%) mils for the pavements with CA base layer. Measured deflection values D_0 indicated variability in all pavement test sections but in general less deflection D_0 values exhibited by pavement test sections with RCA base layers compared with those with CA base layers.

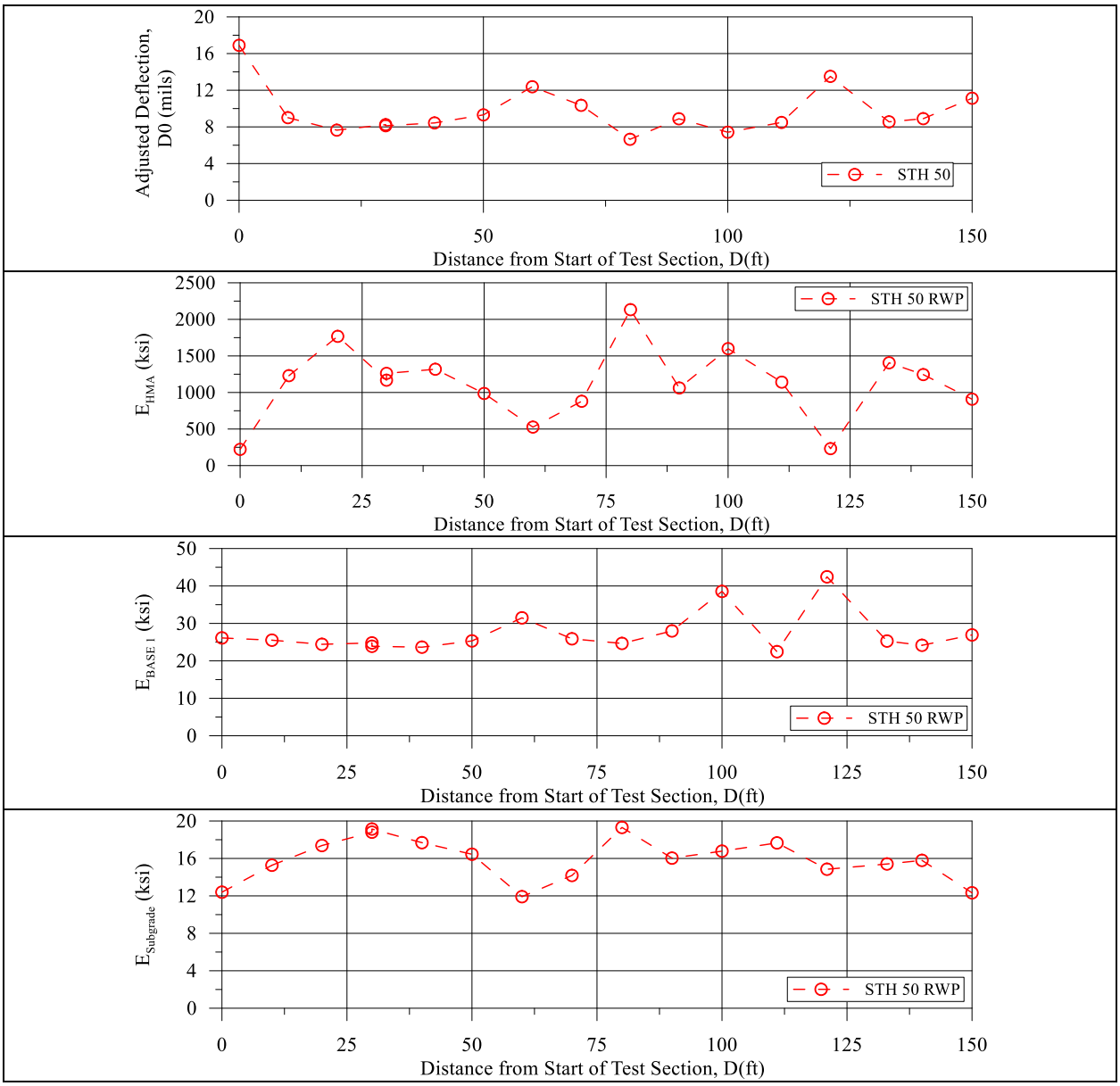

Figure 5.7: Results of FWD tests on a 150 ft section on STH 50 pavement (a) Adjusted deflection under the loading plate (D_0) (corrected for a 9,000 lb drop and temperature), (b) Back-calculated HMA layer modulus, (c) Back-calculated RCA base layer modulus, and (d) Back-calculated subgrade modulus.

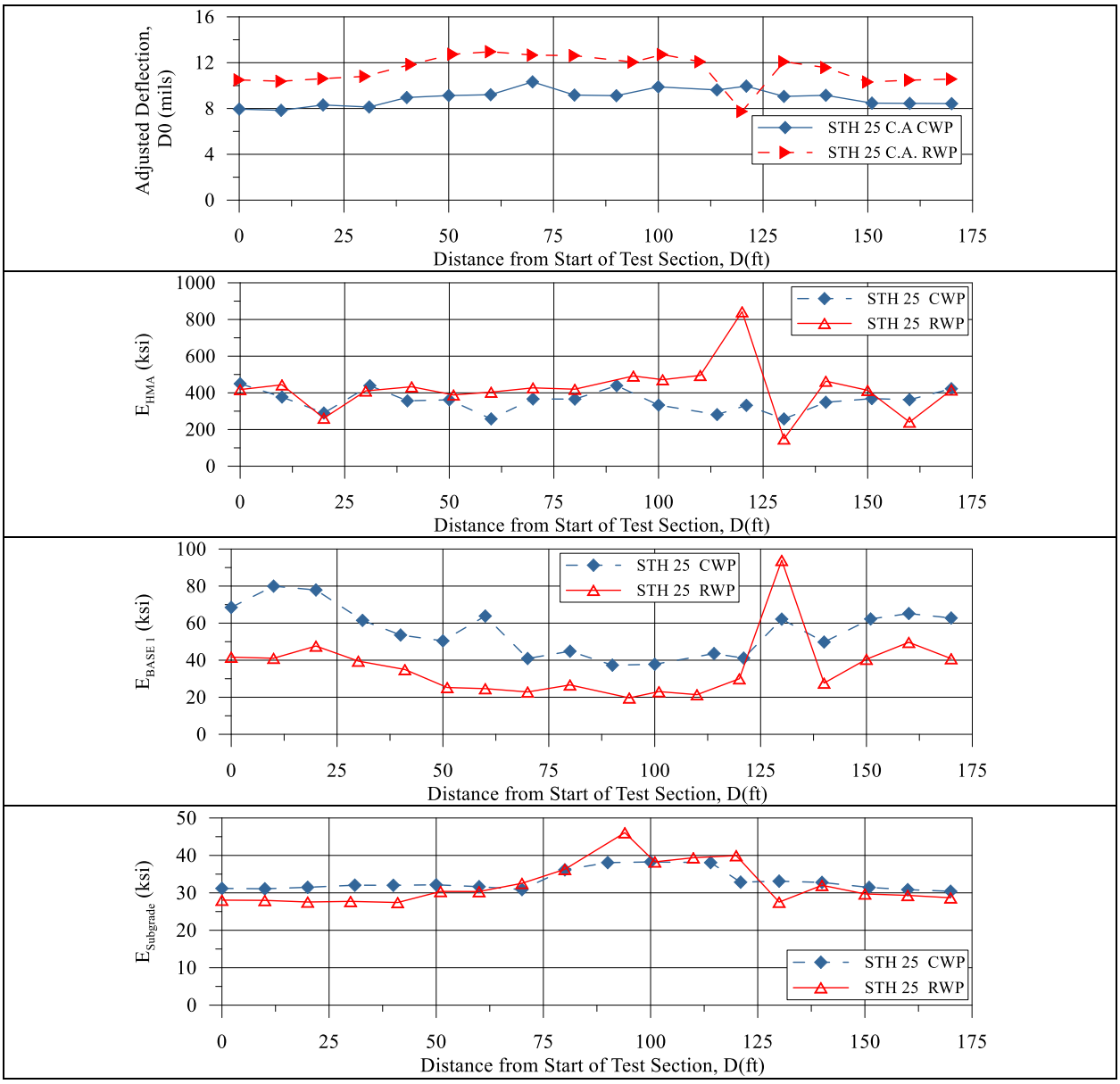

Figure 5.8: Results of FWD tests on a 170 ft section on STH 25 pavement (a) Adjusted deflection under the loading plate (D_0) (corrected for a 9,000 lb drop and temperature), (b) Back-calculated HMA layer modulus, (c) Back-calculated CA base layer modulus, and (d) Back-calculated subgrade modulus.

Table 5.4: Statistical summary of adjusted deflection under loading plate (D_0) normalized to 9,000 lb. load for investigated HMA pavements with RCA and CA base layers.

Pavement Test Section		Average (mils)	COV (%)	Max. (mils)	Min. (mils)
RCA	STH 86	6.9	27.3	10.9	3.6
	STH 50	7.4	36.7	17.0	4.2
	STH 78	9.0	28.9	16.0	4.9
	STH 32	6.2	21.0	10.4	4.1
	Calhoun Rd	5.5	23.4	7.8	4.1
	STH 100	8.5	20.5	14.6	5.8
CA	STH 22-54 Waupaca	13.8	21.4	20.9	9.5
	STH 22 Shawano	10.5	18.6	14.5	7.5
	CTH T	11.4	16.7	14.9	6.6
	STH 25	9.8	18.2	13.0	3.0
	STH 33	12.6	15.4	18.5	7.9
	STH 100	8.5	20.5	14.6	5.8

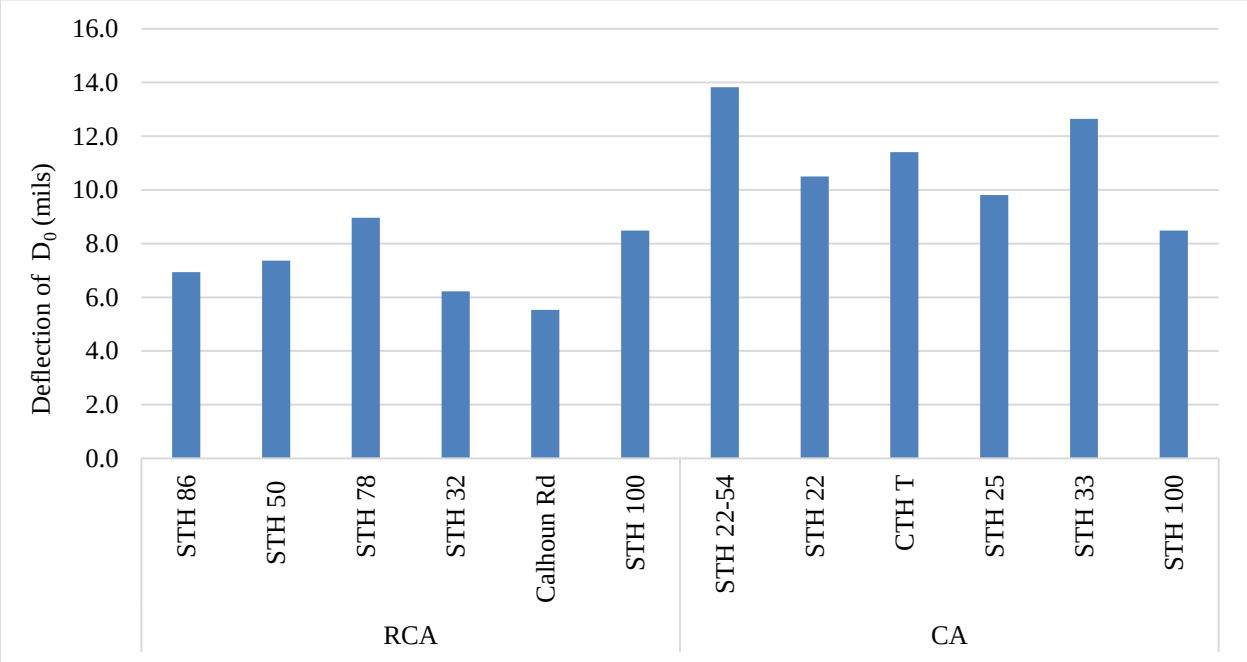

Figure 5.9: Average adjusted deflection under loading plate (D_0) normalized to 9,000 lb load for investigated HMA pavements (average for all test section on each highway pavement).

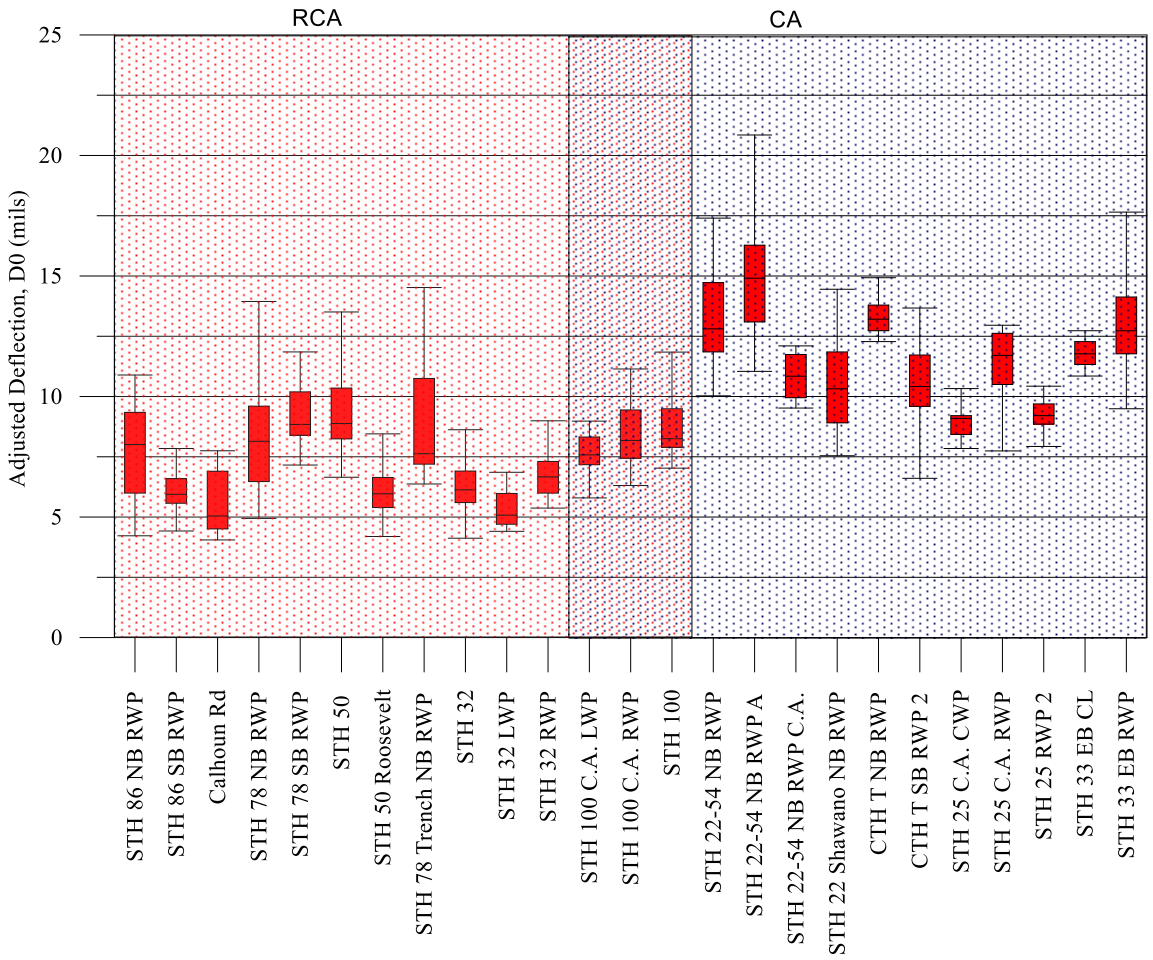

Figure 5.10: Box-Whisker plot of the variability of the adjusted deflection under loading plate (D_0) normalized to 9,000 lb load for the investigated HMA pavements with RCA and CA base layers.

The results of the back-calculation analysis conducted on the FWD results are summarized in Table 5.5. The back-calculated modulus for the HMA layer (E_{HMA}) for all investigated pavements varies significantly among the pavement test sections and within individual pavement sections with COVs ranging between 47% and 1,652% for pavements with RCA base layer compared with 25 to 1,652% for pavements with CA base layers. The variability in EHMA is not necessarily exclusively dependent on the base course layer variability. There are

other factors that may influence the mechanical stability of HMA (mix design, compaction temperature, compaction effort, density) and, most importantly, variability in layer thickness.

Table 5.5: Statistical summary of back-calculated layer moduli for investigated HMA pavements with RCA and CA base layers.

	Pavement Test Section	E_{HMA}				E_{Base1}				E_{Base2}				$E_{subgrade}$			
		Mean (ksi)	COV (%)	Max. (ksi)	Min. (ksi)	Mean (ksi)	COV (%)	Max. (ksi)	Min. (ksi)	Mean (ksi)	COV (%)	Max. (ksi)	Min. (ksi)	Mean (ksi)	COV (%)	Max. (ksi)	Min. (ksi)
RCA	STH-86	5337	47	9000	1001	30	64	92	6	-	-	-	-	24	22	39	17
RCA	STH 50	2300	53	5102	200	39	25	84	15	-	-	-	-	20	19	28	10
RCA	STH 78	421	133	2948	70	981	124	4000	2	49	134	343	4	31	24	52	17
RCA	STH 32	790	47	2008	294	264	74	649	14	143	72	365	17	27	23	41	20
RCA	Calhoun Rd	879	59	2539	368	202	54	391	56	9	28	13	5	39	20	61	28
RCA	STH 100	27	1652	2526	367	175	7	83	2	61	74	210	8	13	27	37	20
CA	STH 22/54	299	25	440	161	29	37	59	13	-	-	-	-	20	15	26	14
CA	STH 22 SHAWANO	850	94	3073	110	27	42	61	10	-	-	-	-	25	20	35	18
CA	CTH T	623	49	2023	84	99	234	1697	11	56	53	145	14	25	17	41	15
CA	STH 25	538	233	9000	149	48	37	94	11	-	-	-	-	33	13	48	27
CA	STH 33	437	20	677	220	20	55	76	8	48	39	125	19	18	23	33	9
CA	STH 100	27	1652	2526	367	175	7	83	2	61	74	210	8	13	27	37	20

The back-calculated moduli for the RCA and CA base layers (E_{Base}) for all investigated pavement test sections are summarized in Table 5.5. There is significant variability of the back-calculated E_{Base} within individual pavement test sections and among pavements. The average back-calculated E_{Base} RCA base layers ranges from 30 to 981 ksi (COV between 7 and 124%), while the average back-calculated E_{Base} CA base layers varies between 20 to 175 ksi (COV between 7 and 234%). Figure 5.11 depicts the average back-calculated layer moduli for the investigated pavements with RCA and CA base layers. Figures 5.12 depicts the back-calculated layer moduli values E_{HMA}, $E_{base\ I}$, and $E_{base\ II}$ for each pavement test section in a box-whisker plot. The plots show the range and median of the back-calculated layer moduli. Comparison of the back-calculated layer moduli values $E_{base\ I}$ for RCA and CA base layer pavement show that there are very high values exhibited by RCA base layers for example at STH 78, which could be attributed to the tufa formation. The formation of C-S-H in the RCA base layer can result in the material to cement together and increase the modulus over time.

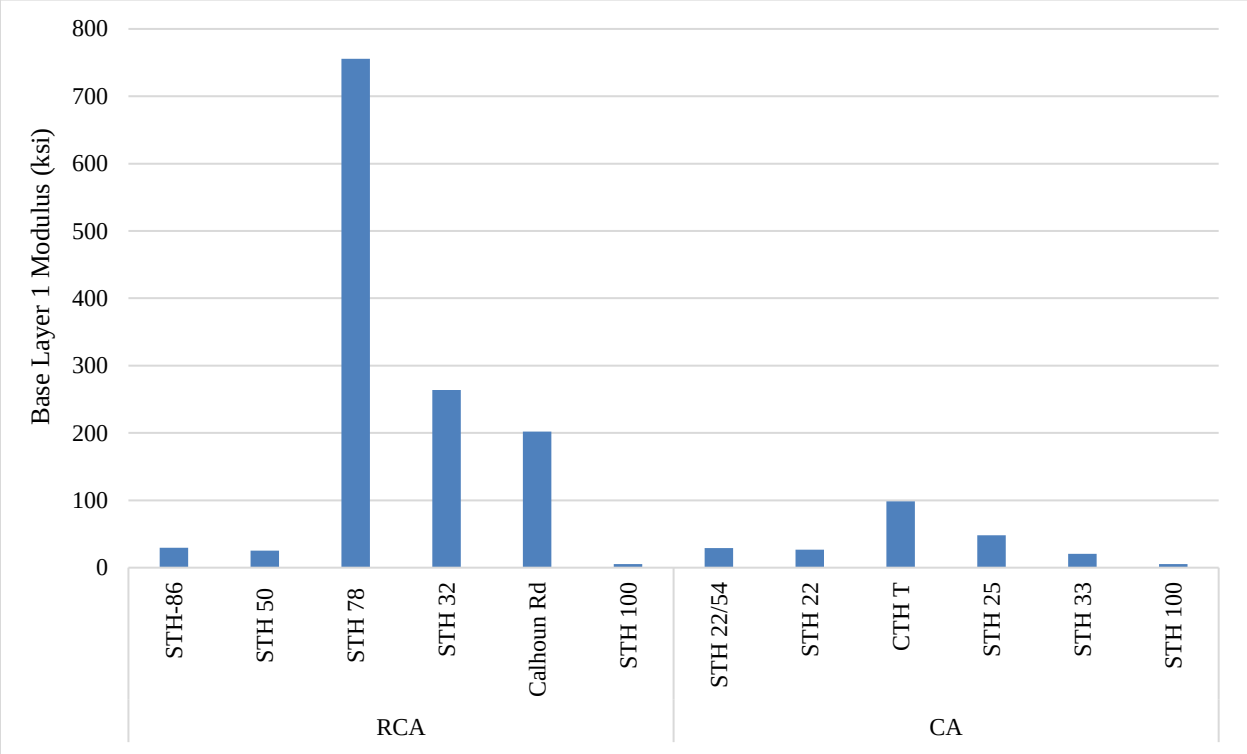

Figure 5.11: Average back-calculated layer moduli for the investigated pavements with RCA and CA base layers.

The results of the back-calculated subgrade modulus ($E_{Subgrade}$) are presented in Table 5.5. Average $E_{Subgrade}$ ranged from 13 to 39 ksi for pavement with RCA base layers compared with 13 to 33 ksi for pavement with CA base layers. Figure 5.13 depicts a Box-whisker plot for back-calculated $E_{subgrade}$ of the investigated pavements with RCA and CA base layers. Inspection of the figure shows the variability in the back-calculated $E_{subgrade}$ within each pavement test section and among all sections but the back-calculated $E_{subgrade}$ values or the pavements with RCA and CA base layers are comparable. The results of the FWD test at all investigated pavements with RCA and CA base layers are presented in Appendix C.

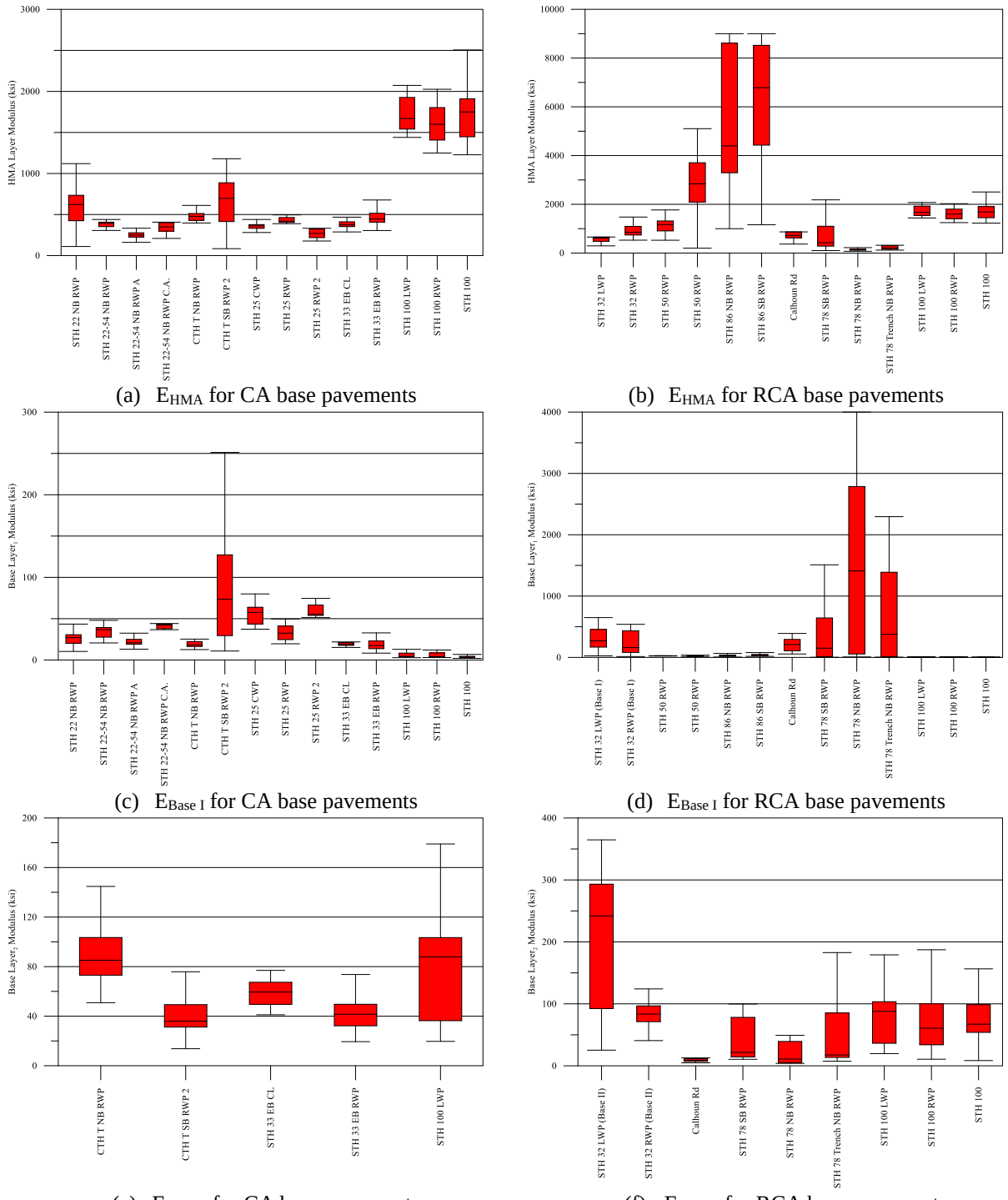

(a) E_{HMA} for CA base pavements

(b) E_{HMA} for RCA base pavements

(c) $E_{Base\ I}$ for CA base pavements

(d) $E_{Base\ I}$ for RCA base pavements

(e) $E_{Base\ II}$ for CA base pavements

(f) $E_{Base\ II}$ for RCA base pavements

Figure 5.12: Box-whisker plot for the back-calculated E_{HMA}, $E_{base\ I}$, and $E_{base\ II}$ for the investigated pavements with RCA and CA base layers.

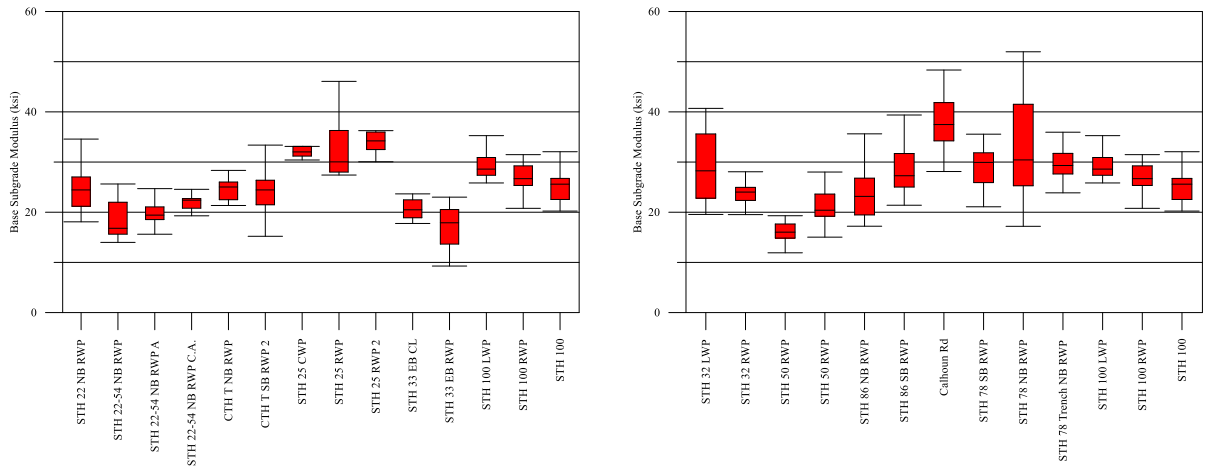

(a) $E_{Subgrade}$ for CA base pavements

(b) $E_{Subgrade}$ for RCA base pavements

Figure 5.13: Box-whisker plot for $E_{subgrade}$ of the investigated pavements.

5.3 Visual and Automated Distress Surveys

Visual distress surveys and pavement surface profile measurements were conducted to obtain the pavement conditions index and ride quality for the investigated HMA pavements with RCA and CA base layers. Figure 5.14 shows a Box-Whisker plot for the pavement condition index of the investigated HMA pavements with RCA and CA base layer. The HMA pavements with RCA base layer exhibited higher PCI values indicating better pavement quality; however, pavement condition index depends largely on the surface layer distresses.

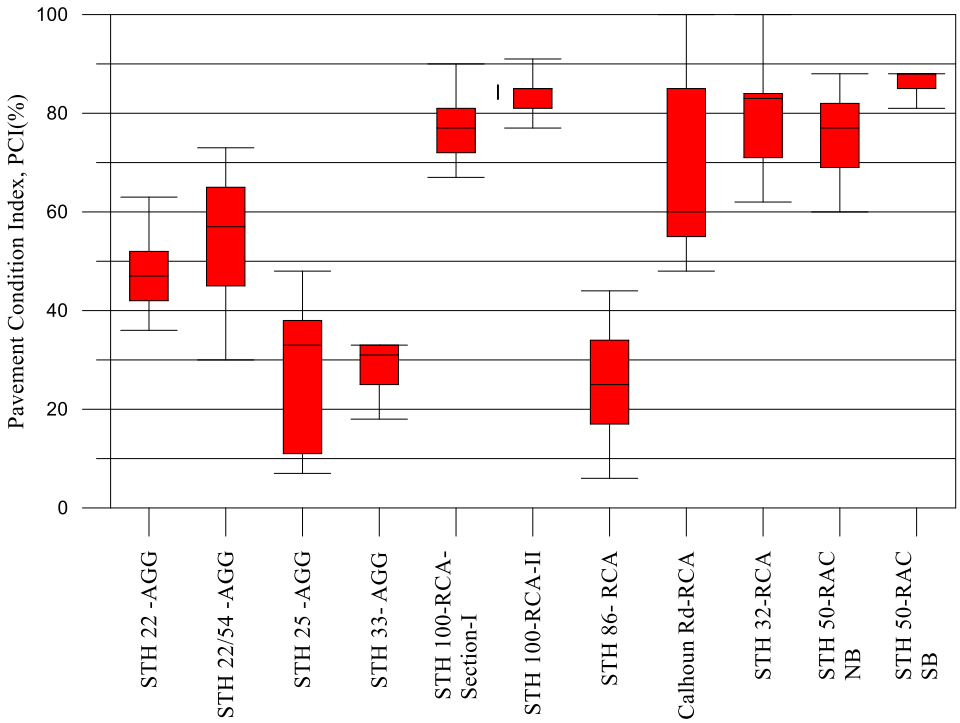

Figure 5.14: Box-Whisker plot for the pavement condition index of the investigated HMA pavements with RCA and CA base layer.

Figure 5.15 depicts the variation of ride quality with distance along 528 ft test sections on STH 50 with RCA base layer and STH 25 with CA base layer. The IRI indicated also the pavement surface roughness.

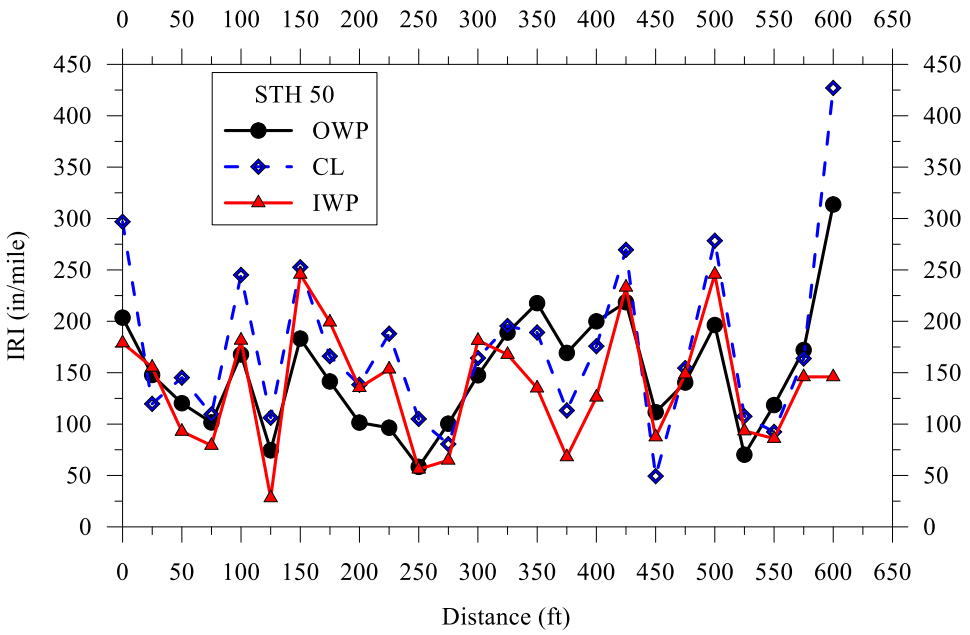

(a) STH 50 with RCA base layer

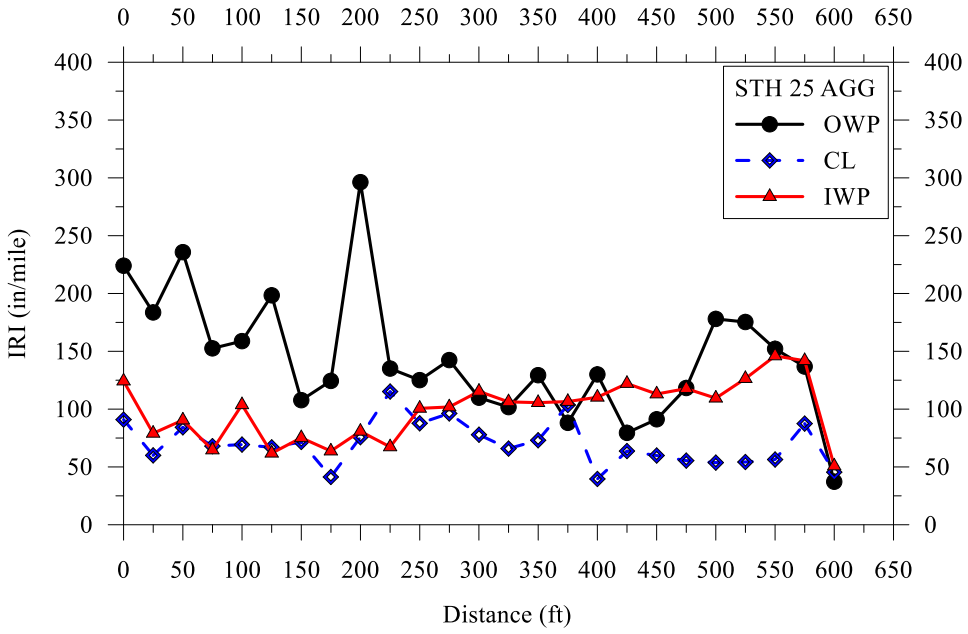

(b) STH 25 with CA base layer

Figure 5.15: Variation of ride quality in terms of IRI for two HMA pavements with RCA and CA base layer.

Figure 5.16 presents a Box-Whisker plot of the measured IRI for the investigated HMA pavements with RCA and CA base layer sections. While there is a very highly variability in the test results, the HMA pavements with CA base layers exhibited lower IRI values compared with the HMA pavements with CA base layers. The IRI profiles with distance for all investigated pavement sections are presented in Appendix D.

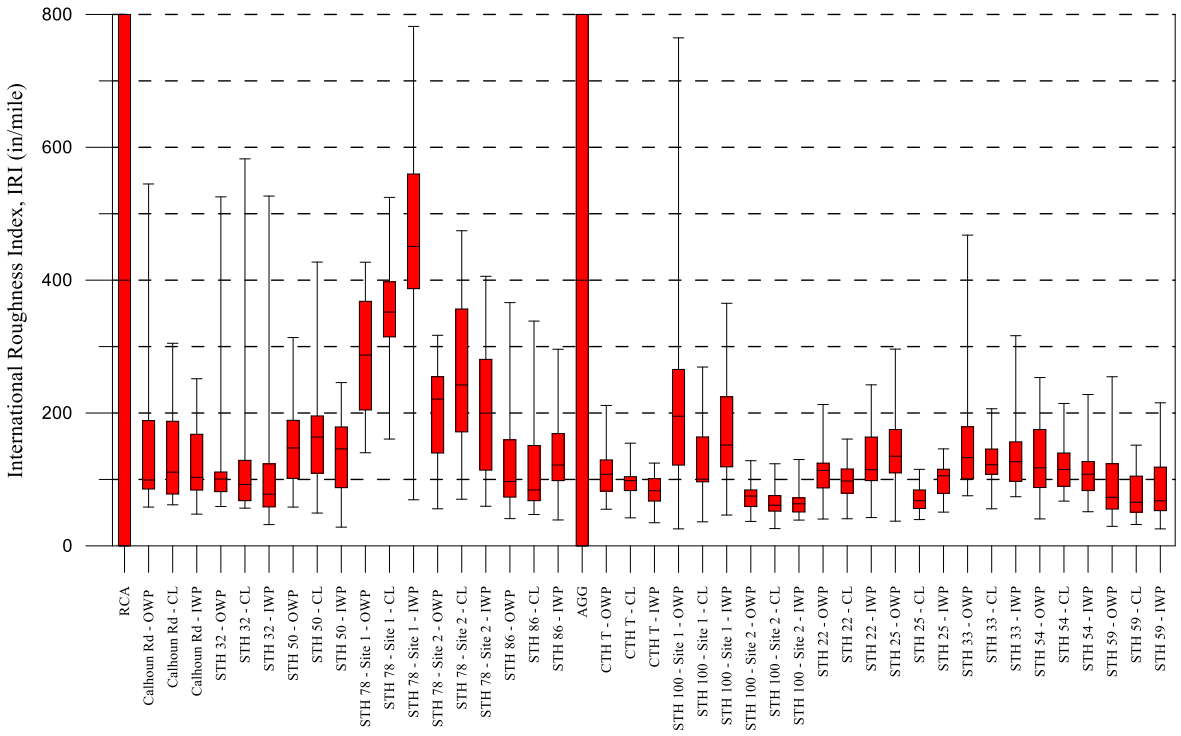

Figure 5.16: Box-Whisker plot of the IRI for the investigated HMA pavements with RCA and CA base layers.

Chapter 6

Summary and Conclusions

This research investigated the influence of the RCA base layers on the HMA pavement performance as compared with CA base layers using laboratory tests on collected base layer materials and field tests on corresponding pavement sections. Comprehensive field and laboratory testing programs were conducted to investigate RCA and CA base layer materials in which identified test sections at the selected pavement sites were subjected to testing using FWD, walking profiler, and DCP. Visual distress surveys were also conducted at the selected pavement sections. RCA and CA base layer samples were collected from these pavement sites and were subjected to a laboratory testing program including: particle size analysis, Micro-Deval abrasion test, absorption, and specific gravity.

The results of the sieve analyses indicated that the particle size distribution for the RCA and CA base materials are in general consistent with WisDOT specifications with few samples of RCA and CA fell partially outside the corresponding WisDOT base aggregate gradation specifications. The investigated RCA base layer materials are found in general to be “finer” than the CA base materials based on the FM and GN values.

The RCA base layer materials possessed higher absorption values compared with CA base materials. The absorption values of the investigated RCA base materials varied between 2.7% to 8.2%. The CA samples possessed absorption values ranging from 1.41% to 3.43%.

Micro-Deval abrasion test results showed that RCA and CA base layer materials exhibited high mass loss, in general, compared with a mean mass loss of 15.05% for Wisconsin virgin coarse aggregates obtained by Tabatabai et al. (2013).

Strength and modulus evaluations of the investigated RCA and CA base materials and pavement test sections were achieved DCP and FWD tests. The DCP test results provided information about the RCA base quality of construction as well as the variability in such quality. DCP test results indicated variability in strength (as predicted by CBR) and modulus (predicted resilient modulus). Test results indicated that the CBR and layer moduli values of both RCA and CA base layer types are comparable. The average predicted CBR ranged from 65 to 96% for the RCA bases and between 58 to 90% for the CA bases. Similar trend is exhibited by average predicted layer modulus with the average range for the RCA bases between 37 and 47 ksi and for the CA bases from 34 and 45 ksi. The CBR and base layer modulus values obtained from the results of the DCP tests indicated in general good properties of the investigated bases.

FWD test results showed variability in pavement surface deflections (D_0) within individual test sections and among the various pavement test sections. In general, less deflection D_0 values exhibited by pavement test sections with RCA base layers compared with those with CA base layers.

The back-calculated moduli for the RCA and CA base layers (E_{Base}) exhibited significant variability within individual pavement test sections and among pavements. The average back-calculated E_{Base} RCA base layers ranges from 30 to 981 ksi, while the average

back-calculated E_{Base} CA base layers varies between 20 to 175 ksi. Comparison of the back-calculated layer moduli values E_{base} for RCA and CA base layer pavement show that there are very high values exhibited by RCA base layers for example at STH 78, which could be attributed to the tufa formation. The formation of C-S-H in the RCA base layer can result in the material to cement together and increase the modulus over time.

The results of the visual distress surveys and pavement profile measurements (in terms of calculated PCI and IRI) for investigated pavement test sections showed variability with classified pavement conditions ranging from poor to good. The HMA pavements with RCA base layers exhibited higher PCI values indicating better pavement quality; however, pavement condition index depends largely on the surface layer distresses. The HMA pavements with CA base layers exhibited lower IRI values compared with the HMA pavements with CA base layers indicating a smoother ride quality for HMA pavement with CA base layer.

References

1) Edil, T., Benson, C., Tinjum, J., Scheartle, G., Bozyurt, O., Nokkaew, K., Chen, J., Bradshaw, S. (2011). “Engineering Properties of Recycled Materials for

2) Butler, L., Tighe, S., West, J. (2013). “Guidelines for Selection and Use of Coarse Recycled-Concrete Aggregates in Structural Concrete”. Transportation

3) Jayakody, S. (2014). “Investigation on Characteristics and Performance or Recycled Concrete Aggregates as Granular Materials for Unbound Pavements”.

4) Gabr, A., Cameron, D. (2012). Properties of Recycled Concrete Aggregate for Unbound Pavement Construction

5) Ceylan, H., Kim, S., Gopalakrishnan, K., (2014). “Use of Crushed/Recycled Concrete as Drainable Base/Subbase and Possible Future Plugging of Pavement

6) Tabatabai, H., Titi, H.H., Lee, C.W., Qamhia, I., and Puerta Fella, G. (2013) “Investigation of Testing Methods to Determine Long-Term Durability of Wisconsin

Appendix A

Dynamic Cone Penetrometer Test Results

Results of DCP tests and corresponding CBR layer values for RCA and CA

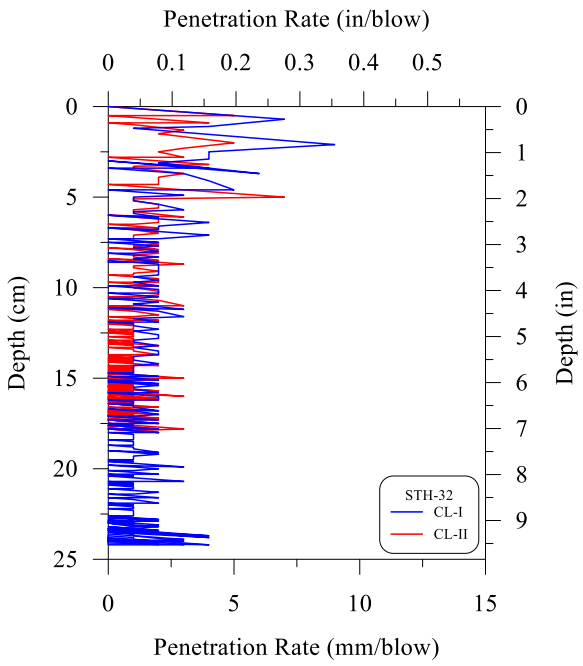

(a) DCP tests STH 32, CL-I, CL-II

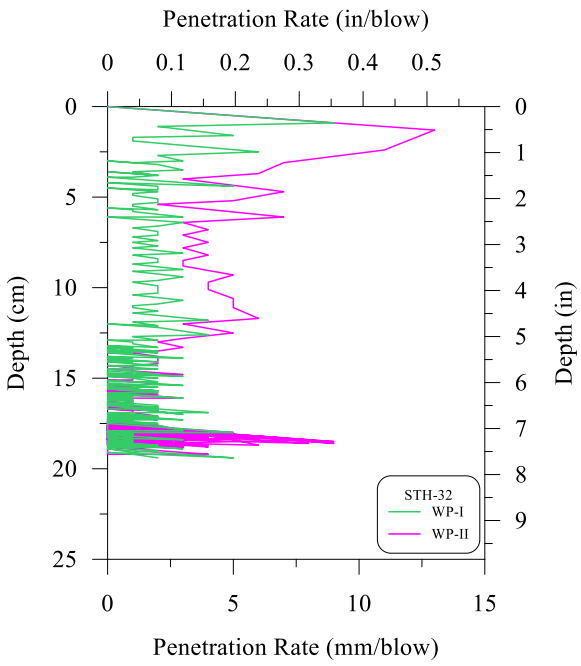

(b) DCP tests STH 32, WP-I, WP-II

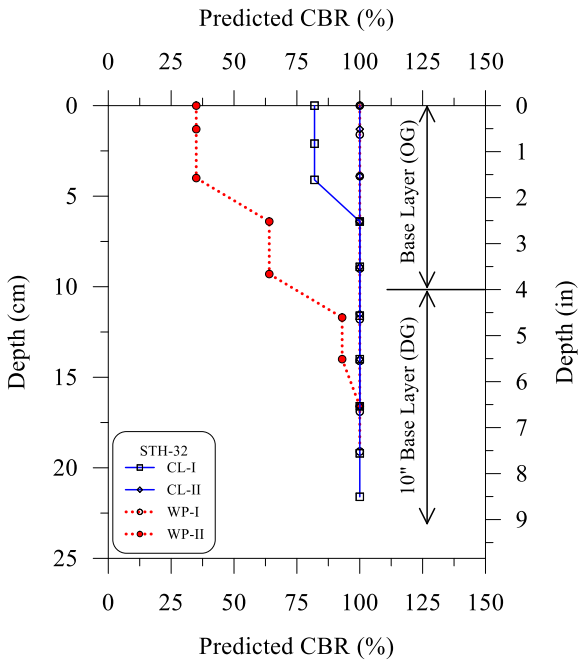

(c) Predicted CBR (%) STH 32

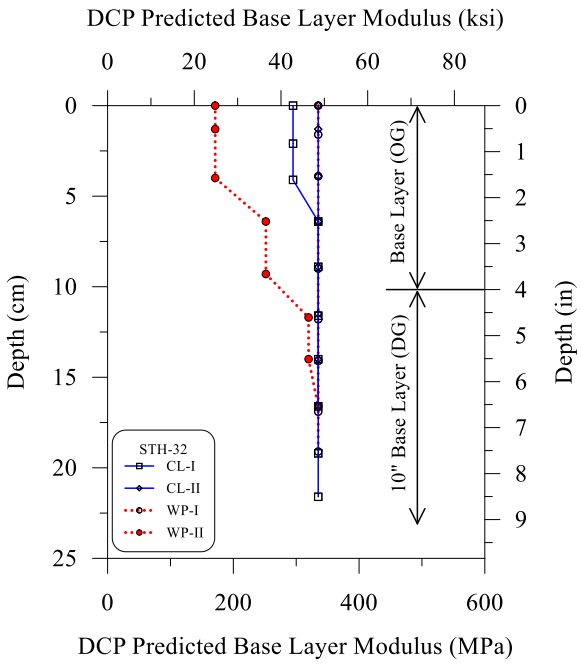

(d) Base layer modulus by DCP test STH 32

Figure 1: Penetration resistance with depth from DCP and distribution with depth of estimated CBR and base layer modulus from DCP test (RCA Base Coarse STH 32)

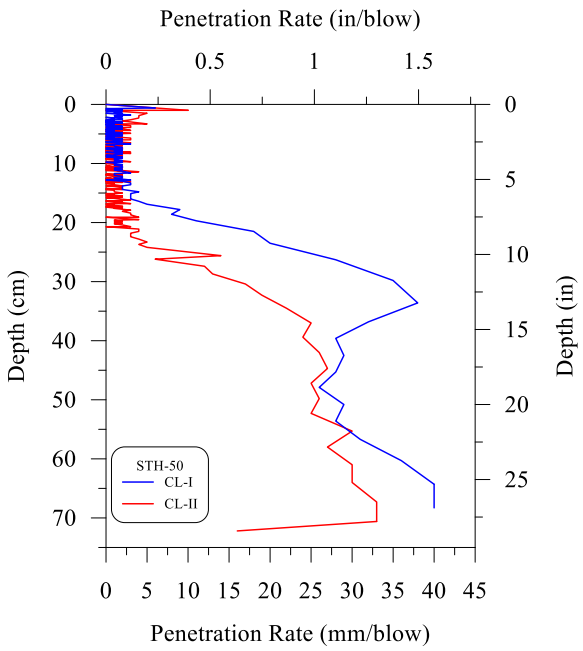

(a) DCP tests STH 50, CL-I, CL-II

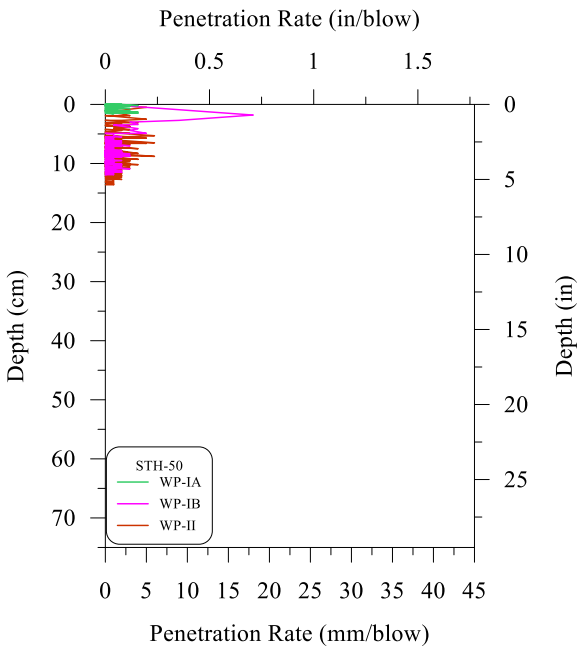

(b) DCP tests STH 50, WP-IA, WP-IB, WP-II

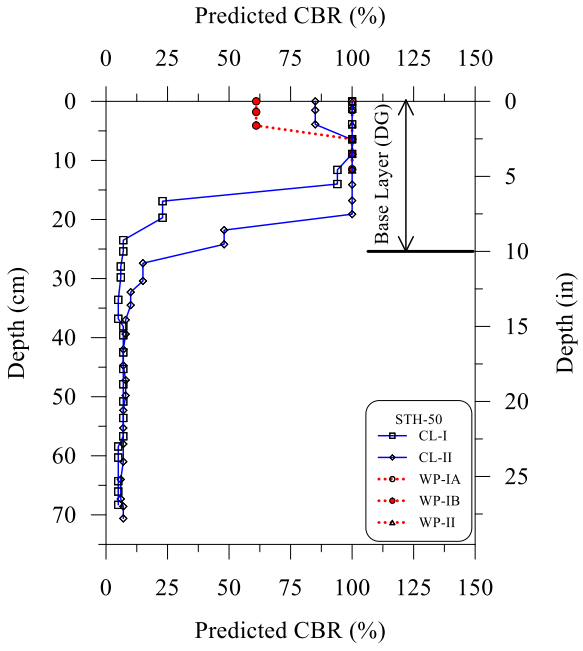

(c) Predicted CBR (%) STH 50

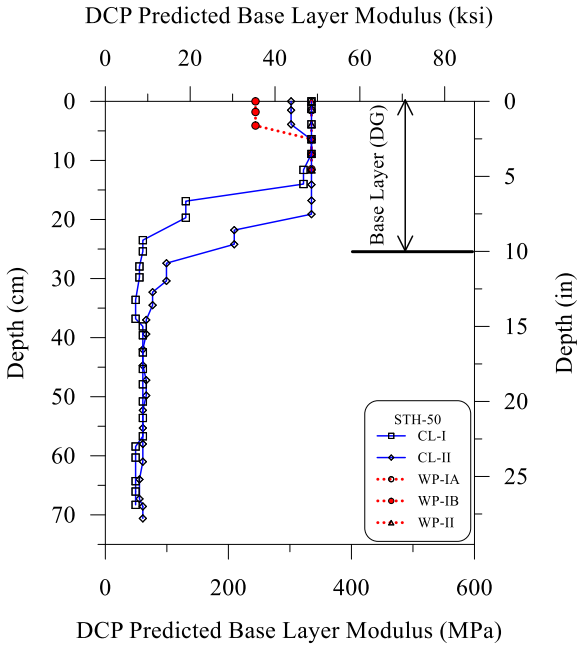

(d) Base layer modulus by DCP test STH 50

Figure 2: Penetration resistance with depth from DCP and distribution with depth of estimated CBR and base layer modulus from DCP test (RCA Base Coarse STH 50)

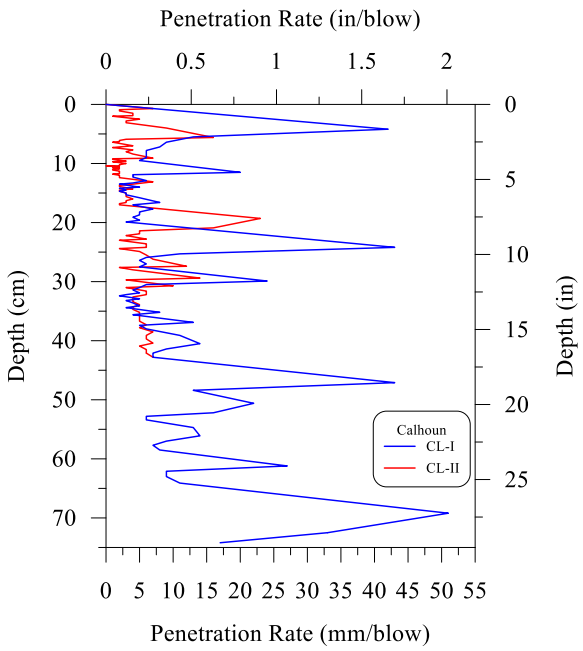

(a) DCP tests Calhoun, CL-I, CL-II

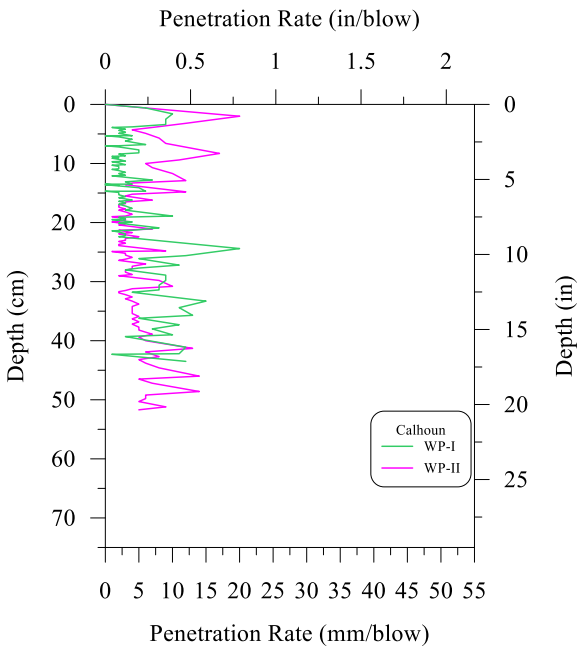

(b) DCP tests Calhoun, WP-I, WP-II

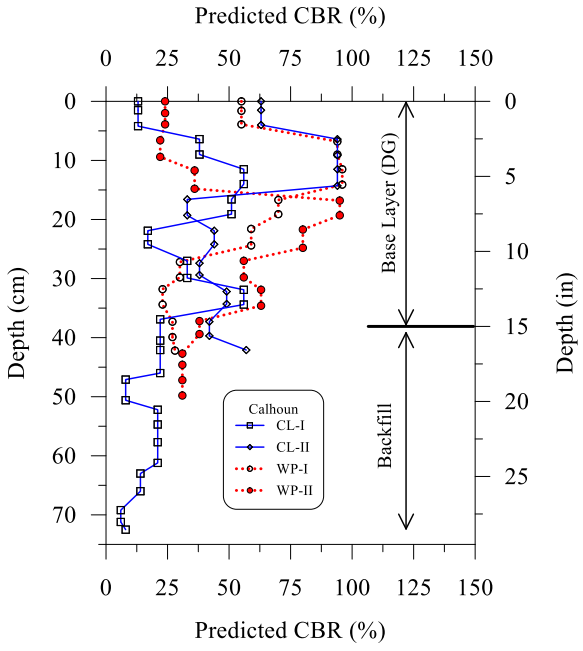

(c) Predicted CBR (%) Calhoun

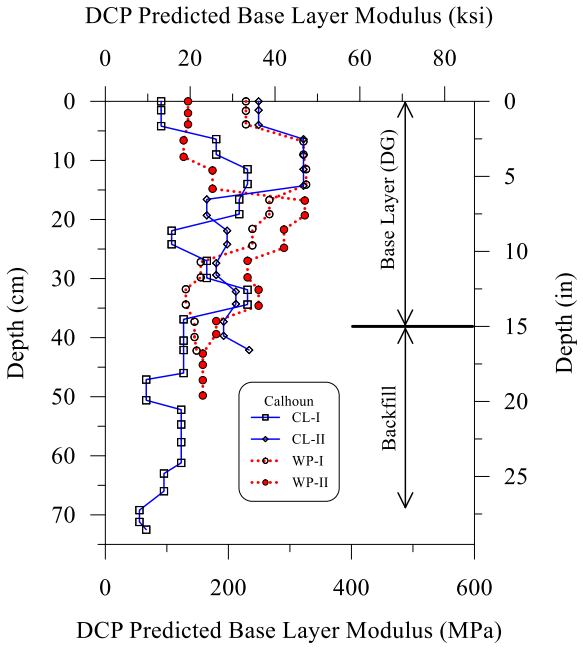

(d) Base layer modulus by DCP test Calhoun

Figure 3: Penetration resistance with depth from DCP and distribution with depth of estimated CBR and base layer modulus from DCP test (RCA Base Coarse Calhoun)

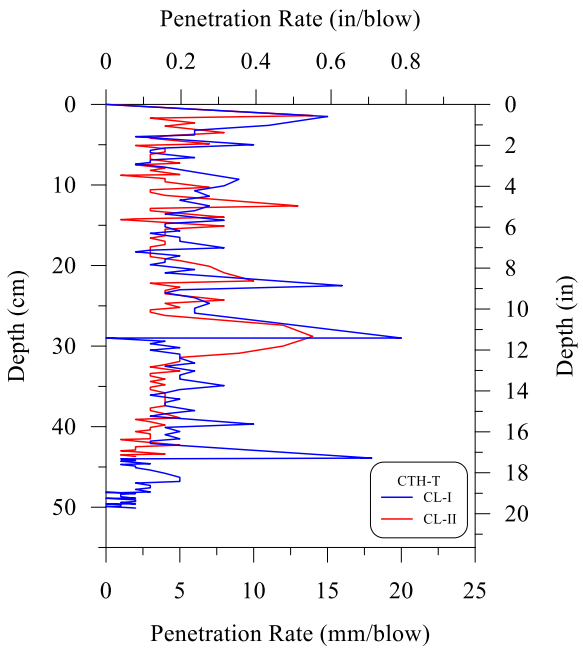

(a) DCP tests CTH T, CL-I, CL-II

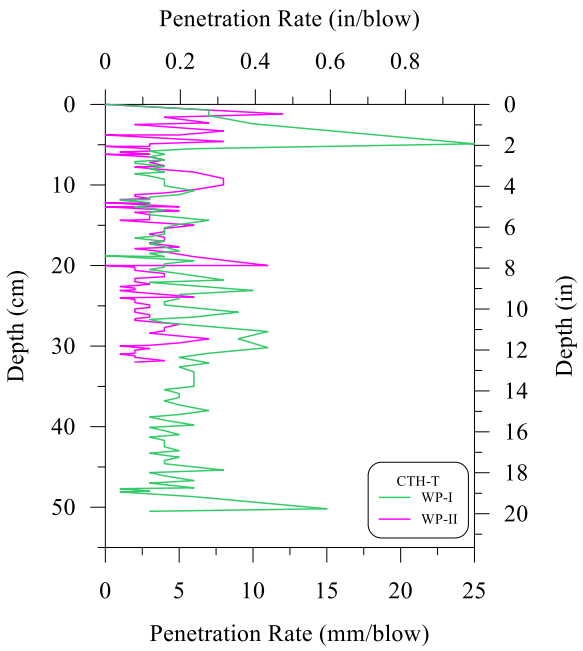

(b) DCP tests CTH T, WP-I, WP-II

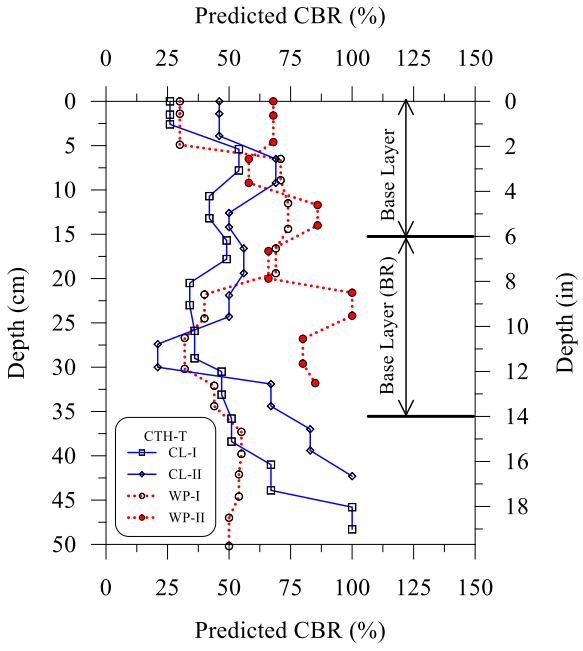

(c) Predicted CBR (%) CTH T

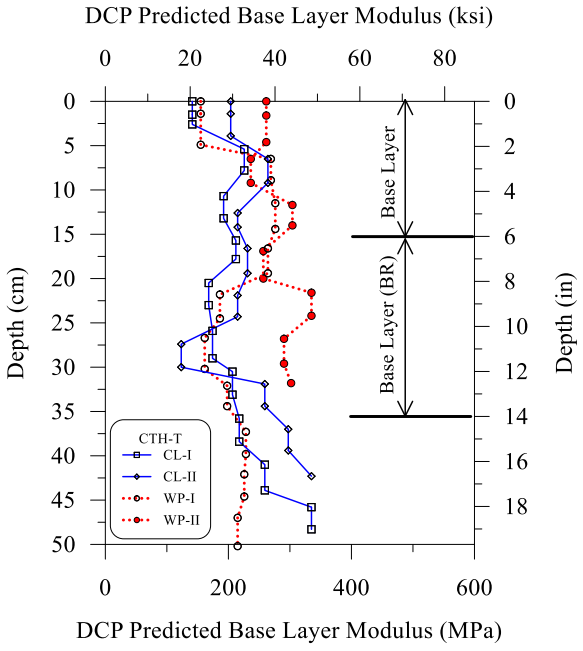

(d) Base layer modulus by DCP test CTH T

Figure 4: Penetration resistance with depth from DCP and distribution with depth of estimated CBR and base layer modulus from DCP test (CA CTH T)

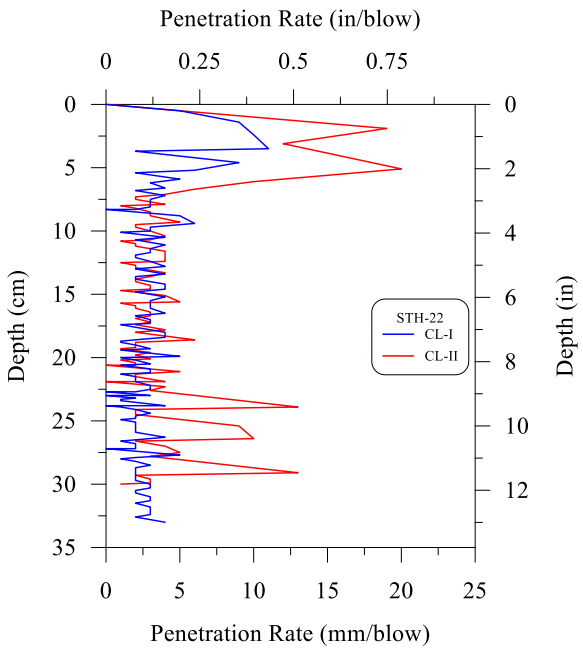

(a) DCP tests STH 22, CL-I, CL-II

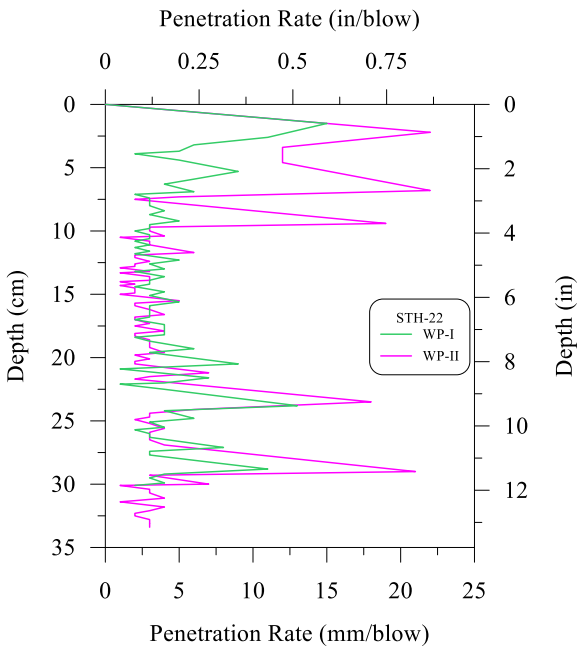

(b) DCP tests STH 22, WP-I, WP-II

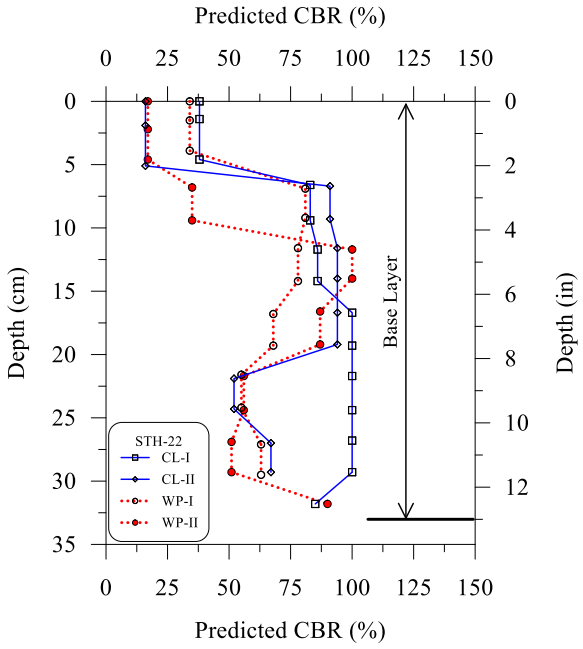

(c) Predicted CBR (%) STH 22

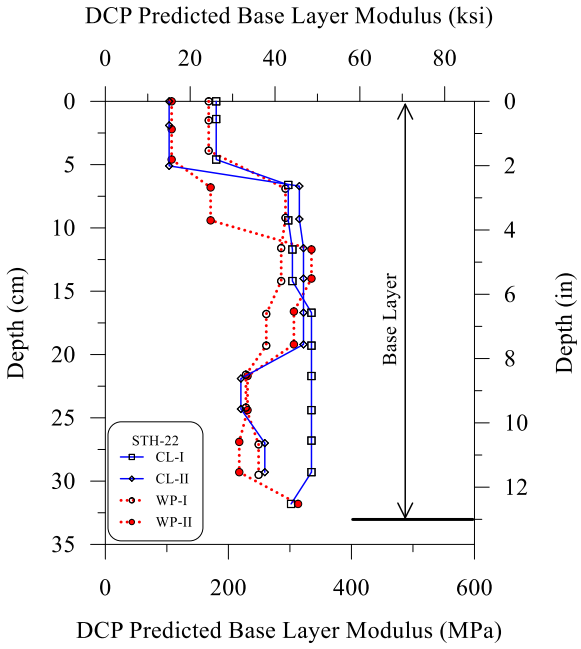

(d) Base layer modulus by DCP test STH 22

Figure 5: Penetration resistance with depth from DCP and distribution with depth of estimated CBR and base layer modulus from DCP test (CA STH 22)

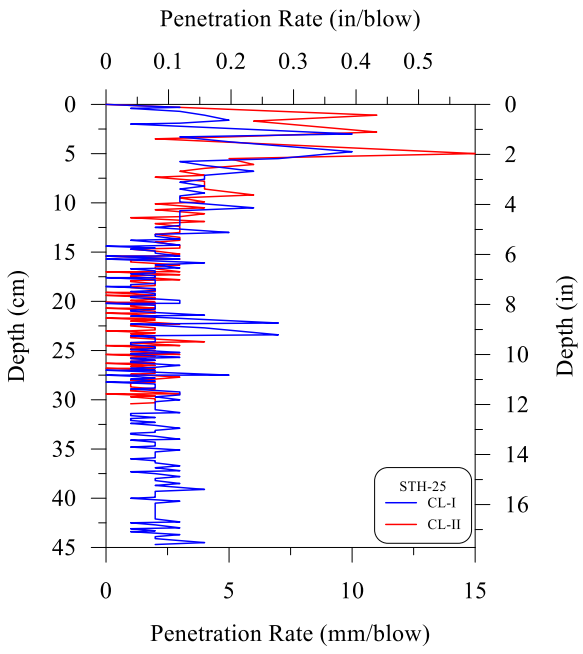

(a) DCP tests STH 25, CL-I, CL-II

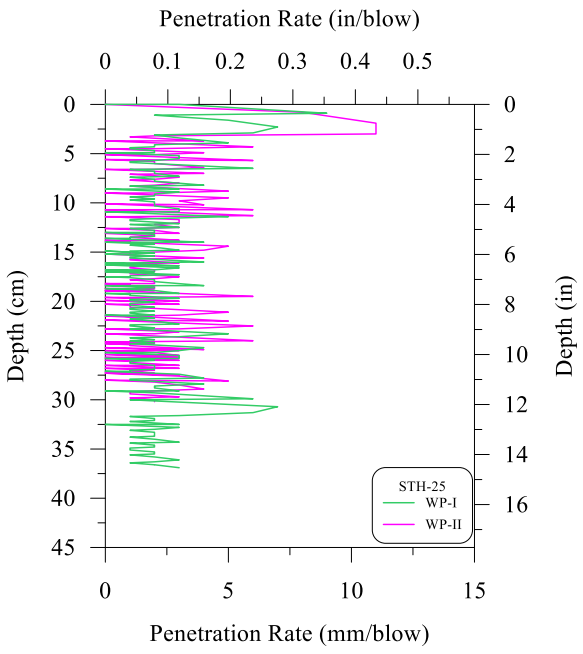

(b) DCP tests STH 25, WP-I, WP-II

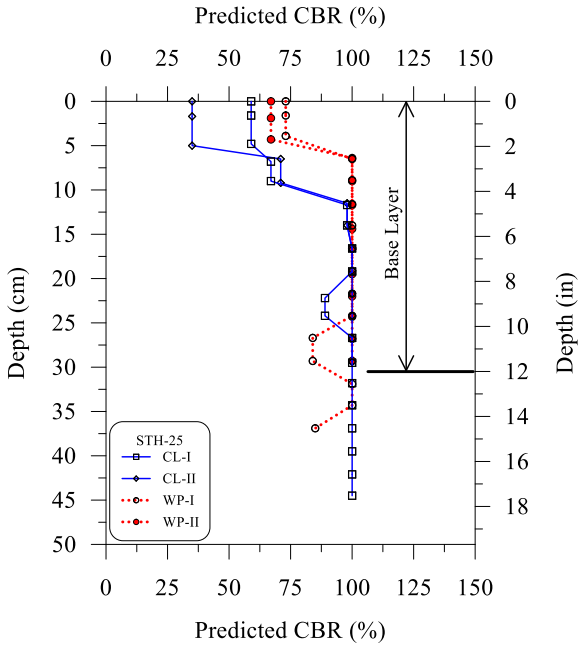

(c) Predicted CBR (%) STH 25

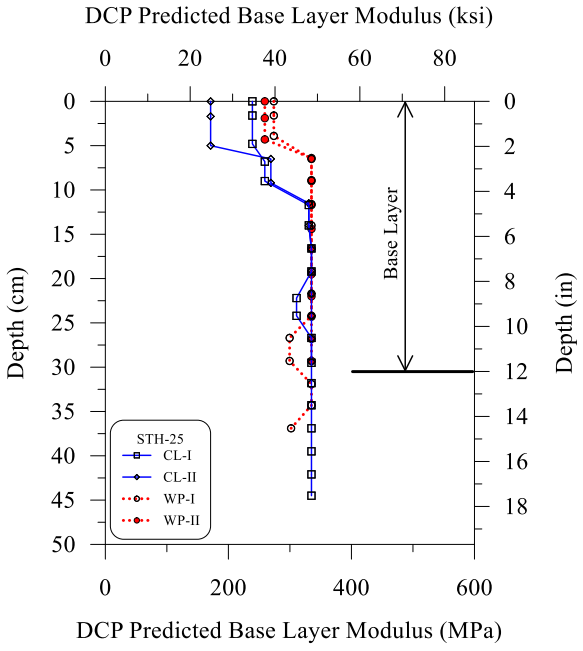

(d) Base layer modulus by DCP test STH 25

Figure 6: Penetration resistance with depth from DCP and distribution with depth of estimated CBR and base layer modulus from DCP test (CA STH 25)

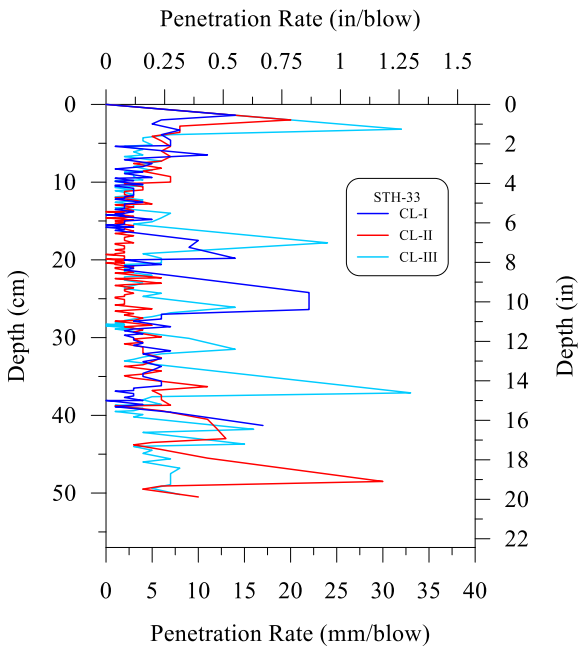

(a) DCP tests STH 33, CL-I, CL-II, CL-III

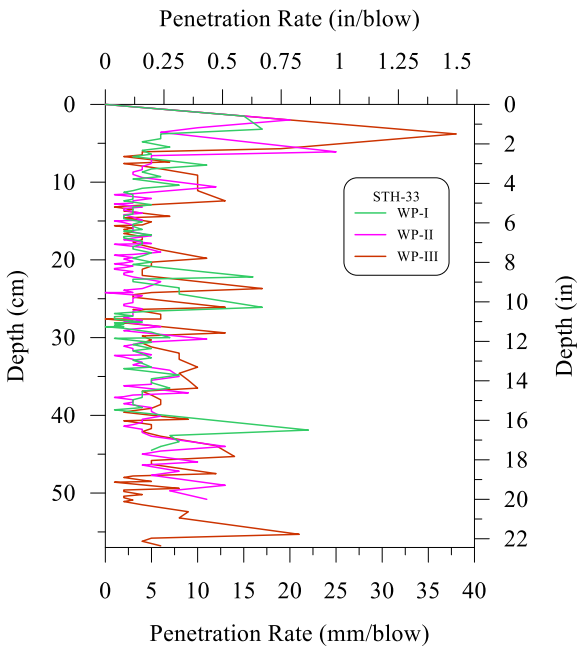

(b) DCP tests STH 33, WP-I, WP-II, WP-III

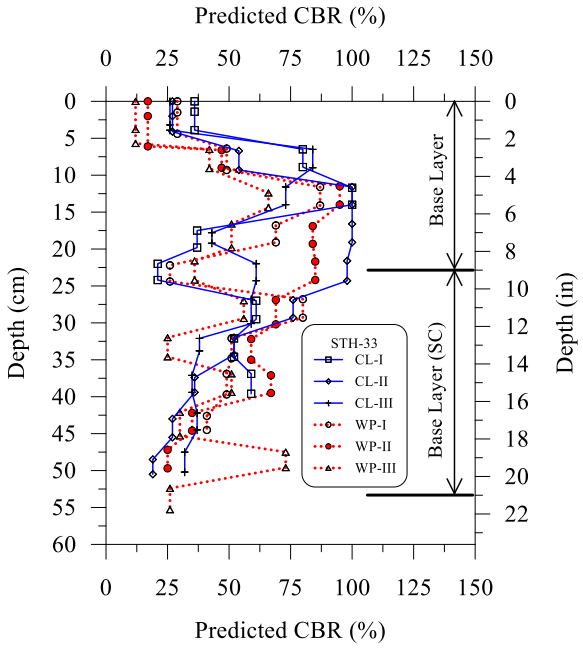

(c) Predicted CBR (%) STH 33

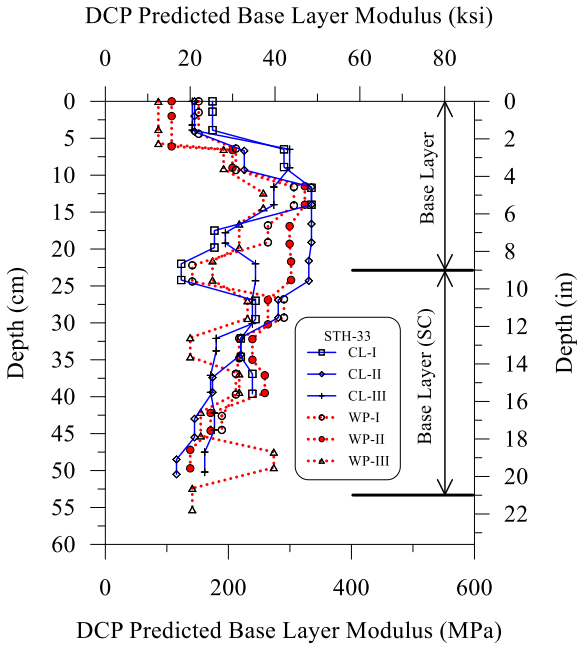

(d) Base layer modulus by DCP test STH 33

Figure 7: Penetration resistance with depth from DCP and distribution with depth of estimated CBR and base layer modulus from DCP test (CA STH 33)

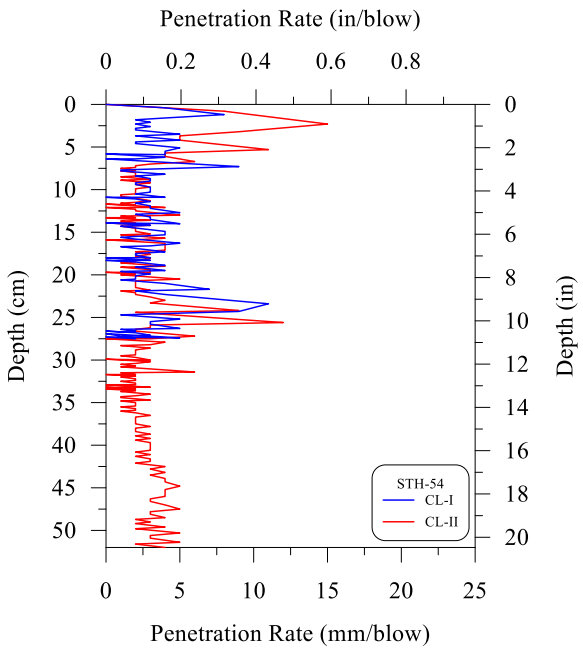

(a) DCP tests STH 54, CL-I, CL-II

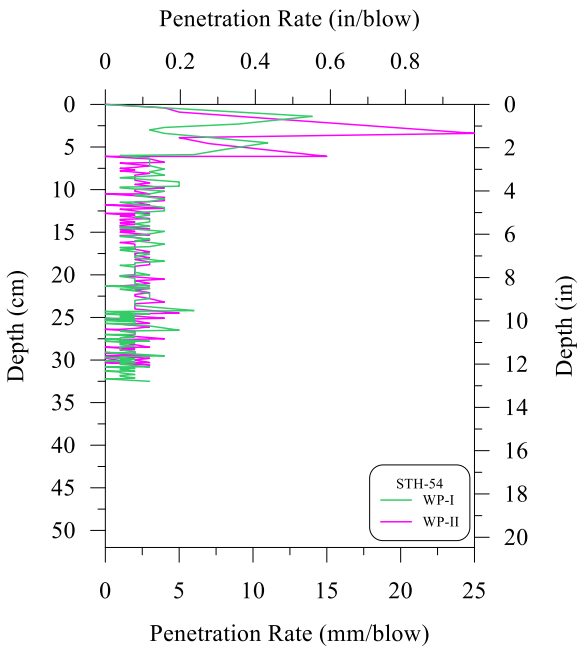

(b) DCP tests STH 54, WP-I, WP-II

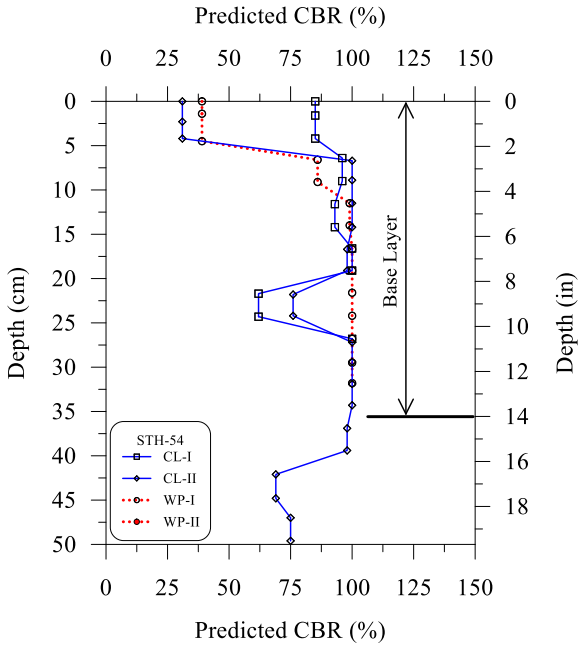

(c) Predicted CBR (%) STH 54

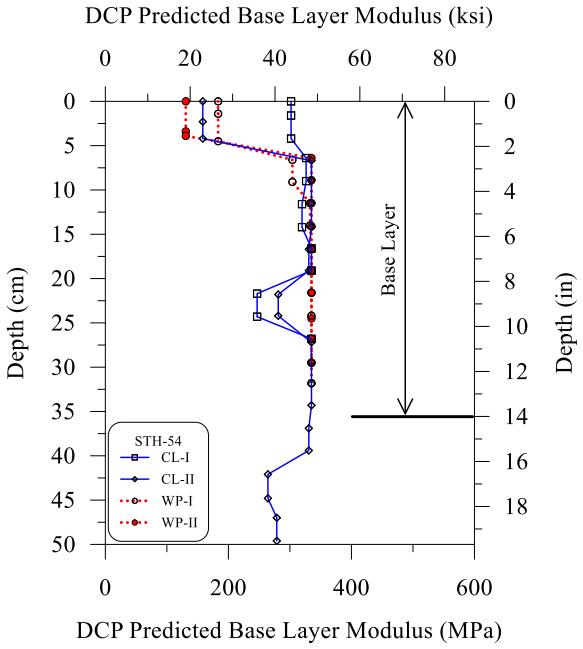

(d) Base layer modulus by DCP test STH 54

Figure 8: Penetration resistance with depth from DCP and distribution with depth of estimated CBR and base layer modulus from DCP test (CA STH 54)

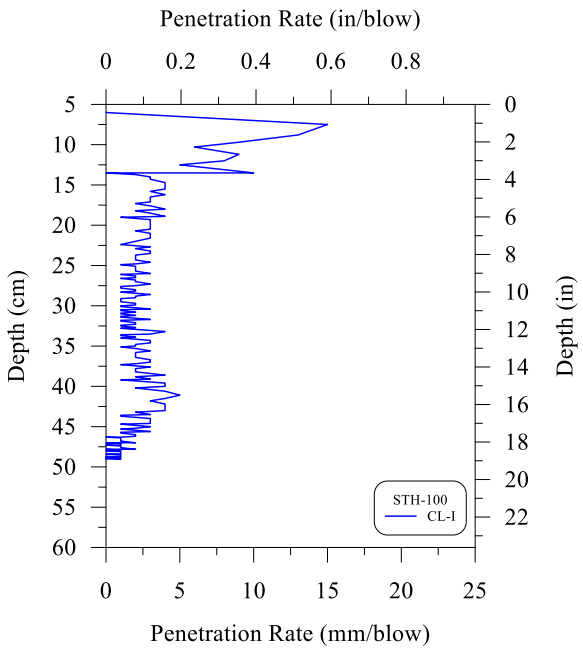

(a) DCP tests STH 100, CL-I

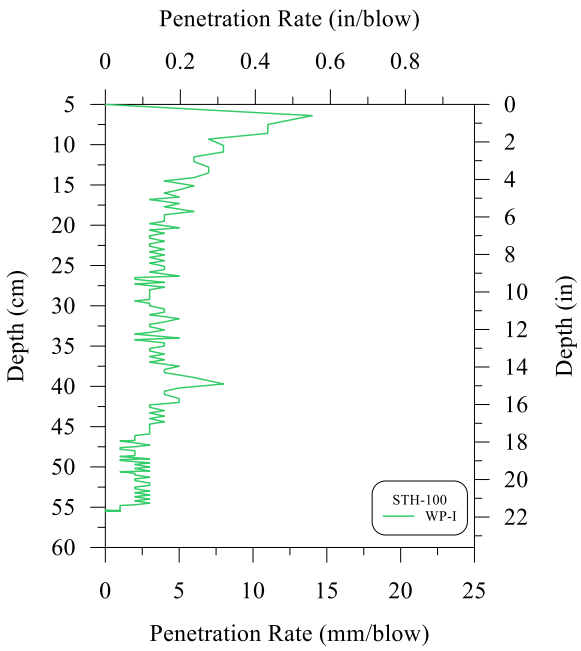

(b) DCP tests STH 100, WP-I

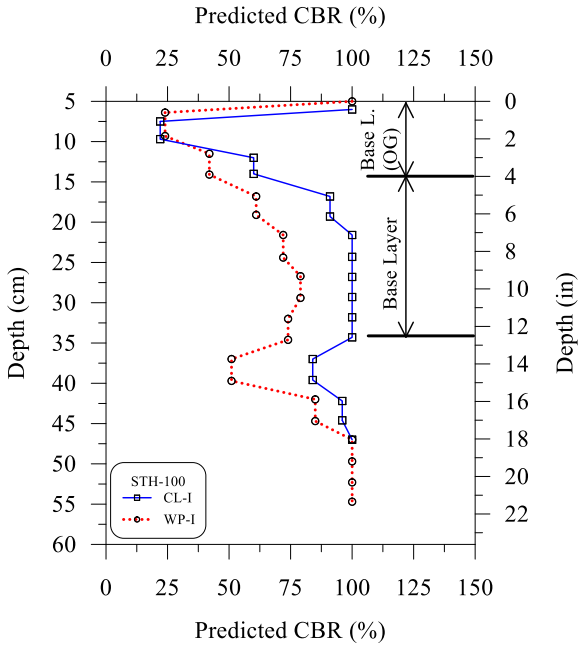

(c) Predicted CBR (%) STH 100

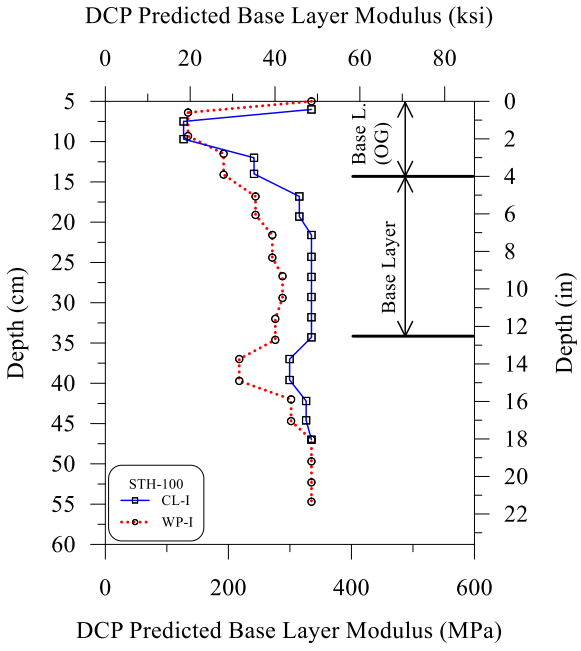

(d) Base layer modulus by DCP test STH 100

Figure 9: Penetration resistance with depth from DCP and distribution with depth of estimated CBR and base layer modulus from DCP test (CA STH 100)

Appendix B

Typical Sections of all Investigated Pavements

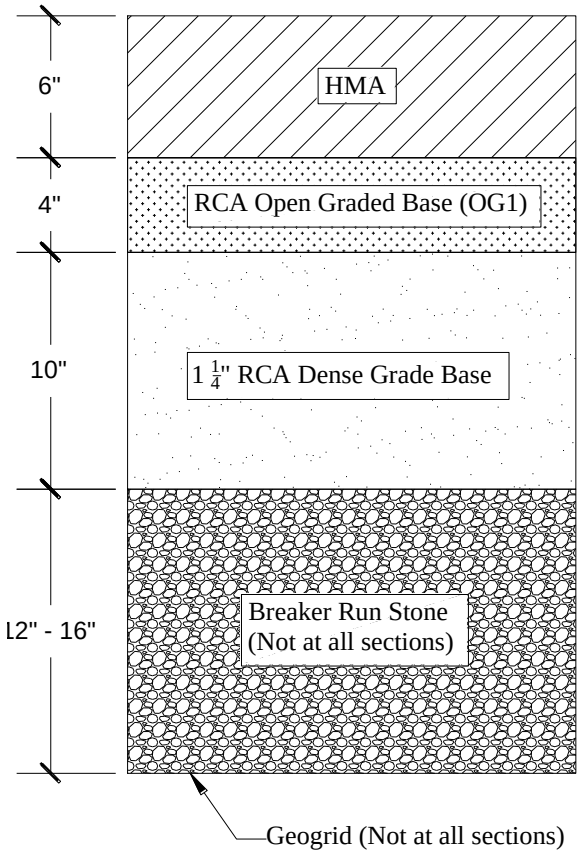

Figure 1: STH 32 RCA

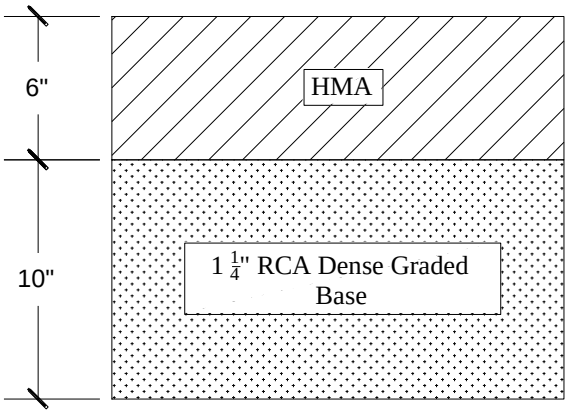

Figure 2: STH 50 RCA

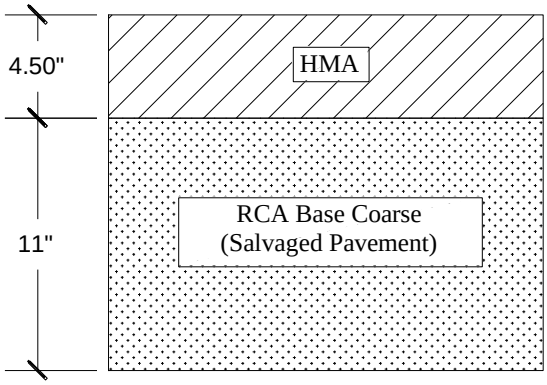

Figure 3: STH 86 RCA

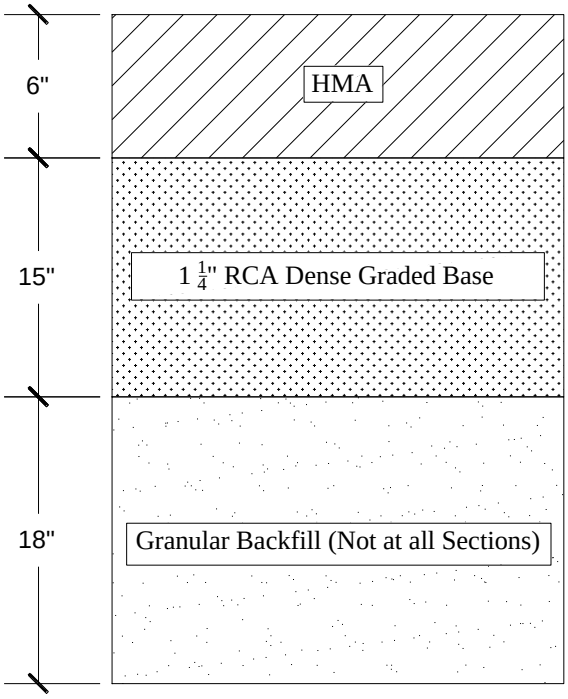

Figure 4: Calhoun RCA

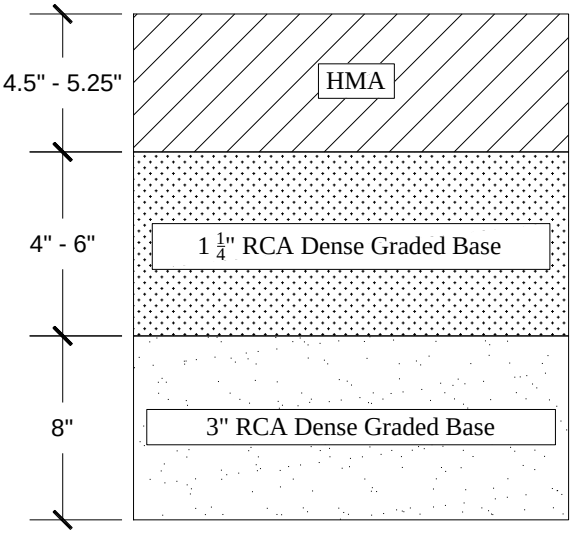

Figure 5: STH 78 RCA

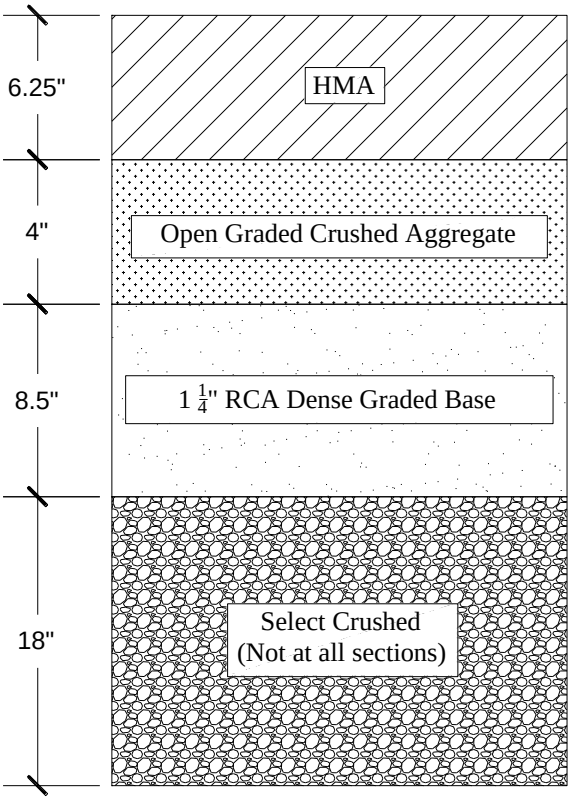

Figure 6: STH 100 RCA

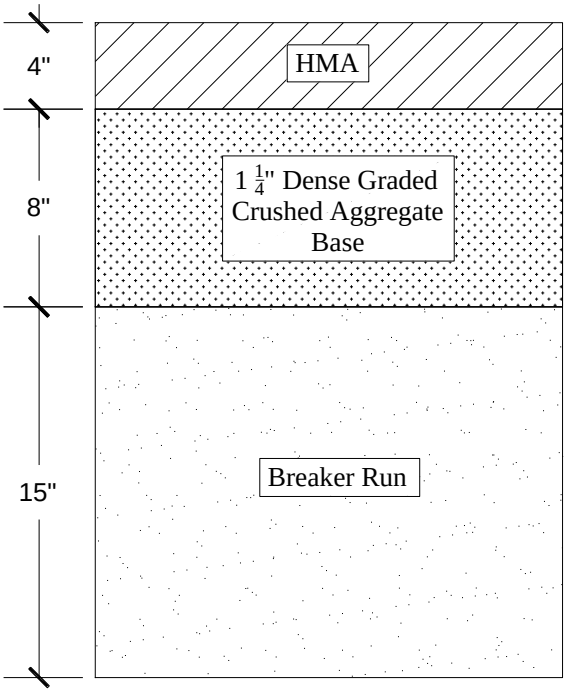

Figure 7: STH 59 CA

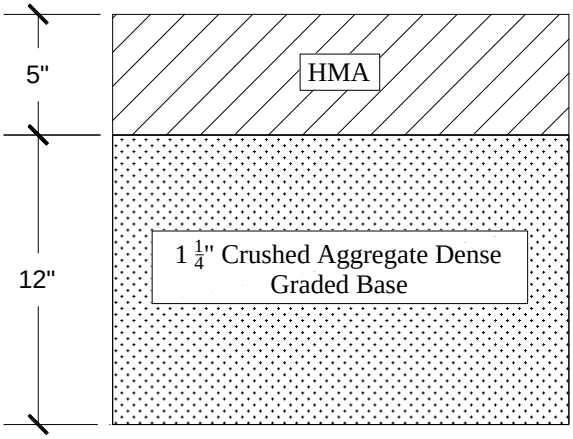

Figure 8: STH 25 CA

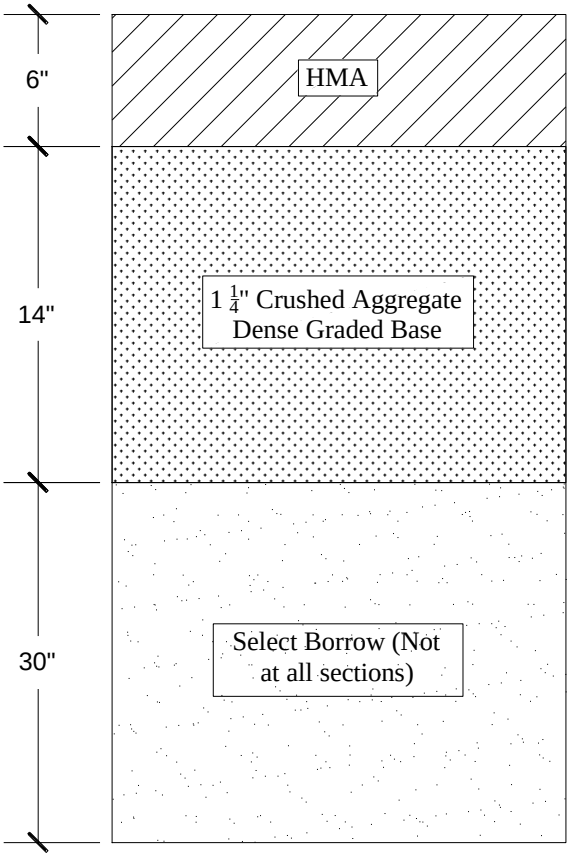

Figure 9: STH 54-22 Waupaca CA

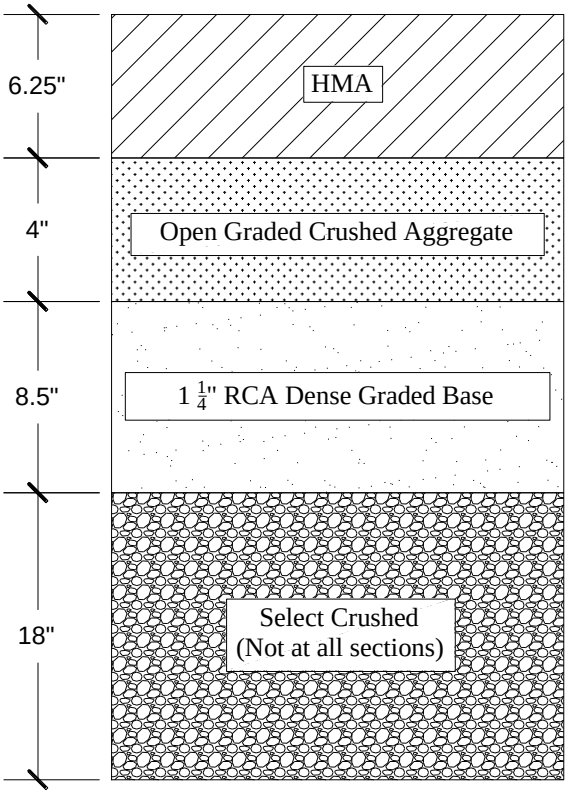

Figure 10: STH 100 CA

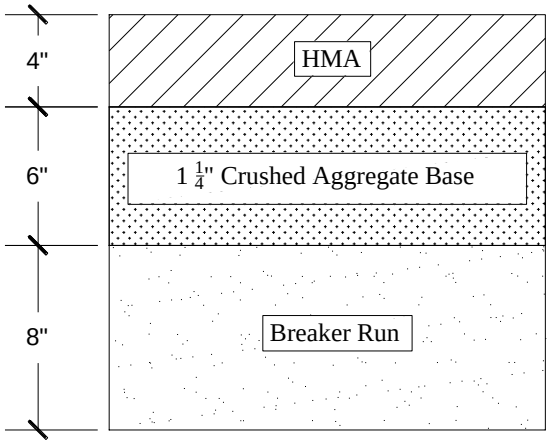

Figure 11: CTH T CA

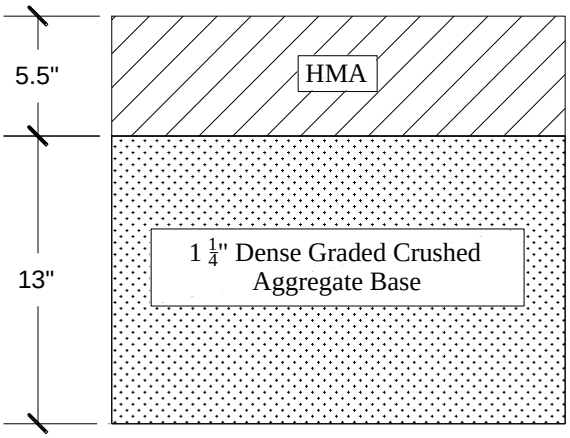

Figure 12: STH 22 CA

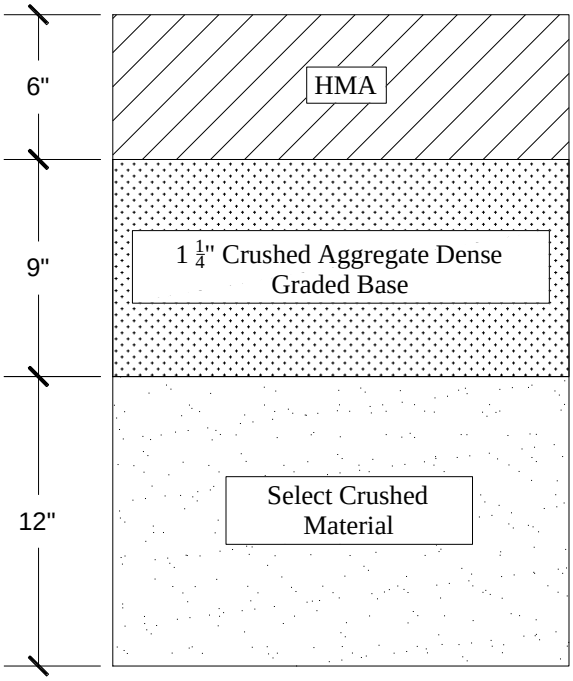

Figure 13: STH 33 CA

Appendix C

Falling Weight Deflectometer Test Results

Plots of Deflection Under the Loading Plate (D_0) and the Corresponding Backcalculated Layer Moduli with Distance for Various Pavement Test Sections

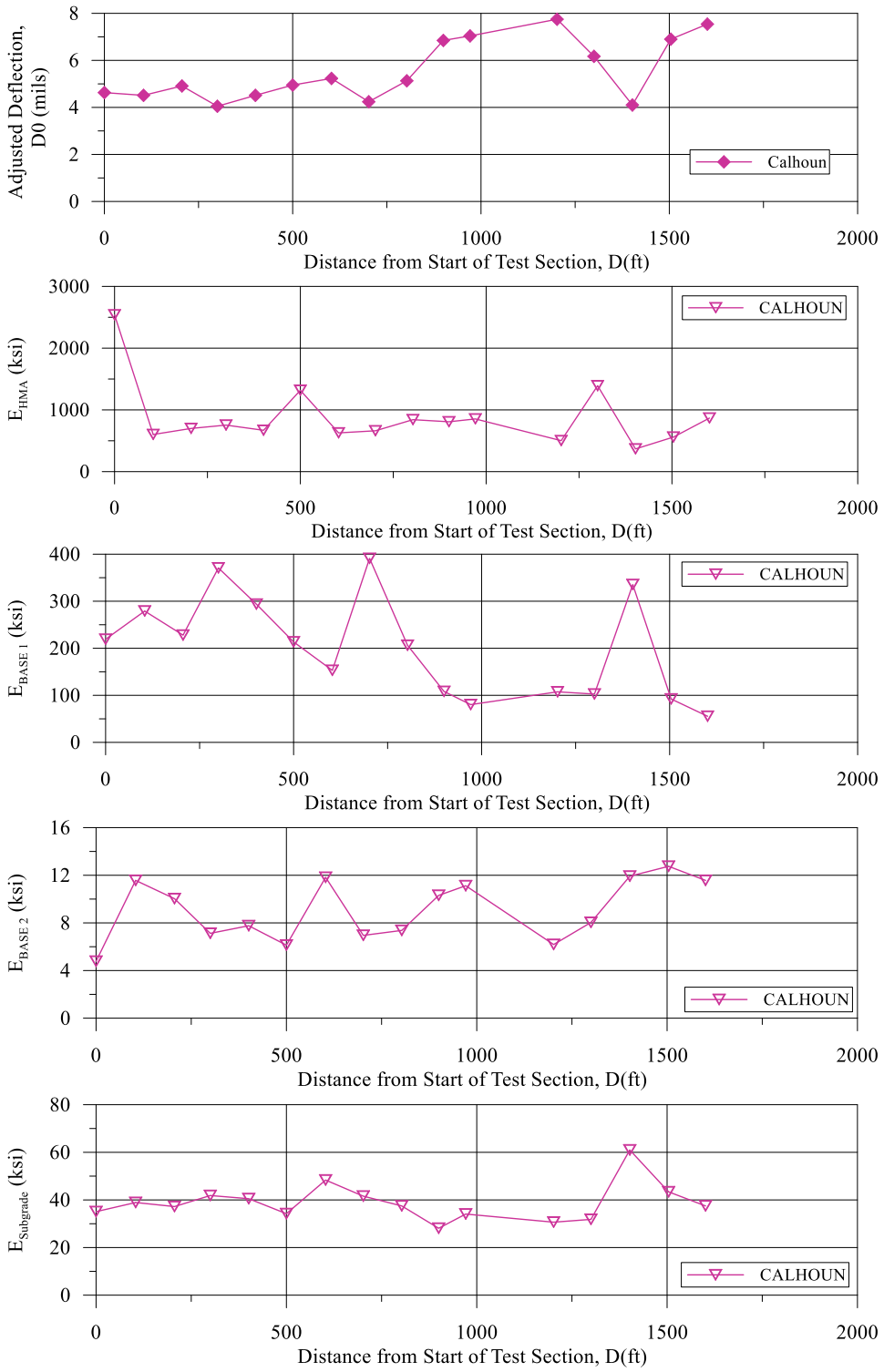

Figure 1: Results of FWD tests on Calhoun Road pavement (a) Adjusted deflection under the loading plate (D_0) (corrected for a 9,000 lb drop and temperature), (b) Back-calculated HMA layer modulus, (c) Back-calculated base layer modulus, and (d) Back-calculated subgrade modulus.

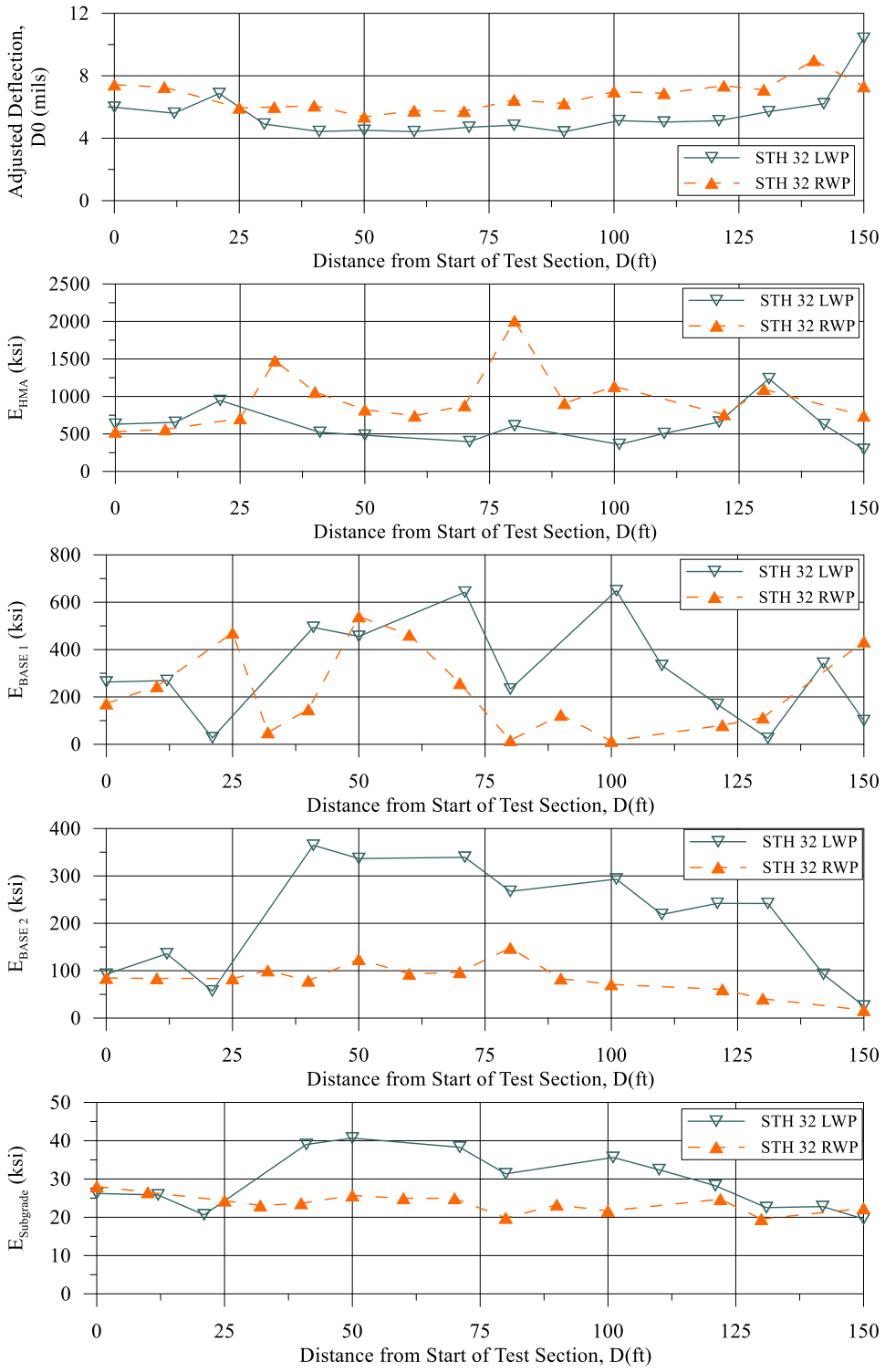

Figure 2: Results of FWD tests on STH 32 pavement (a) Adjusted deflection under the loading plate (D_0) (corrected for a 9,000 lb drop and temperature), (b) Back-calculated HMA layer modulus, (c) Back-calculated base layer modulus, and (d) Back-calculated subgrade modulus.

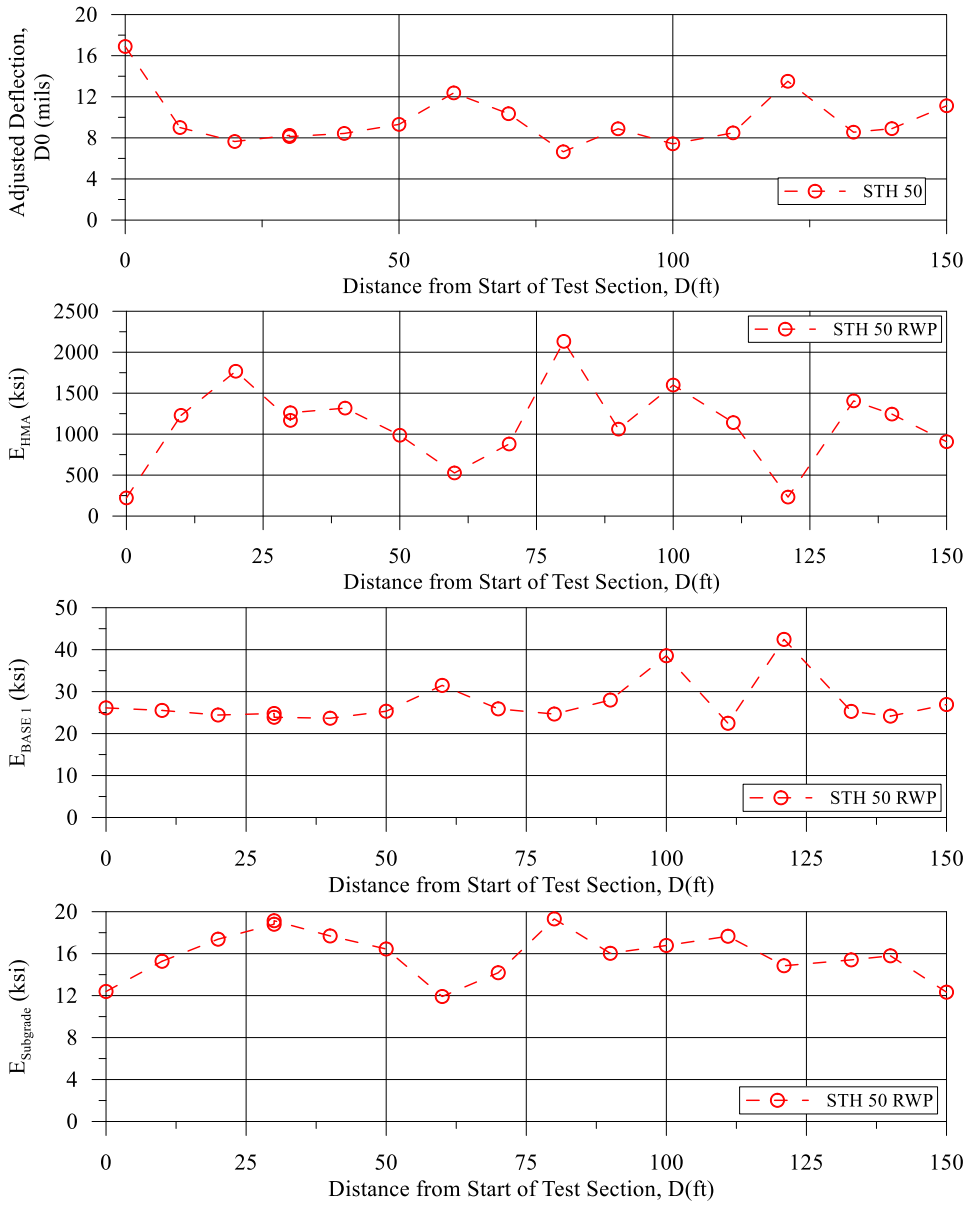

Figure 3: Results of FWD tests on STH 50 pavement (a) Adjusted deflection under the loading plate (D_0) (corrected for a 9,000 lb drop and temperature), (b) Back-calculated HMA layer modulus, (c) Back-calculated base layer modulus, and (d) Back-calculated subgrade modulus.

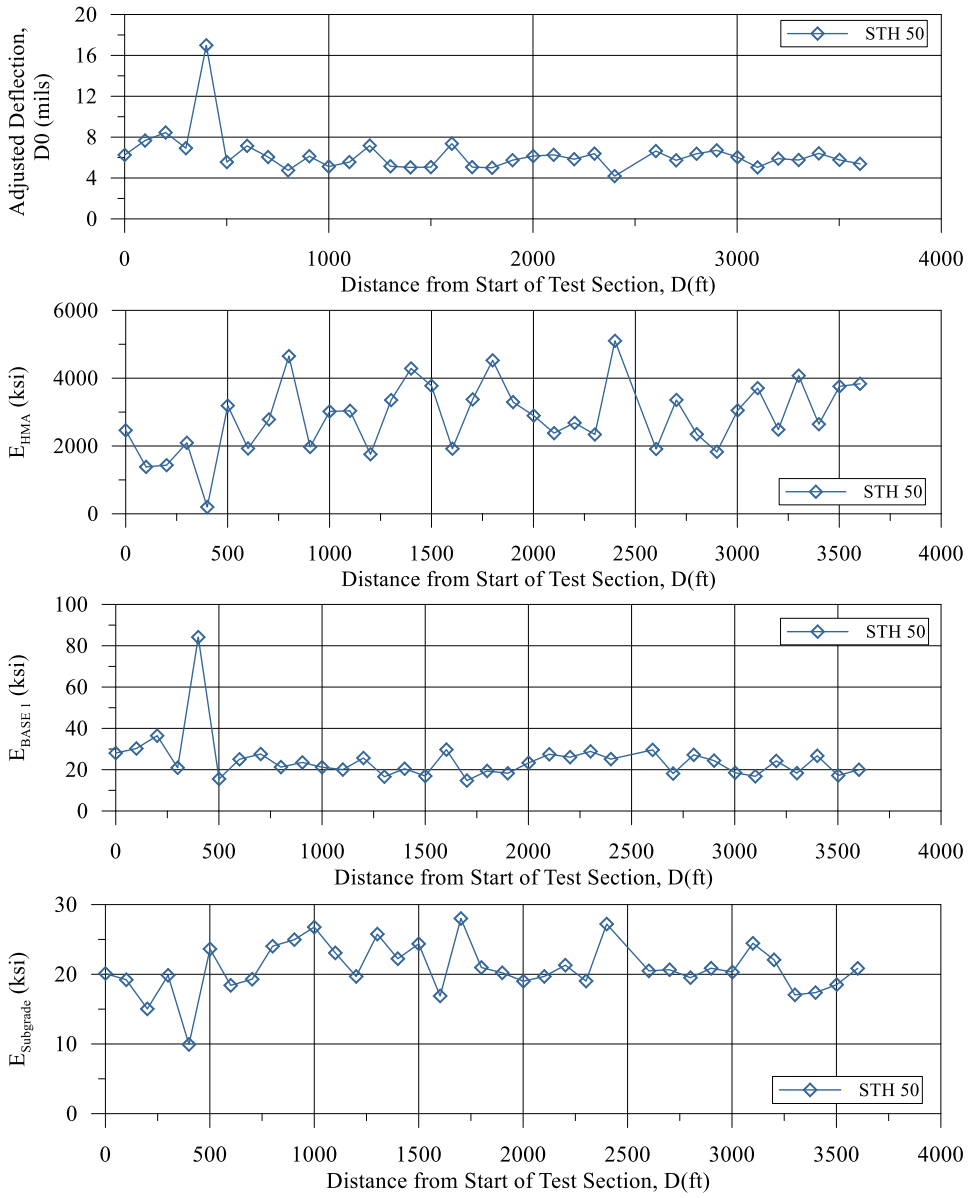

Figure 4: Results of FWD tests on STH 50 pavement (a) Adjusted deflection under the loading plate (D_0) (corrected for a 9,000 lb drop and temperature), (b) Back-calculated HMA layer modulus, (c) Back-calculated base layer modulus, and (d) Back-calculated subgrade modulus.

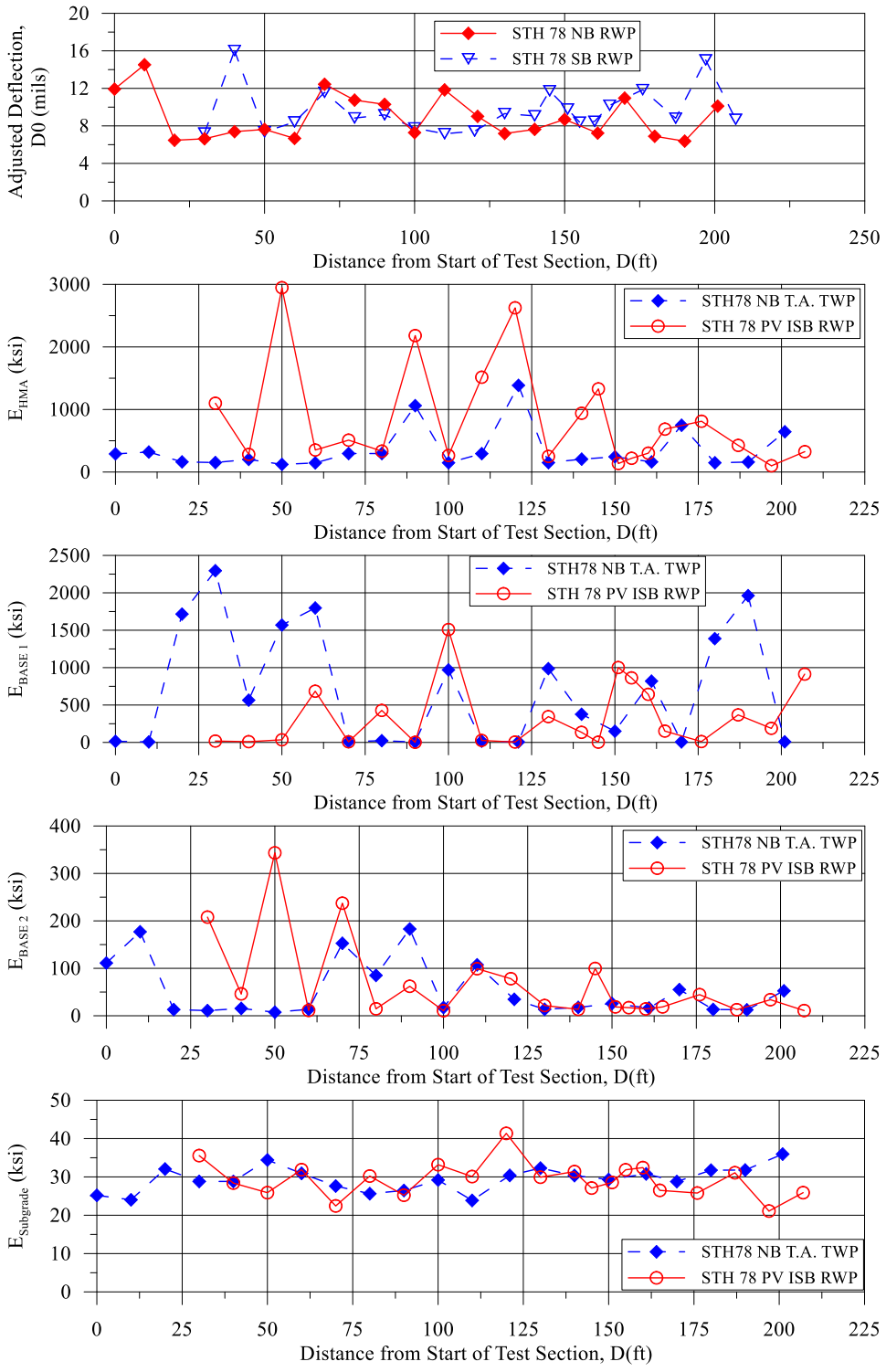

Figure 5: Results of FWD tests on STH 78 pavement (a) Adjusted deflection under the loading plate (D_0) (corrected for a 9,000 lb drop and temperature), (b) Back-calculated HMA layer modulus, (c) Back-calculated base layer modulus, and (d) Back-calculated subgrade modulus.

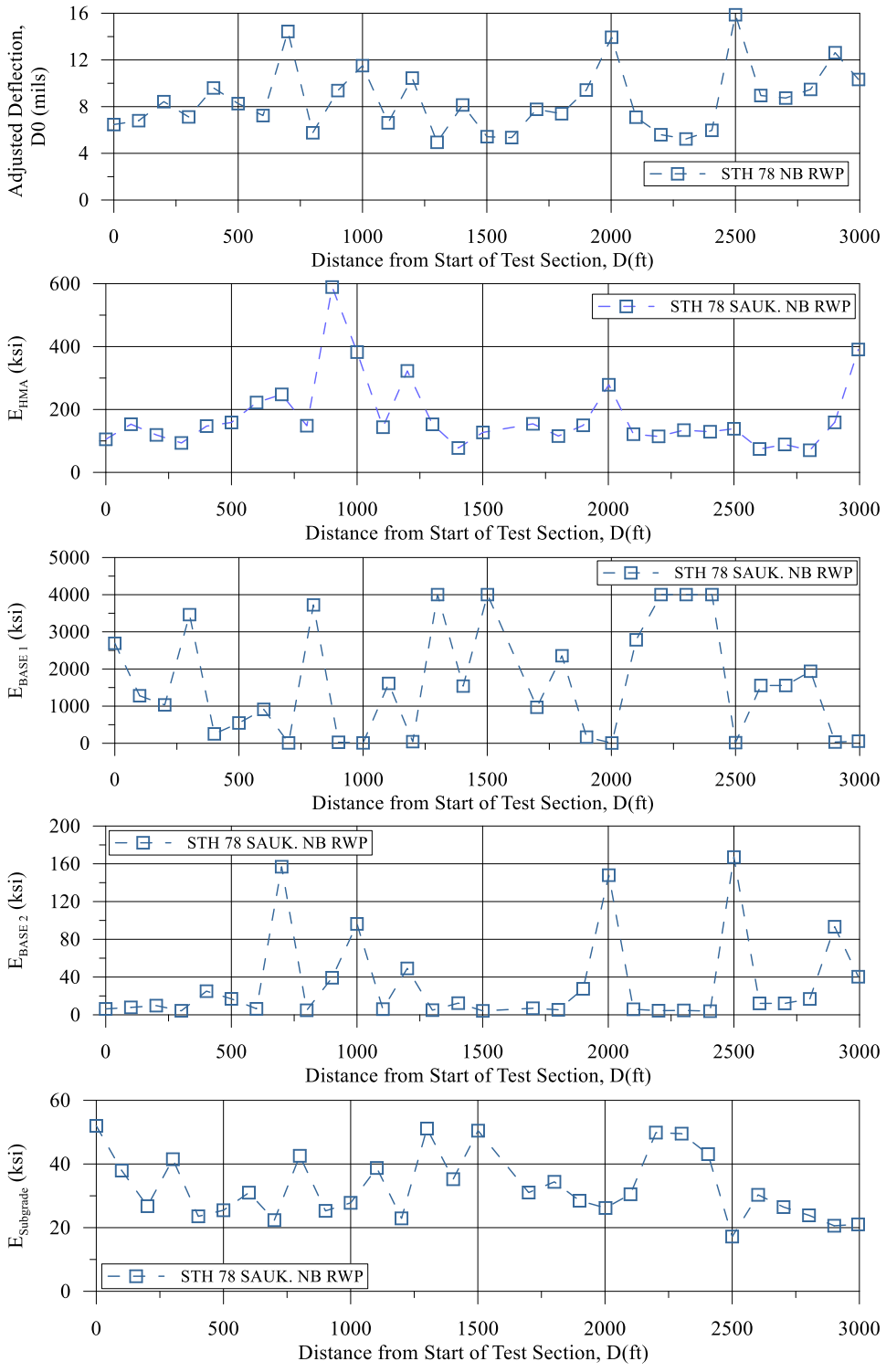

Figure 6: Results of FWD tests on STH 78 pavement (a) Adjusted deflection under the loading plate (D_0) (corrected for a 9,000 lb drop and temperature), (b) Back-calculated HMA layer modulus, (c) Back-calculated base layer modulus, and (d) Back-calculated subgrade modulus.

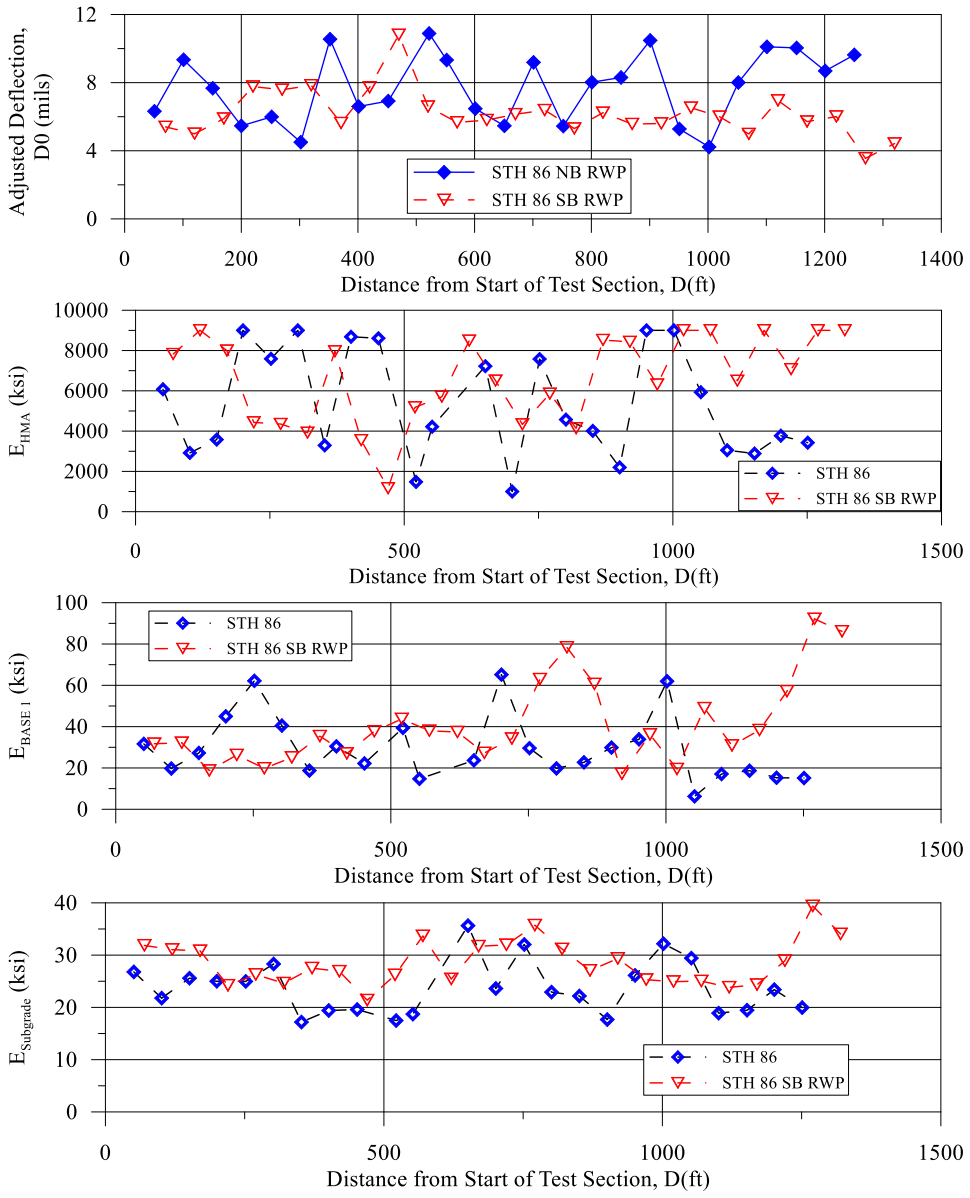

Figure 7: Results of FWD tests on STH 86 pavement (a) Adjusted deflection under the loading plate (D_0) (corrected for a 9,000 lb drop and temperature), (b) Back-calculated HMA layer modulus, (c) Back-calculated base layer modulus, and (d) Back-calculated subgrade modulus.

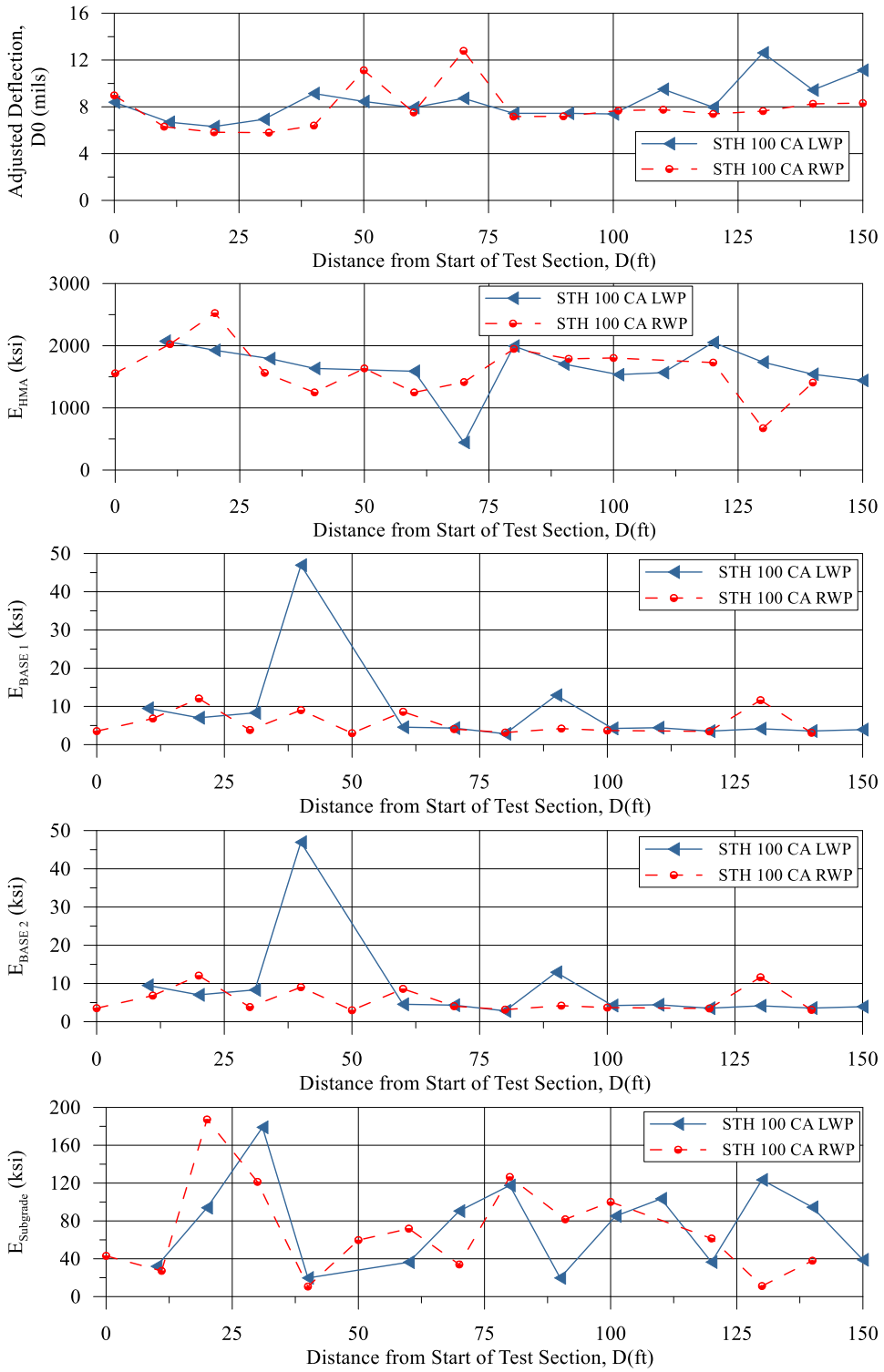

Figure 8: Results of FWD tests on STH 100 pavement (a) Adjusted deflection under the loading plate (D_0) (corrected for a 9,000 lb drop and temperature), (b) Back-calculated HMA layer modulus, (c) Back-calculated base layer modulus, and (d) Back-calculated subgrade modulus.

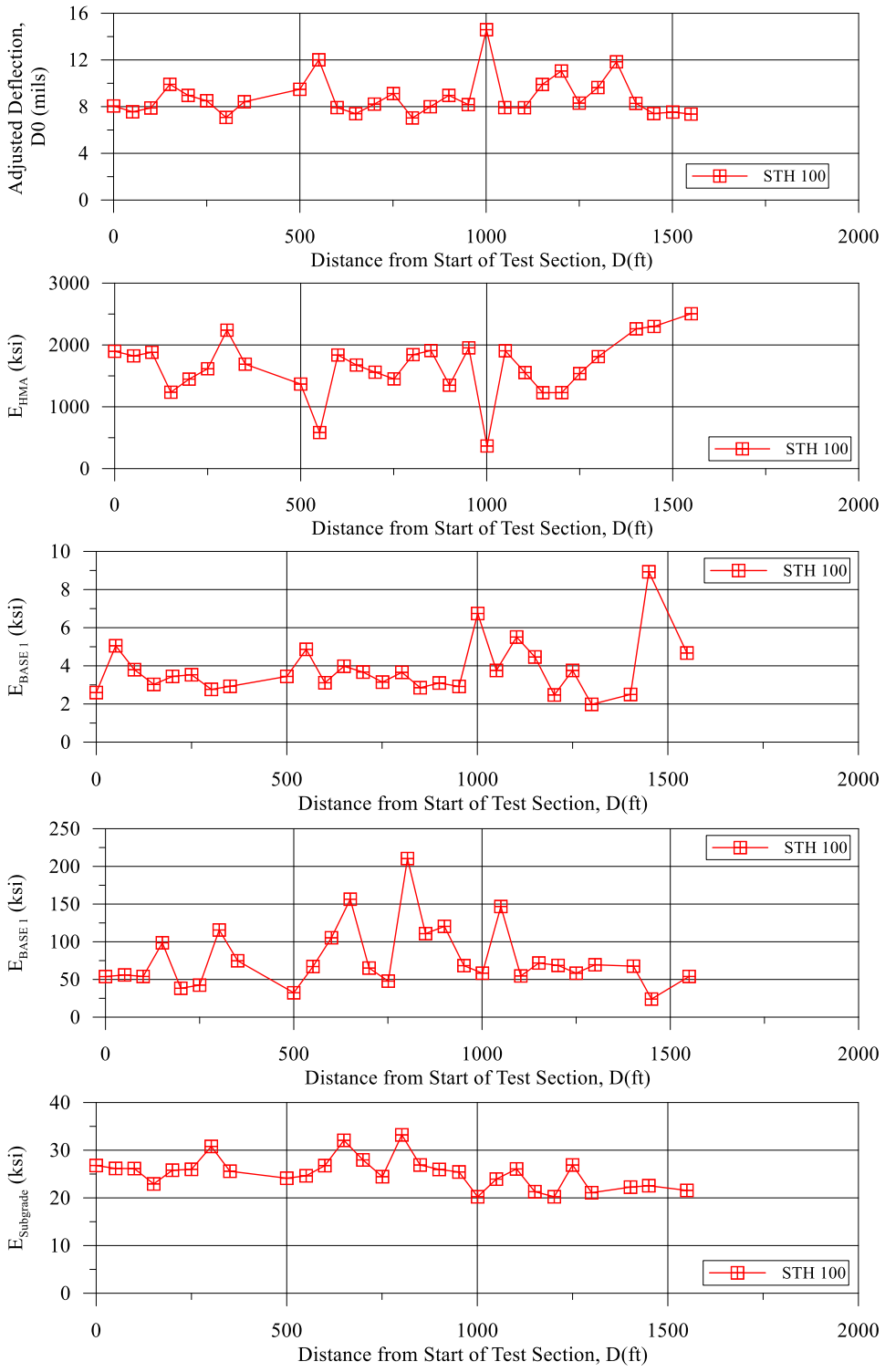

Figure 9: Results of FWD tests on STH 100 pavement (a) Adjusted deflection under the loading plate (D_0) (corrected for a 9,000 lb drop and temperature), (b) Back-calculated HMA layer modulus, (c) Back-calculated base layer modulus, and (d) Back-calculated subgrade modulus.

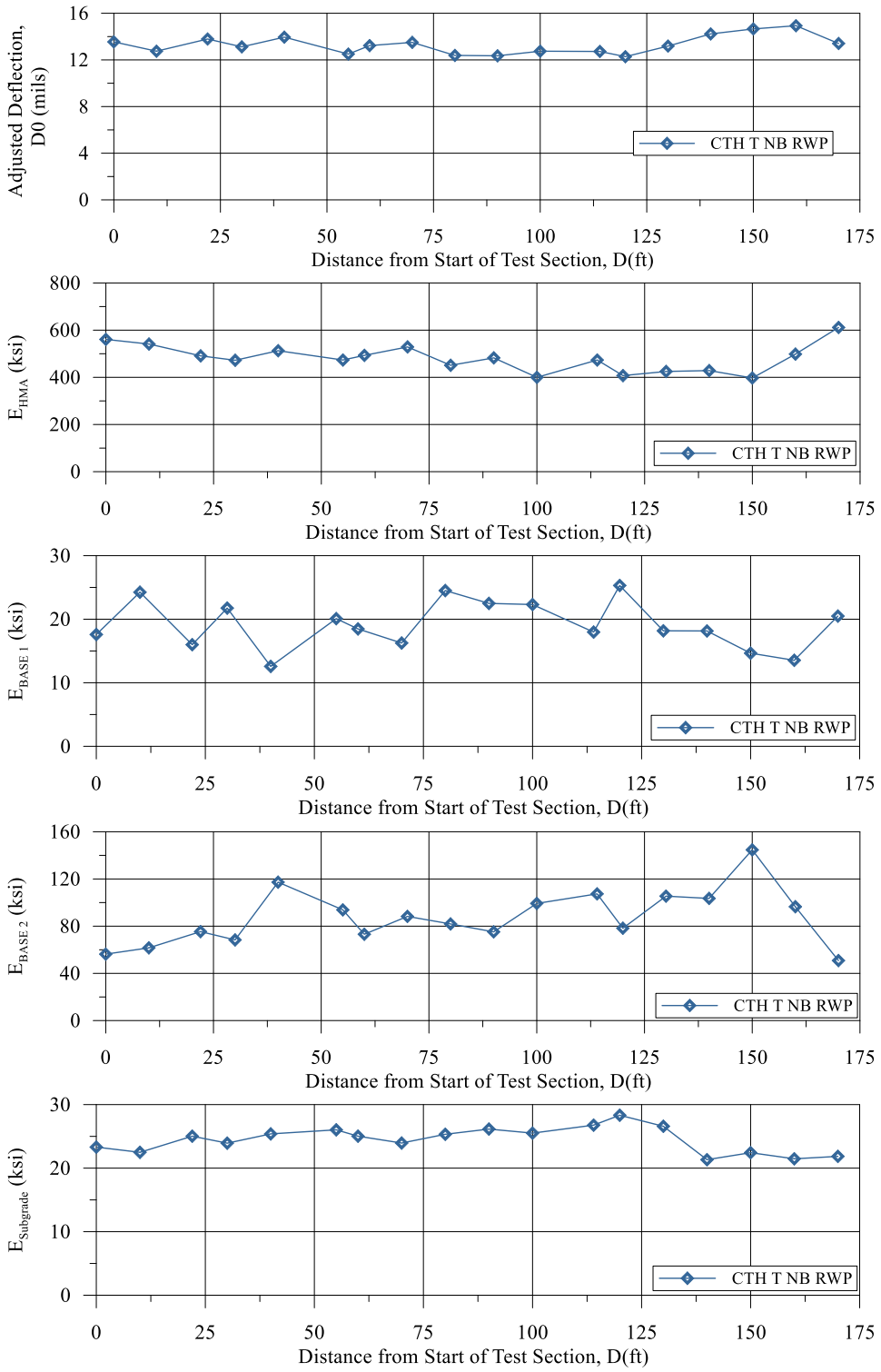

Figure 10: Results of FWD tests on CTH T pavement (a) Adjusted deflection under the loading plate (D_0) (corrected for a 9,000 lb drop and temperature), (b) Back-calculated HMA layer modulus, (c) Back-calculated base layer modulus, and (d) Back-calculated subgrade modulus.

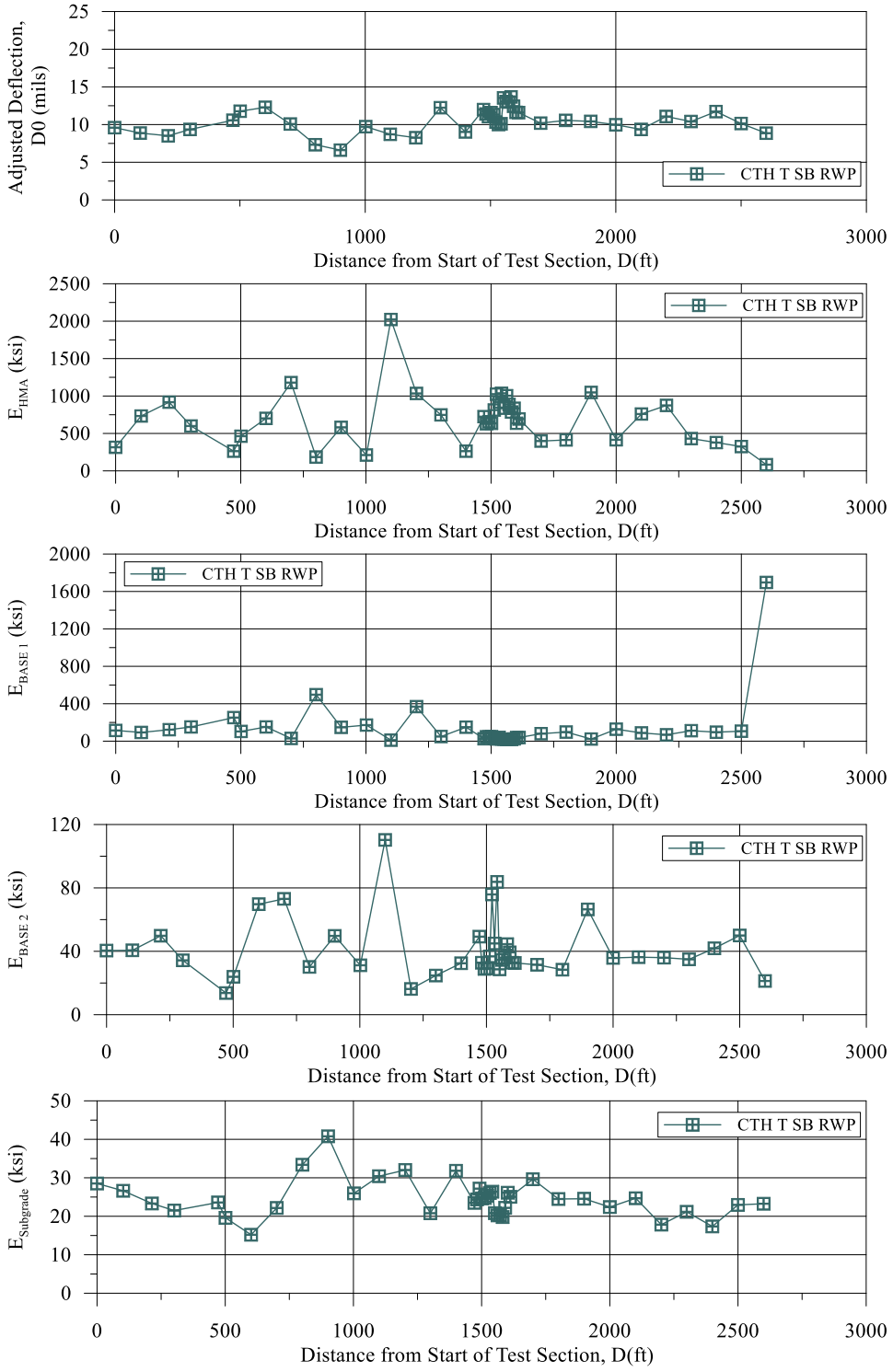

Figure 11: Results of FWD tests on CTH T pavement (a) Adjusted deflection under the loading plate (D_0) (corrected for a 9,000 lb drop and temperature), (b) Back-calculated HMA layer modulus, (c) Back-calculated base layer modulus, and (d) Back-calculated subgrade modulus.

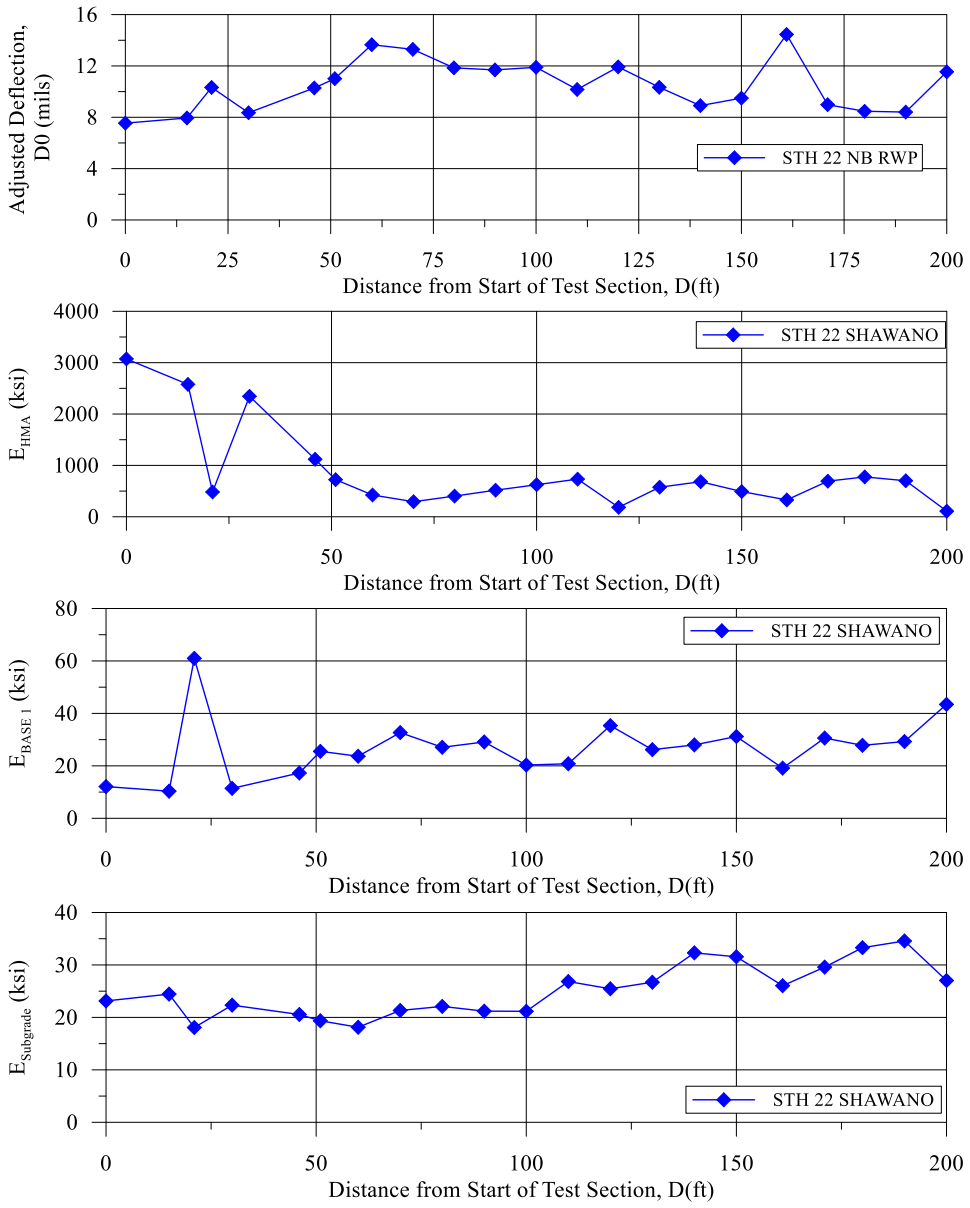

Figure 12: Results of FWD tests on STH 22 Shawano pavement (a) Adjusted deflection under the loading plate (D_0) (corrected for a 9,000 lb drop and temperature), (b) Back-calculated HMA layer modulus, (c) Back-calculated base layer modulus, and (d) Back-calculated subgrade modulus.

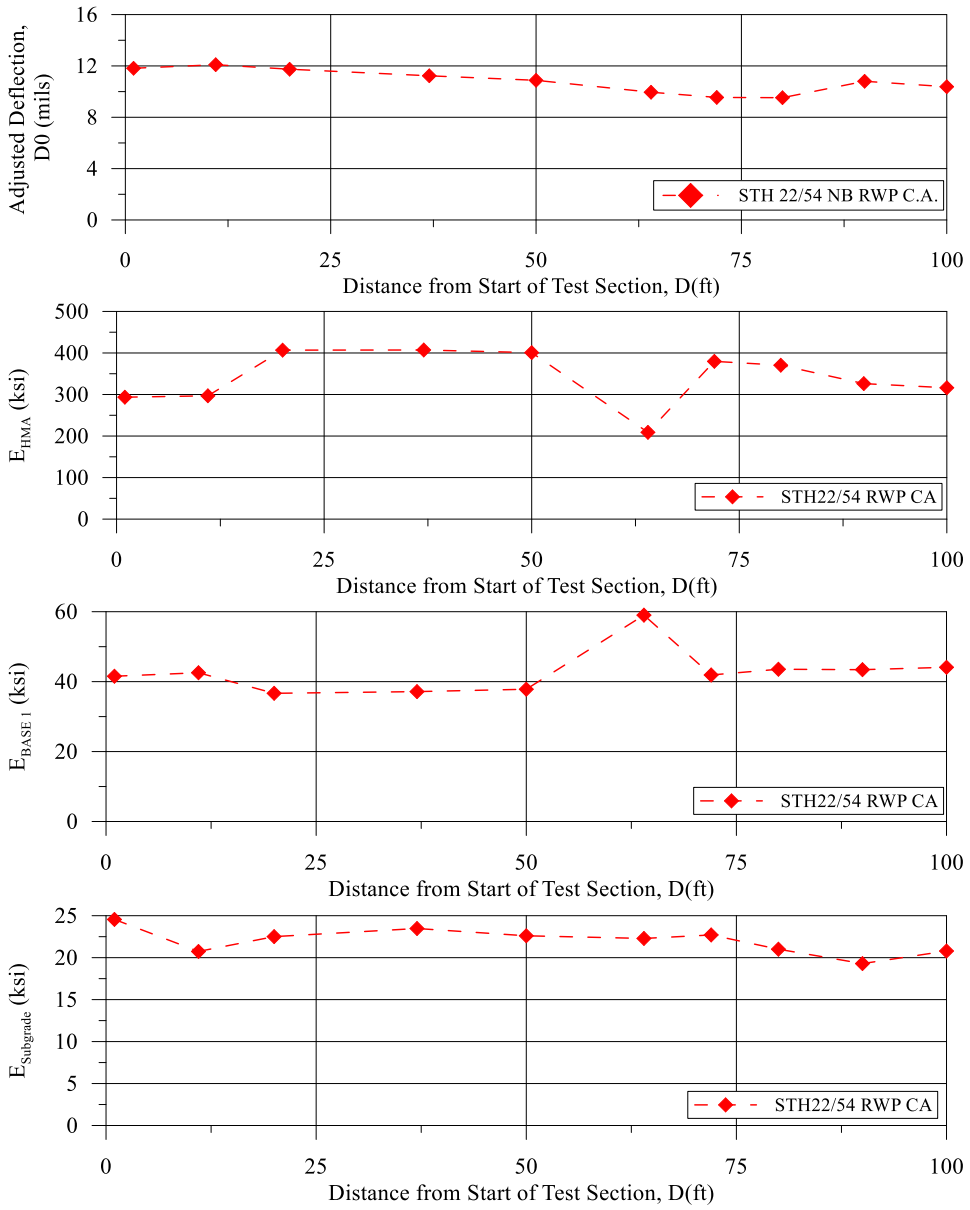

Figure 13: Results of FWD tests on STH 22-54 pavement (a) Adjusted deflection under the loading plate (D_0) (corrected for a 9,000 lb drop and temperature), (b) Back-calculated HMA layer modulus, (c) Back-calculated base layer modulus, and (d) Back-calculated subgrade modulus.

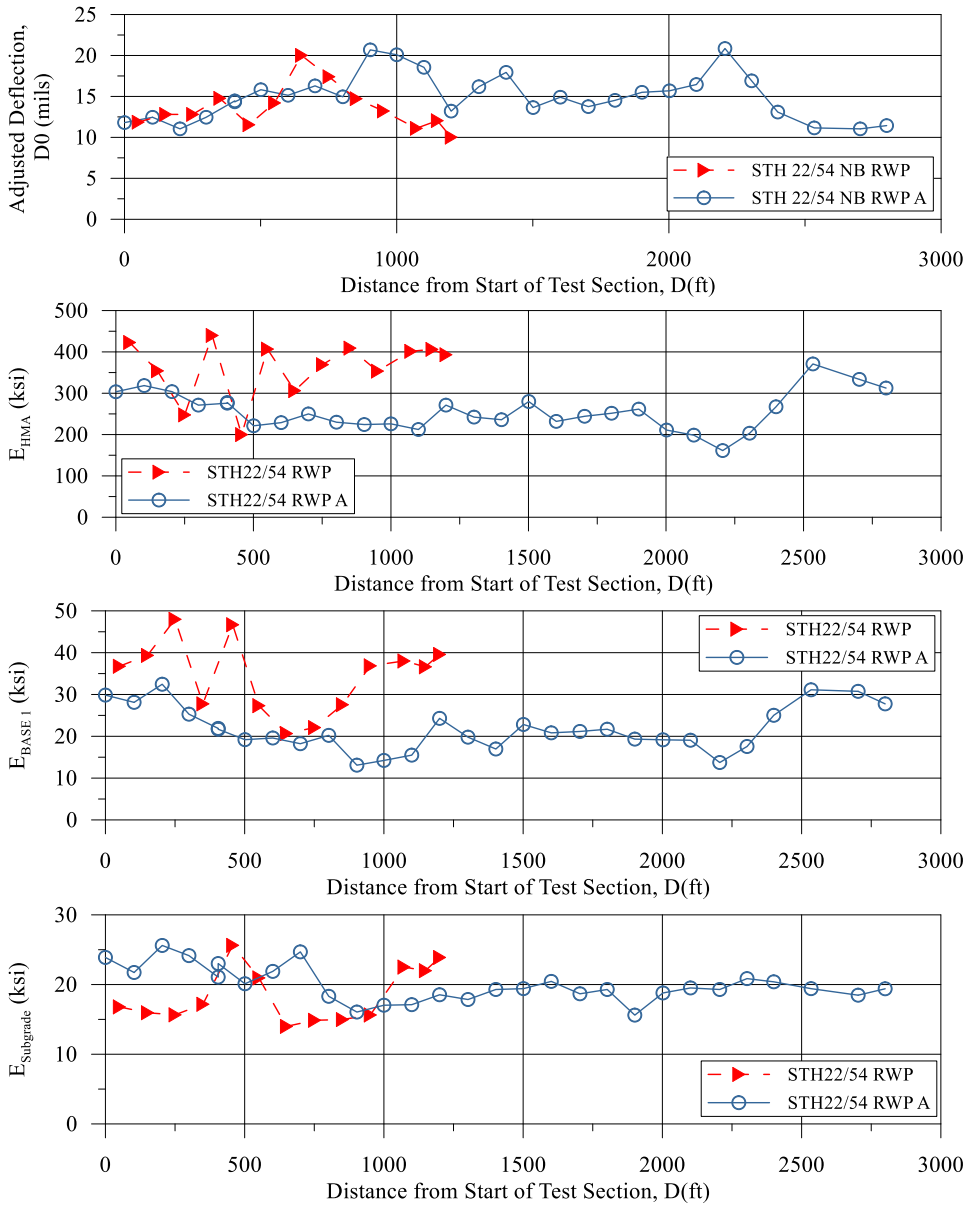

Figure 14: Results of FWD tests on STH 22-54 pavement (a) Adjusted deflection under the loading plate (D_0) (corrected for a 9,000 lb drop and temperature), (b) Back-calculated HMA layer modulus, (c) Back-calculated base layer modulus, and (d) Back-calculated subgrade modulus.

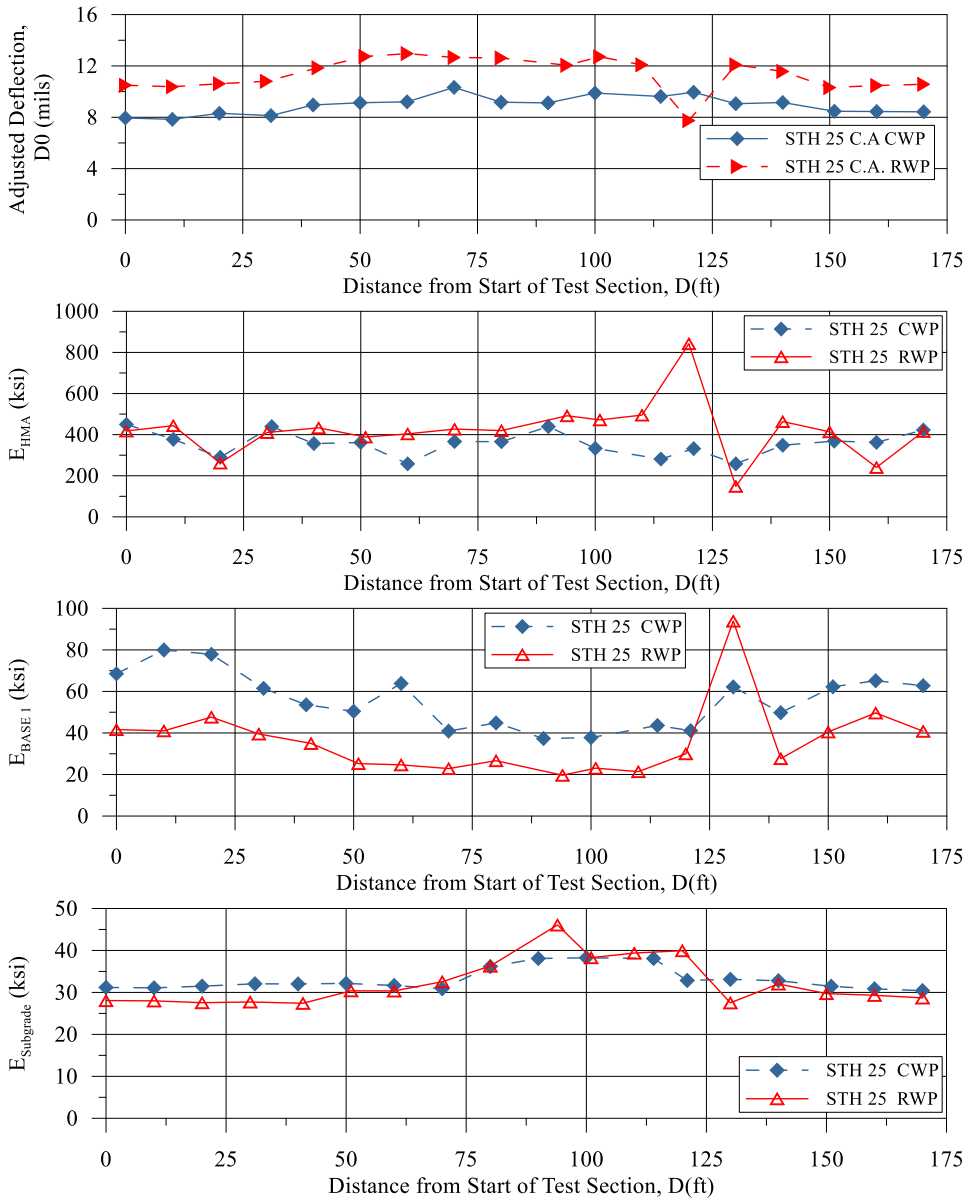

Figure 15: Results of FWD tests on STH 25 pavement (a) Adjusted deflection under the loading plate (D_0) (corrected for a 9,000 lb drop and temperature), (b) Back-calculated HMA layer modulus, (c) Back-calculated base layer modulus, and (d) Back-calculated subgrade modulus.

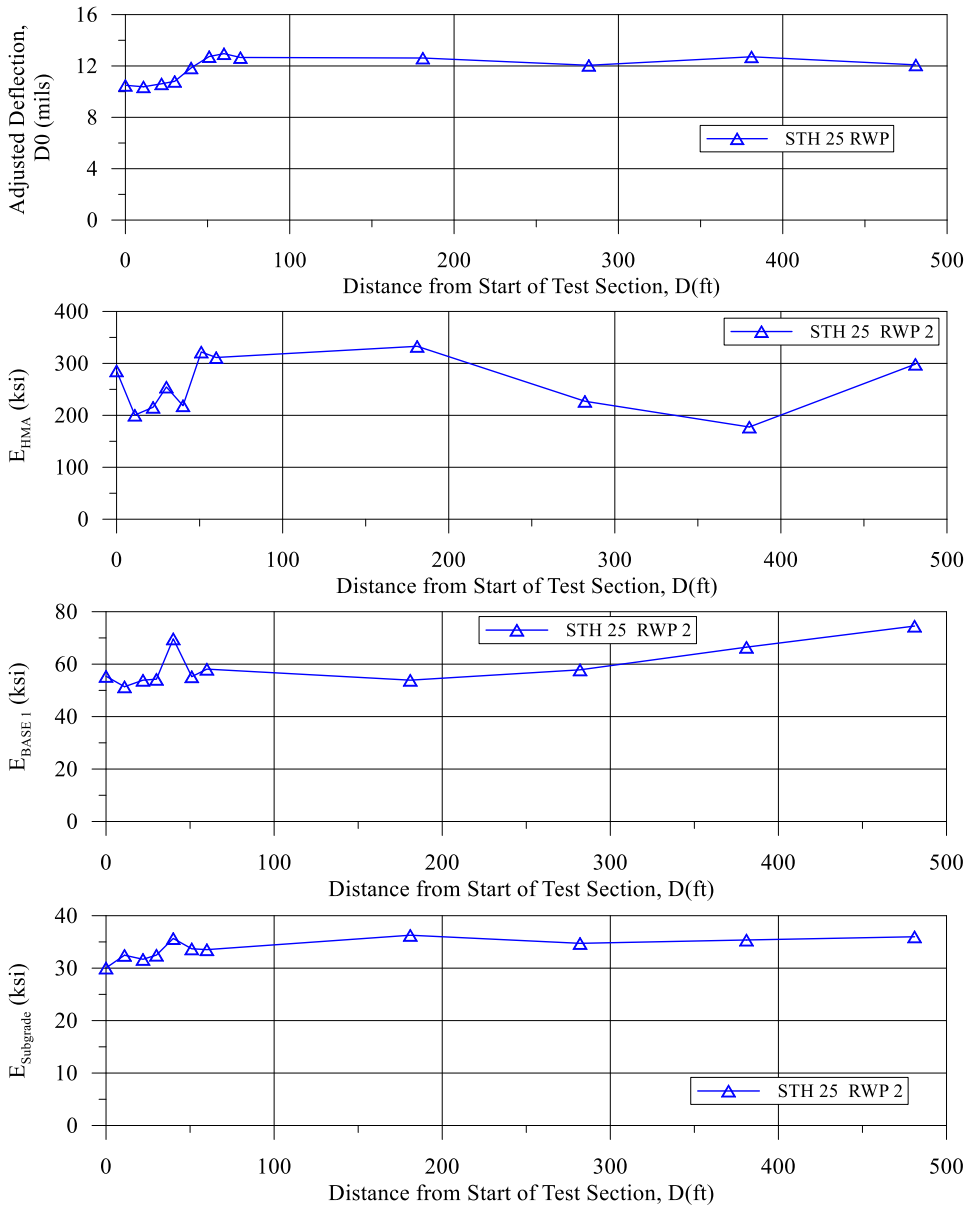

Figure 16: Results of FWD tests on STH 25 pavement (a) Adjusted deflection under the loading plate (D_0) (corrected for a 9,000 lb drop and temperature), (b) Back-calculated HMA layer modulus, (c) Back-calculated base layer modulus, and (d) Back-calculated subgrade modulus.

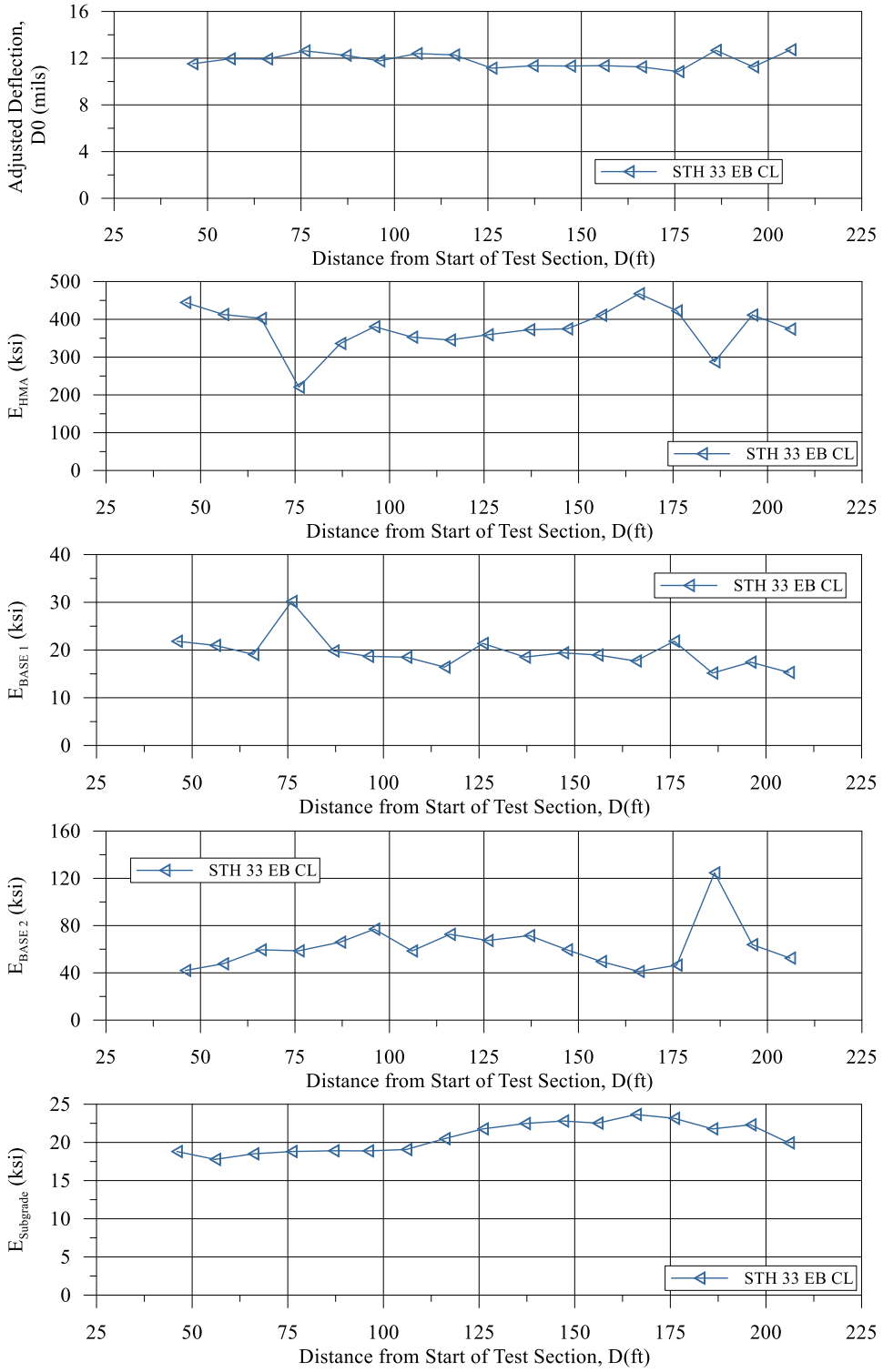

Figure 17: Results of FWD tests on STH 33 pavement (a) Adjusted deflection under the loading plate (D_0) (corrected for a 9,000 lb drop and temperature), (b) Back-calculated HMA layer modulus, (c) Back-calculated base layer modulus, and (d) Back-calculated subgrade modulus.

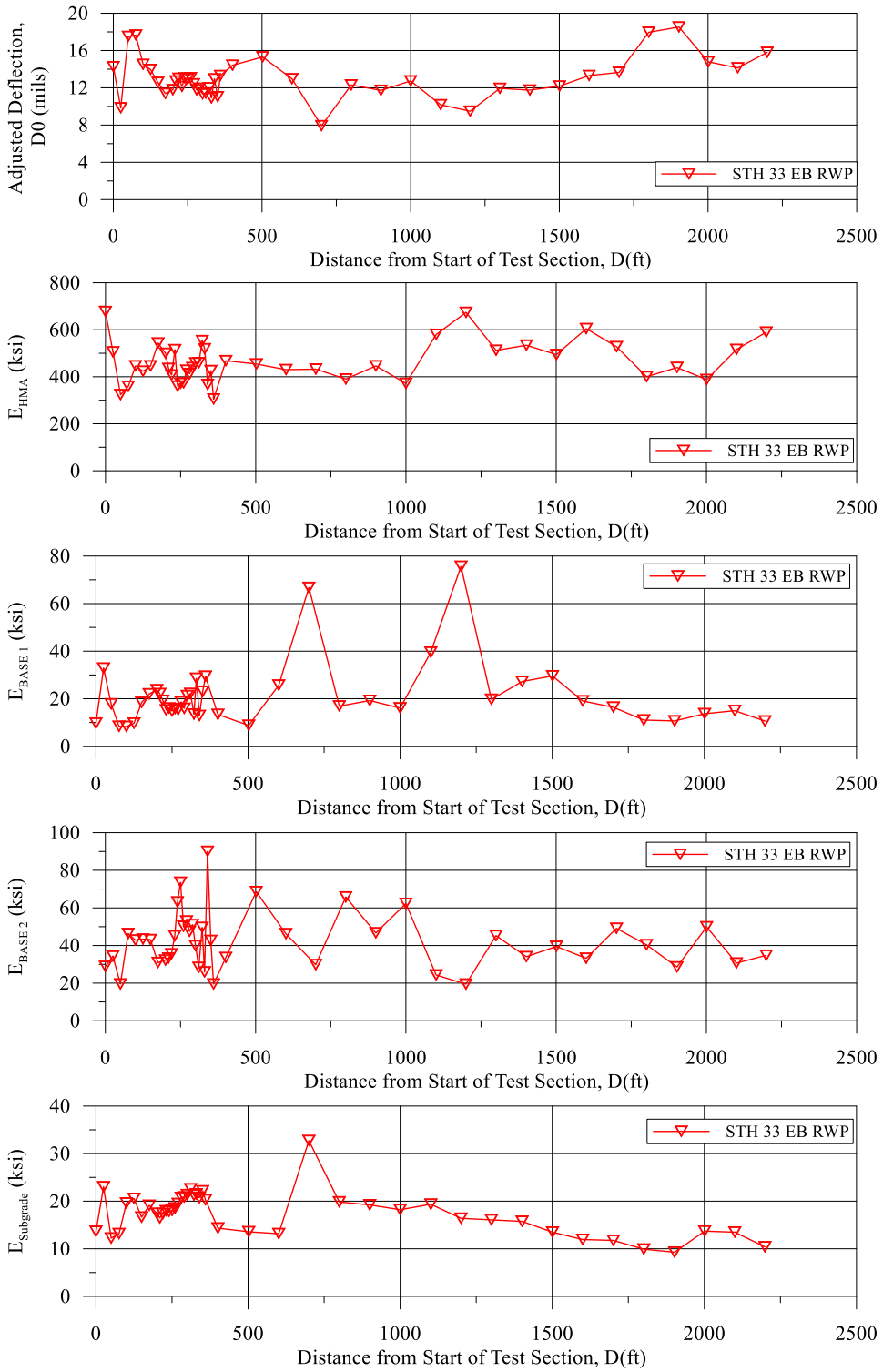

Figure 18: Results of FWD tests on STH 33 pavement (a) Adjusted deflection under the loading plate (D_0) (corrected for a 9,000 lb drop and temperature), (b) Back-calculated HMA layer modulus, (c) Back-calculated base layer modulus, and (d) Back-calculated subgrade modulus.

Appendix D

International Roughness Index Profiles

IRI profiles with distance for all investigated pavement sections

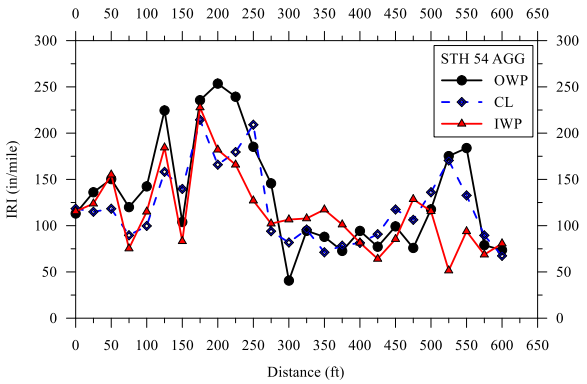

CA STH 22/54

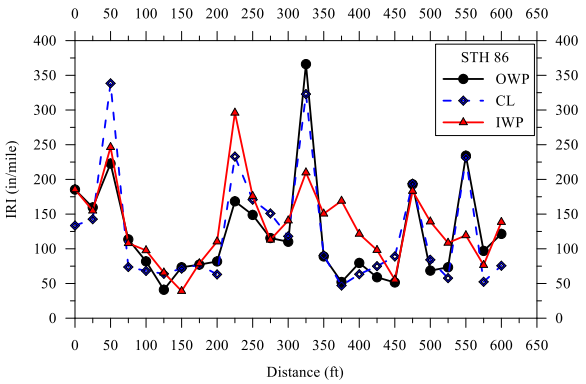

RCA STH 86

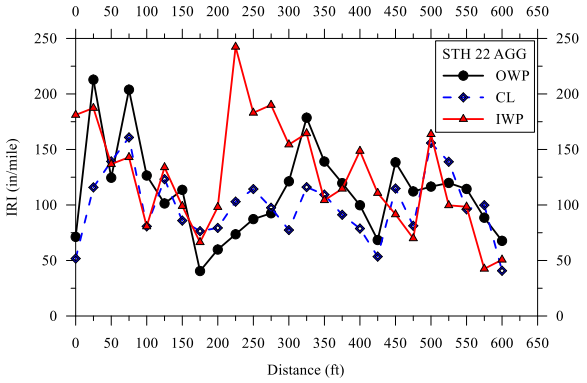

CA STH 22 Shawano

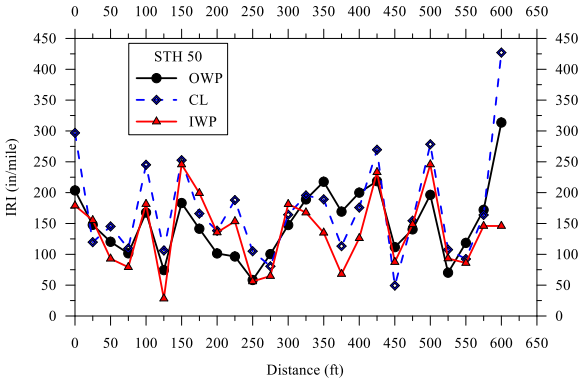

RCA STH 50

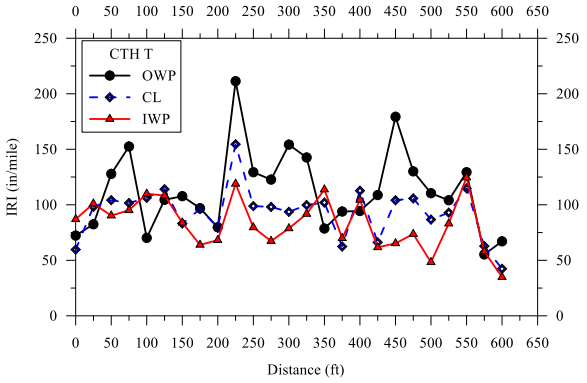

CA CTH T

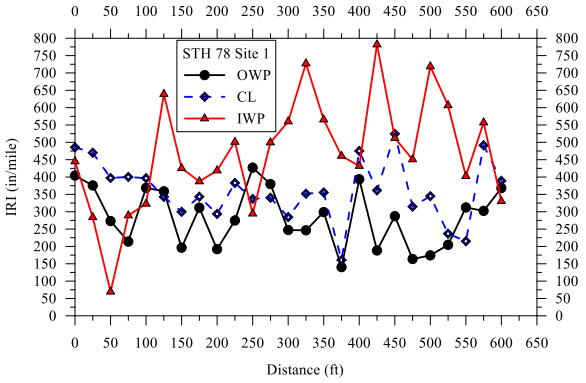

RCA STH 78 Site 1

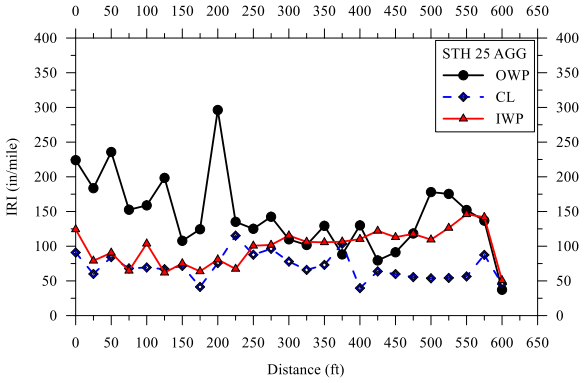

CA STH 25

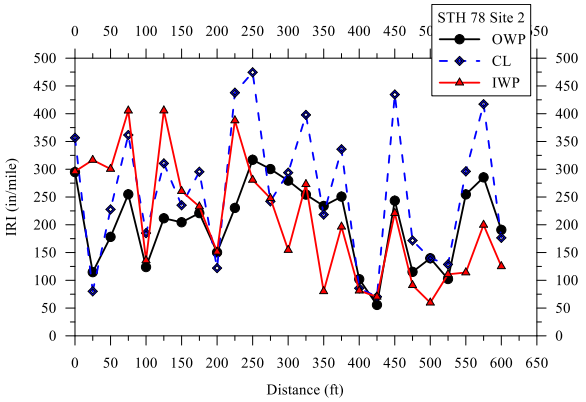

RCA STH 78 Site 2

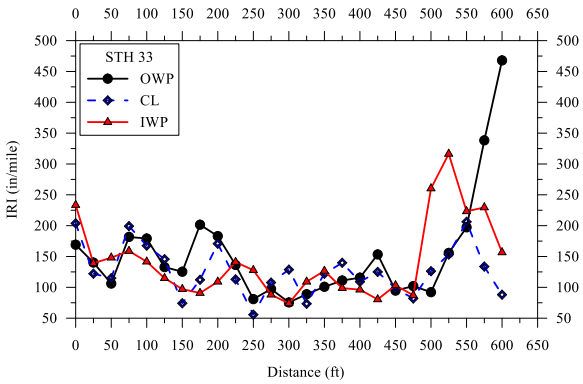

CA STH 33

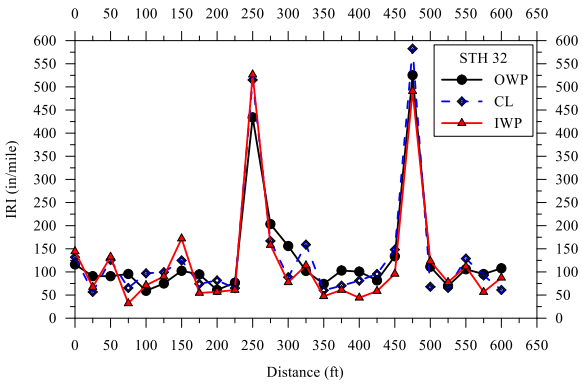

RCA STH 32

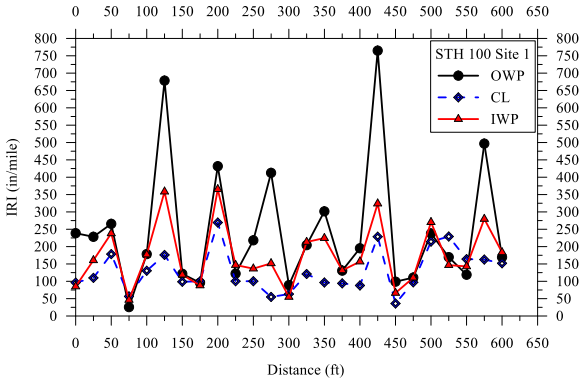

CA STH 100 Site 1

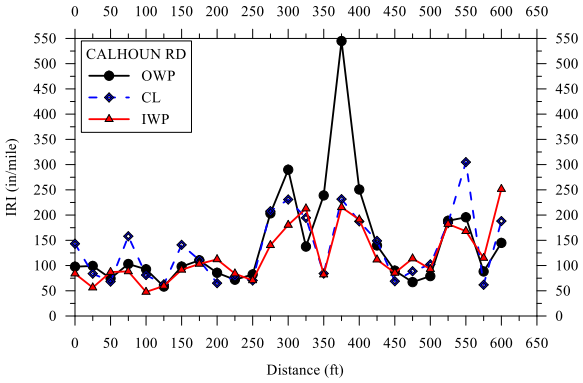

RCA Calhoun

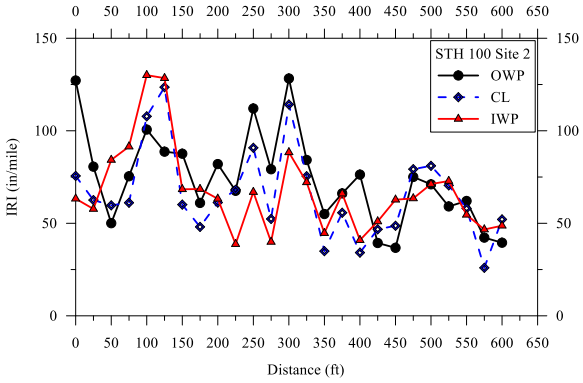

CA STH 100 Site 2

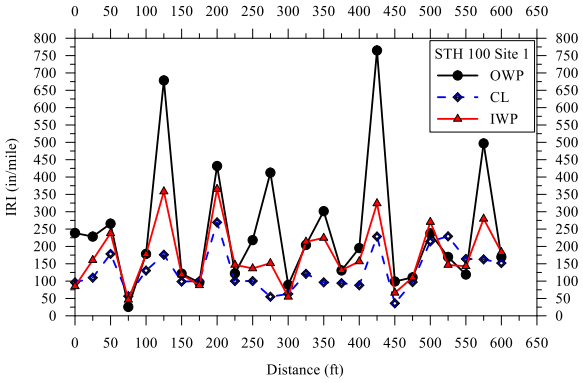

RCA STH 100 Site 1

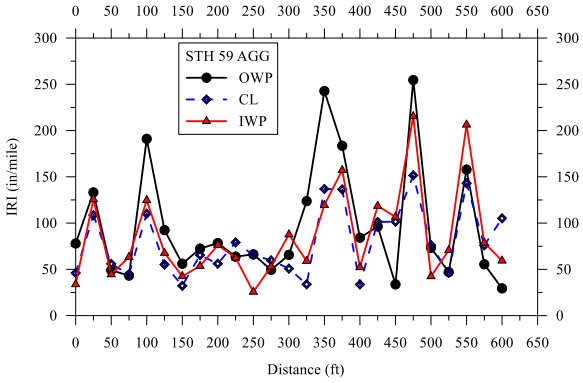

CA STH 59

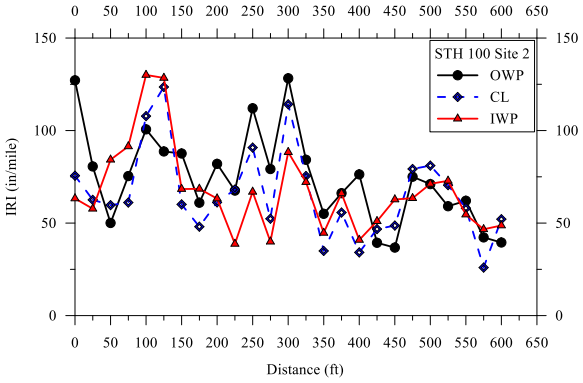

RCA STH 100 Site 2

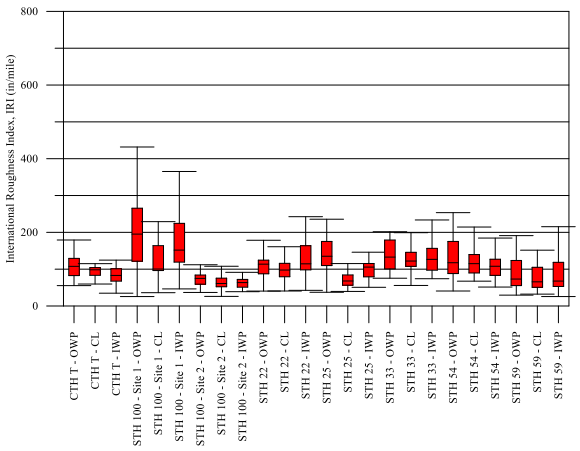
International Roughness Index, IRI (in/mile)
800
600
400
200
0
CTH T - OWP
CTH T - CL
CTH T - IWP
STH 100 - Site 1 - OWP
STH 100 - Site 1 - CL
STH 100 - Site 1 - IWP
STH 100 - Site 2 - OWP
STH 100 - Site 2 - CL
STH 100 - Site 2 - IWP
STH 22 - OWP
STH 22 - CL
STH 22 - IWP
STH 25 - OWP
STH 25 - CL
STH 25 - IWP
STH 33 - OWP
STH 33 - CL
STH 33 - IWP
STH 54 - OWP
STH 54 - CL
STH 54 - IWP
STH 59 - OWP
STH 59 - CL
STH 59 - IWP

CA

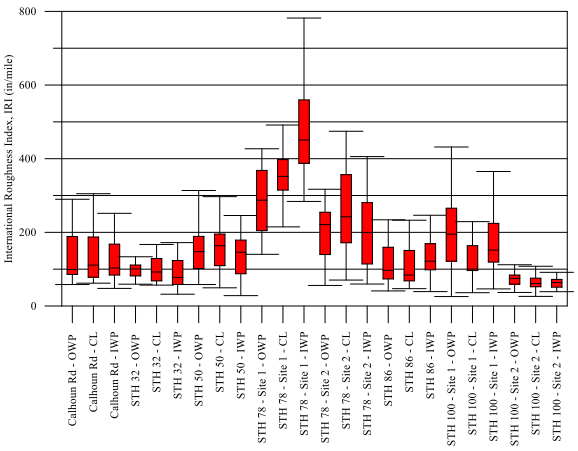
International Roughness Index, IRI (in/mile)
800
600
400
200
0
Calhoun Rd - OWP
Calhoun Rd - CL
Calhoun Rd - IWP
STH 32 - OWP
STH 32 - CL
STH 32 - IWP
STH 50 - OWP
STH 50 - CL
STH 50 - IWP
STH 78 - Site 1 - OWP
STH 78 - Site 1 - CL
STH 78 - Site 1 - IWP
STH 78 - Site 2 - OWP
STH 78 - Site 2 - CL
STH 78 - Site 2 - IWP
STH 86 - OWP
STH 86 - CL
STH 86 - IWP
STH 100 - Site 1 - OWP
STH 100 - Site 1 - CL
STH 100 - Site 1 - IWP
STH 100 - Site 2 - OWP
STH 100 - Site 2 - CL
STH 100 - Site 2 - IWP

RCA